UNIVERSITA' DEGLI STUDI DI CATANIA

DOTTORATO DI RICERCA IN BIOTECHNOLOGIE

XXVIII Ciclo

The role of mTOR signaling in Alzheimer's disease

TESI DI DOTTORATO

Dottorando:

Dott.ssa Antonella Caccamo

Tutor:
Chiar.ma Prof.ssa Angela Messina

Coordinatore:
Chiar.mo Prof. Vito De Pinto

TRIENNIO ACCADEMICO 2013-2016

ABSTRACT

The majority (>95%) of Alzheimer's disease (AD) cases are sporadic and of unknown causes. The single major risk factor for AD is aging and molecular changes that occur in the brain as a function of age may facilitate the development of AD. However, little is known as to how the aging process facilitates the development of AD.

Overwhelming evidence shows that reducing the activity of the mammalian target of rapamycin (mTOR) increases lifespan and health-span in several genetically different species. mTOR is a ubiquitously expressed protein kinase that plays a key role in regulating protein synthesis and cell growth. mTOR also is a negative regulator of autophagy induction. By simultaneously regulating protein synthesis and degradation, mTOR is key in controlling protein homeostasis, a process that is altered in AD and other proteinopathies. Another known function of mTOR signaling is the regulation of synaptic plasticity and function.

Using two widely used animal models of AD, known as Tg2576 and 3xTg-AD mice, we employed multidisciplinary approaches to dissect the role of mTOR signaling in AD. We found that genetic reduction of mTOR signaling reduced amyloid-β deposits and tau pathology and rescued memory deficits in Tg2576 mice. Mechanistically, the reduction in mTOR signaling led to an increase in autophagy induction and restored the hippocampal gene expression signature of the Tg2576 mice to wild type levels. Consistent with these findings, we also found that that genetic reduction of the ribosomal protein S6 kinase 1 (S6K1), a protein kinase directly downstream of mTOR, improved synaptic plasticity and spatial memory deficits, and reduced the accumulation of amyloid-β and tau, in 3xTg-AD mice. Mechanistically, these changes were linked to reduced translation of tau and the beta-site APP cleaving enzyme 1 (BACE-1), a key enzyme in the generation of amyloid-β.

Given the overwhelming evidence showing that reducing mTOR signaling increases lifespan and health span, the data presented here have profound clinical implications for aging and AD and provide the molecular basis for how aging may contribute to AD pathology. Our results implicate hyperactive mTOR/S6K1 signaling as a previous unidentified signaling pathway underlying gene-expression dysregulation, synaptic and cognitive deficits in Alzheimer's disease.

SUMMARY

1. INTRODUCTION

1.1 Alzheimer's disease

Alzheimer's disease (AD) is the most common neurodegenerative disorder. It is estimated that 26 million people worldwide are living with AD and by 2050 the number of people with this disorder can reach 100 million (Thies et al., 2013). Currently there are no effective cures for AD and patients perish of comorbidities 3 to 9 years after diagnosis.

More than 95% of AD cases are sporadic and of unknown causes, with aging being the major risk factor for the development of the disease. It is estimated that 33-50% of people older than 85 have AD (Bird, 2008). In the Western Countries, the aging population is the fastest segment of society; thus the number of AD cases is predicted to greatly increase by mid-century (Bird, 2008). The remaining cases are caused by mutations in one of three genes, presenilin 1 and 2 and amyloid precursor protein (APP; Querfurth and LaFerla, 2010).

One of the first clinical manifestation of AD is deficits in episodic memory (i.e., the ability to recall previous events; Artero et al., 2003; Welsh et al., 1992). As the disease progresses, other cognitive domains are impacted and deficits in executive functions, language, and learning tasks appear evident. Eventually, patients become bedridden and perish due to other comorbidities.

The two hallmark neuropathological lesions that characterize AD are plaques, mainly composed of amyloid-β (Aβ) peptide, and neurofibrillary tangles (NFT), mainly formed by hyperphosphorylated tau (Selkoe, 2001). The events triggering AD pathology and the molecular mechanisms linking aging to AD are not known.

1.1.1 Biology of Aβ

Aβ is derived from a longer precursor molecule, the amyloid precursor protein (APP), which is encoded by a gene located on chromosome 21 (St George-Hyslop et al., 1987). APP can be processed along two different pathways: a non-amyloidogenic pathway, which prevents the generation of Aβ, and an amyloidogenic pathway, which eventually leads to Aβ formation (Selkoe, 2001; Fig. 1). The non-amyloidogenic pathway involves the activity of α-secretase, which cleaves APP in the middle of the Aβ sequence, thereby preventing the formation of Aβ. In contrast, the

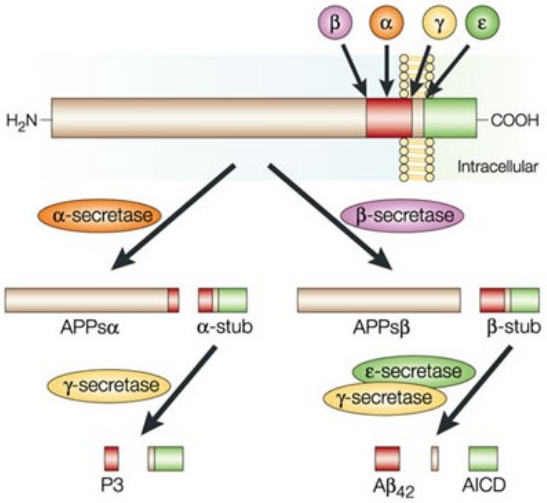

Figure 1. Schematic representation of APP processing. APP is cleaved by an α-secretase, which cuts APP in the middle of the Aβ sequence thus precluding Aβ formation. In the contrary, the sequential activity of β- and γ-secretase enzymes lead to the formation of Aβ. This diagram is from (LaFerla, 2002).

amyloidogenic pathway involves a cleavage of APP at the β-secretase site by the β-site APP cleaving enzyme (BACE; Vassar et al., 1999), leading to the production of the C99 fragment, which serves as the substrate for another secretase known as γ-secretase. γ-secretase cleaves C99 predominantly at two different positions, generating either $A\beta_{40}$ or $A\beta_{42}$. The longer species is more amyloidogenic than the shorter isoforms. Several clinical mutations in the APP gene have

been identified and most of them are localized to positions near the α, β and γ-secretase sites (Goate et al., 1991; Mullan et al., 1992) and reviewed by (Haass and Selkoe, 1993). These mutations lead to autosomal-dominant, early-onset familial Alzheimer's disease (FAD), likely by increasing total Aβ production or by selectively increasing of the longer more amyloidogenic $A\beta_{42}$ species (Citron et al., 1992; Suzuki et al., 1994).

1.1.2 Biology of presenilins

Two other proteins are directly involved in the pathogenesis of AD: presenilin 1 (PS1) and presenilin 2 (PS2) (Levy-Lahad et al., 1995; Rogaev et al., 1995; Sherrington et al., 1995). These are transmembrane proteins that are part of a high molecular weight complex that is responsible for the γ-secretase activity (Kimberly et al., 2000; Wolfe et al., 1999). Both PS1 and PS2 are membrane proteins with multiple transmembrane regions that are expressed in the brain and in the periphery (Rogaev et al., 1995; Sherrington et al., 1995). Within neurons, PS2 is mainly expressed in the cell body whereas PS1 is expressed in cell bodies and neuronal processes (Blanchard et al., 1997). Both proteins undergo proteolytic cleavage; PS1 is rapidly cleaved into a ~28 kDa amino terminal and a ~ 19-kDa carboxy-terminal fragment, whereas PS2 is cleaved into two polypeptides of 34 kDa and 20 kDa, respectively. Mutations in the genes encoding these proteins (located on chromosome 14 and 1, respectively) lead to early-onset AD (Rogaev et al., 1995; Sherrington et al., 1995). Indeed, mutations in the PS1 gene, which account for the majority of all early-onset AD cases (Cruts et al., 1996), can cause AD in people as young as 16 years of age. The mechanism by which these mutations lead to AD seems to be linked to Aβ formation (Scheuner et al., 1996).

1.1.3 Biology of tau

As mentioned above, tau is the main component of NFT. Tau is a microtubule-associated protein that promotes microtubule assembly and stabilization (Drechsel et al., 1992; Lindwall and Cole, 1984; Trinczek et al., 1995). These functions are highly regulated by post-translational modifications including the addition and removal of phosphate groups by the activity of several phosphates and kinases. Tau is highly expressed in neurons although low expression levels are also detected in astrocytes and oligodendrocytes (Binder et al., 1985; LoPresti et al., 1995). Six different isoforms are expressed in the adult brain and all of them are generated from the

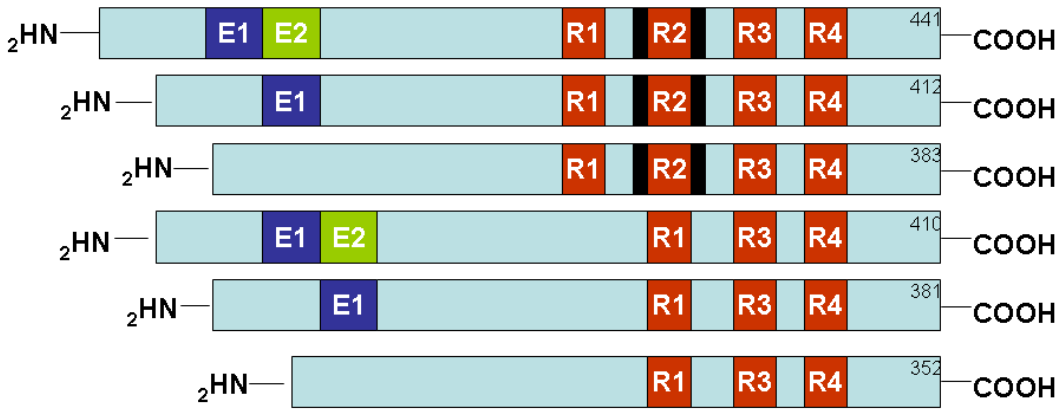

Figure 2. Schematic illustration of the human tau gene. Tau is encoded by a single gene, MAPT, located on chromosome 17. Six isoforms are generated via alternative splicing of exons 2, 3 or 10. Exons 2 and 3 encode repeated regions, whose function is not well understood. The red boxes R1-R4 represent microtubules binding domains. In humans, equal ratio of 3R and 4R is expressed in the adult brain, whereas in mice, the 3R is predominately expressed. This diagram is not drawn to scale and is from (LaFerla and Oddo, 2005).

alternative splicing of a single gene located on chromosome 17 (Fig. 2). Mutations in the tau gene cause frontotemporal dementia and Parkinsonism linked to chromosome 17 (FTDP-17), a disease characterized by intracellular accumulation of tangles similar to those present in AD brains (Hutton et al., 1998).

1.1.4 Amyloid cascade hypothesis

As discussed above, the majority of the clinical mutations known to cause AD lead to Aβ mis-metabolism. This genetic evidence was the basis for the formulation of the amyloid cascade hypothesis, which states that Aβ is the trigger of all cases of AD (Hardy and Selkoe, 2002; Hardy and Higgins, 1992; Selkoe, 1991). Based on this hypothesis, all the other pathological events are a consequence of Aβ accumulation, which can be a consequence of mis-metabolism, overproduction, or a reduction in clearance mechanisms. Indeed, steady-state levels of two Aβ-degrading enzymes decrease in the cortex and cerebellum of NonTg mice and humans as a function of age but do not change in the cerebellum. Moreover, the steady-state levels of these enzymes are always higher in the cerebellum (Caccamo et al., 2005). These results clearly suggest that the levels of these enzymes can play an important role in Aβ deposition.

1.1.5 Synaptic dysfunctions

Synaptic loss is another major neuropathological hallmarks of AD and is the best correlate of cognitive deficits (Koffie et al., 2011). Hippocampal synapses begin to degenerate in patients with mild cognitive impairment, where a reduction of about 25% in the presynaptic vesicle protein synaptophysin has been reported (Querfurth and LaFerla, 2010). With the progression of the disease, the loss of synapses becomes severe, especially in brain regions surrounding plaques. These observations suggests that Aβ may be the cause of synaptotoxicity. To this end, Aβ inhibits long-term potentiation (LTP), one of the major cellular mechanisms that underlies learning and memory, and a measure of synaptic strength and plasticity (Koffie et al., 2011). Consistent with this results, inhibiting the formation of Aβ oligomers rescues LTP induced by treating brain slices with media containing Aβ. In addition to inhibit LTP, Aβ facilitates the induction of long-term depression (LTD) in hippocampal synapses. Impairments in LTP and facilitation of LTD cause synaptic depression and damages in neuronal networks (Palop and

Mucke, 2010). The molecular mechanisms underlying the Aβ-mediated synapse dysfunction is very complex and it is an area of active research. For example, Aβ can induce calcium dyshomeostasis, trigger activation of caspases and calcineurin, and modulate the activity of synaptic excitatory receptors and receptor tyrosine kinases, instigating a cascade of molecular events that culminate in synapses loss and eventually impairment of cognitive and memory functions (Koffie et al., 2011).

1.1.6 Transgenic mice

Considering the complex nature of AD pathology, it is very difficult to study the molecular mechanisms underlying this disease in humans. In human *post mortem* brain tissue, it is difficult to establish the damage due to Aβ and the downstream damage due to degenerative processes occurring in the last years of the patient's life. Moreover, other complications that can occur during the last years of the patient's life can complicate the pathological *post mortem* analysis of these brains. Therefore, several groups have attempted to generate transgenic models of AD, soon after the isolation of the APP gene (Higgins et al., 1993; Mucke et al., 1994; Quon et al., 1991; Sandhu et al., 1991).

<u>APP and PS transgenic models.</u> The first successful model to reproduce Aβ pathology was the PDAPP mice, which overexpress the human APP minigene encoding for APP_{V717F} under the control of the PDGF promoter (Games et al., 1995). The overexpression levels of the human APP were more than 10-fold over endogenous mouse APP levels, and this probably contributed to their success in reproducing Aβ pathology. These mice develop age-dependent Aβ deposits, which start around 6-9 months of age in the hippocampus, corpus callosum and cerebral cortex. The PDAPP mice also develop neuritic plaques, synaptic loss, astrocytosis and microgliosis (Games et al., 1995). Moreover, they show a behavioral deficit in the radial-maze, Morris water-

maze and object-recognition tasks (Chen et al., 2000; Dodart et al., 1999) Another mouse-model (Tg2576) was subsequently developed by overexpressing human APP_{695} containing the Swedish double mutation (K670N, M671L) under the control of the PrP (Hsiao et al., 1996). The Tg2576 mice overexpress APP to about 6-fold over endogenous levels, develop all the AD-like pathology observed in the PDAPP mice starting around 9-10 months; they also develop an age-dependent memory deficit tested by the water-maze paradigm (Hsiao et al., 1996; Westerman et al., 2002).

Other groups subsequently developed models showing AD-like pathology by overexpressing the APP gene (Calhoun et al., 1999; Chishti et al., 2001; Davis et al., 2004; Moechars et al., 1999; Mucke et al., 2000; Sturchler-Pierrat et al., 1997). The majority of these animal models develop Aβ pathology, dystrophic neurites and cognitive impairments (Phinney et al., 2003). However, they do not develop NFT nor do they have appreciable cell loss. This is surprising because a single mutation in the APP, PS1 or PS2 genes leads to the development of the full spectrum of AD neuropathology, in humans. Curiously, mice harboring an FAD mutation in PS1 and/or PS2 do not develop plaques (see for example (Chui et al., 1999; Duff et al., 1996; Guo et al., 1999) but show an increase in $A\beta_{42}$ levels. Double transgenic mice have been generated by crossing APP and PS1 transgenic mice (see for example (Borchelt et al., 1997; Holcomb et al., 1998)). The common observation in these double transgenic mice is that Aβ deposition is accelerated compared to single APP transgenic mice. Remarkably, despite the increase and early onset in Aβ accumulation in the double transgenic mice, they still do not develop NFT. Several reasons might account for the lack of NFT in these models. For example, it is possible that mice do not live long enough to develop NFT or that the mouse tau gene is somehow protective (Andorfer et al., 2003).

Tau transgenic models. The major component of NFT is hyperphosphorylated tau. Mutations in

the tau gene lead to FTDP-17 (Hutton et al., 1998), a disorder characterized by tangle accumulation in brain regions that are also affected in AD cases. The FTDP-17 patients do not develop any Aβ pathology, suggesting that tau pathology is not likely the factor that triggers AD pathology, but may lead to neurodegeneration downstream of Aβ. Moreover, these cases show that tau pathology can be induced by other factors independent from Aβ.

To better study NFT formation and their involvement in neurodegenerative disease, different groups have generated transgenic models overexpressing human tau_{P301L}, a mutation known to cause FTDP-17. In 2000, Nature Genetics published the characterization of the first transgenic model harboring the human tau_{P301} under the control of prion promoter (Lewis et al., 2000). These mice accumulate NFT in different areas of the brain stem and spinal cord, leading to a profound motor deficit and early death (Lewis et al., 2000). Considering the motor deficit and early mortality that occurs in these mice, their utility for studying neurodegenerative disorders, such as AD or FTDP-17 has been limited. Another group overexpressed the human tau_{P301L} using the Thy1.2 promoter (Gotz et al., 2001a). These mice accumulate NFT in the CA1 region of the hippocampus and in the neocortex. Apoptotic cells were also present in selected areas of the somatosensory cortex (Gotz et al., 2001a). No reports of cognitive impairments in neither of these two transgenic mice are present in the literature.

It is clear that high levels of Aβ in mice do not lead to tau pathology, and likewise high levels of tau pathology do not lead to Aβ pathology. Consequently, to obtain a model with both plaques and tangles, it is necessary to use strategies that are more aggressive. Toward this goal, two major approaches have been used: microinjecting pathological protein into the brains of single transgenic mice (Gotz et al., 2001b) or crossing individual transgenic mice harboring APP and tau mutations (Lewis et al., 2000).

Gotz *et al.* showed that injection of fibrillar Aβ into the somatosensory cortex of transgenic mice overexpressing human tau_{P301L} caused a 5-fold increase in NFT in the amygdala. By injecting a retrograde tracer in the somatosensory cortex, they showed that the affected neurons in the amygdala project to the injected area. This finding suggests that synaptic damage due to Aβ accumulation can induce NFT in the cell bodies. They also concluded that Aβ can accelerate NFT formation, although no other reports have yet been published that replicate these findings.

Using a different approach, Lewis *et al.* (2001) arrived at similar conclusions. They crossed two independent transgenic lines, one overexpressing mutant APP and the other overexpressing mutant tau. The double transgenic mice developed Aβ pathology at the same age as the single APP transgenic mice but showed enhanced tau pathology. This led the authors to conclude that either APP or Aβ influences tau pathology *in vivo*. However, other conclusions might explain their results. For instance, it has been shown that the genetic background of mice can modulate pathological events such as susceptibility to excitotoxic cell death in transgenic mice (Schauwecker and Steward, 1997; Steward et al., 1999). By crossing mice of different genetic backgrounds, Lewis *et al*. generated a new set of mice where the genetic background was different compared to the parental strain. This might have changed the susceptibility of specific neurons to tau pathology or altered the expression patter of the transgene. Moreover, these mice show a profound motor deficit due to extensive pathology in the brain stem. This deficit and the fact that the mice die prematurely make this model unsuitable for any behavior or immunological studies. Therefore, other animal models with both plaques and tangles in AD-affected brain regions, without the confounding variable of mixing different genetic backgrounds, still need to be derived.

3xTg-AD mice. The development of both plaques and tangles is necessary in a model of AD. The 3xTg-AD mice develop age- and region-dependent accumulation of plaques and tangles (Oddo et al., 2003b). These transgenic mice harbor three mutant human genes, APP_{Swe}, Tau_{P301L}, and $PSN1_{M146V}$. One of the earliest neuropathological manifestation in the 3xTg-AD mice is the accumulation of intraneuronal Aβ, which is detected in the hippocampus as earlier as four to five months of age (Oddo et al., 2003b), and correlates with the onset of cognitive deficits (Billings et al., 2005). Extracellular plaques appear by 12 months in the entorhinal cortex and become more widespread in the hippocampus and in the cortex by 14 months. Accumulation of tau occur in the hippocampus by 8 months of age and became aggregated and hyperphosphorylated and it is detectable in cortex as well (Oddo et al., 2003b; Oddo et al., 2008). Synaptic dysfunction, LTP deficits and cognitive impairment occur before the accumulation of plaques and tangles. The presence of both lesions is critical to study the molecular interaction between plaques and tangles and to test the efficacy of anti-Alzheimer treatments on both pathologies.

1.1.7 Aβ and tau interaction

One major hypothesis for AD is the amyloid cascade hypothesis (Hardy and Selkoe, 2002; Hardy and Higgins, 1992; Selkoe, 1991), which stipulates that Aβ is the trigger of all cases of AD, and tau pathology is a consequence of the Aβ pathology. In other words, it proposes the existence of a link (direct or indirect) between Aβ and tau, where Aβ is the trigger of a cascade of events that lead to the accumulation of NFT that are then responsible for the cell death observed in AD (Hardy, 2003). Different studies have supported the amyloid cascade hypothesis reaffirming the idea of a direct link between Aβ and tau. However, the molecular mechanisms linking the two pathologies are yet not understood. In the previous section, I referred to some *in vivo* evidence produced by us and other groups supporting this interaction (Gotz et al., 2001b; Lewis et al., 2001; Oddo et al., 2003a; Oddo et al., 2003b). Here I will analyze some of the *in vitro* data supporting

this interaction.

Several reports have shown that Aβ is toxic to primary rat and human neuron cultures (Busciglio et al., 1993; Pike et al., 1992; Yankner et al., 1989) and some of them have suggested that tau maybe a possible downstream mediator of Aβ toxicity (Alvarez et al., 1999; Busciglio et al., 1995; Takashima et al., 1993). Takashima and colleagues published the first report for a possible role of tau in Aβ-induced pathology. They showed that treatment of primary hippocampal cultures with Aβ causes an increase in the activity of TPK1 (a GSK3β homologous) that correlates with the Aβ-induced neurotoxicity. More interestingly, TPK1 antisense oligonucleotides protect these neurons from Aβ-induced toxicity (Takashima et al., 1993). Considering that Aβ-treated neurons were also positive for Alz50, a conformational specific tau antibody, (Yankner et al., 1989) and that TPK 1 has been involved in the phosphorylation of tau (Ishiguro et al., 1988; Ishiguro et al., 1992), this study implies that Aβ can induce tau pathology. The involvement of TPK 1 / GSK3β in Aβ-induced toxicity has been confirmed by other studies (Hoshi et al., 2003; Hoshi et al., 1996; Imahori and Uchida, 1997).

CDK5 is another key enzyme implicated in tau phosphorylation (Alvarez et al., 2001; Alvarez et al., 1999; Lee et al., 1999; Patrick et al., 1999). The activity of CDK5 is regulated by a small peptide of 35 amino acids (p35), which binds to CDK5 and activates it (Patrick et al., 1999). Proteolytic cleavage of p35 by calpain (a calcium-dependent protease) leads to the formation of a truncated peptide of 25 amino acids (p25), which binds to CDK5 causing its unregulated activation (Patrick et al., 1999). Primary hippocampal neurons treated with Aβ show increased CDK5 activity as well as cell death (Alvarez et al., 1999). When a CDK5 inhibitor or CDK5 antisense oligonucleotides are added to the Aβ-treated neurons, they partially rescue the Aβ-induced cell death (Alvarez et al., 1999). The mechanism by which Aβ increases the activity of

CDK5 is not fully understood. Increases in intracellular Ca^{2+}, which can be caused by Aβ or FAD mutations (LaFerla, 2002; Leissring et al., 2001; Leissring et al., 1999a; Leissring et al., 1999b; Mattson et al., 1992), has been proposed to be the upstream event leading to increased CDK5 activity. The raise in intracellular Ca^{2+} concentration activates calpain, which in turn produces more p25 (Lee et al., 2000; Patrick et al., 1999) eventually leading to higher CDK5 activity and more tau phosphorylation.

Taken together, these studies show that Aβ can enhance the activity of different kinases that phosphorylate tau. It is still possible, however, that tau phosphorylation could be an epiphenomenon, and all these activated kinases are toxic to the neurons by other pathways independent of tau phosphorylation. The direct evidence that tau is actually necessary for Aβ-induced toxicity has been shown using tau knock-out mice. Treatment of hippocampal neurons from tau null mice with fibrillar Aβ did not produce signs of degeneration, whereas neurons from wild-type mice or from mice expressing human tau show profound signs of neurites degeneration within 24 hours of treatment and they die after 96 hours (Rapoport et al., 2002). Moreover, neurons from human tau transgenic mice generated in a tau null background reacquired their susceptibility to Aβ showing the same signs of degeneration as wild-type mice (Rapoport et al., 2002).

It is well established that different factors, including Aβ, can induce apoptosis in both AD and transgenic mice (Gervais et al., 1999; LaFerla et al., 1995; Nakagawa et al., 2000; Rohn et al., 2001; Su et al., 1994; Troy et al., 2000; Zhao et al., 2003). Incubation of primary neurons with fibrillar Aβ induces activation of caspase 3, which can cleave tau removing 20 amino acids from its C-terminal (Gamblin et al., 2003; Rissman et al., 2004). *In vitro* studies show that the N-terminal portion of this truncated form of tau (delta-au) forms filaments more rapidly in vitro that

full-length tau (Gamblin et al., 2003; Rissman et al., 2004). Moreover, when tau is incubated in the presence of small amount of delta-tau, filament formation is greatly increased (Rissman et al., 2004). Delta-tau is also present in NFT that accumulate in AD and transgenic mice (Gamblin et al., 2003; Novak et al., 1993; Rissman et al., 2004) and inversely correlate with cognitive function (Rissman et al., 2004). These data identify a new link between Aβ and tau that is independent of the tau kinases, although it remains to be established if hyperphosphorylated tau is a better substrate for these caspases. If this turns out to be the case, the increase in CDK5 and GSK3β activity, due to Aβ, could facilitate the assembly of tau in NFT.

1.2 THE MAMMALIAN TARGET OF RAPAMYCIN

The mammalian target of rapamyicn (mTOR) is a serine/threonine-protein kinase, which is involved in the regulation of both protein synthesis and degradation, longevity, and cytoskeletal formation (Johnson et al., 2013; Wullschleger et al., 2006). mTOR is the key catalytic unit of two separate large multimeric protein complexes, mTOR complex 1 (mTORC1) and 2 (mTORC2; Fig. 3).

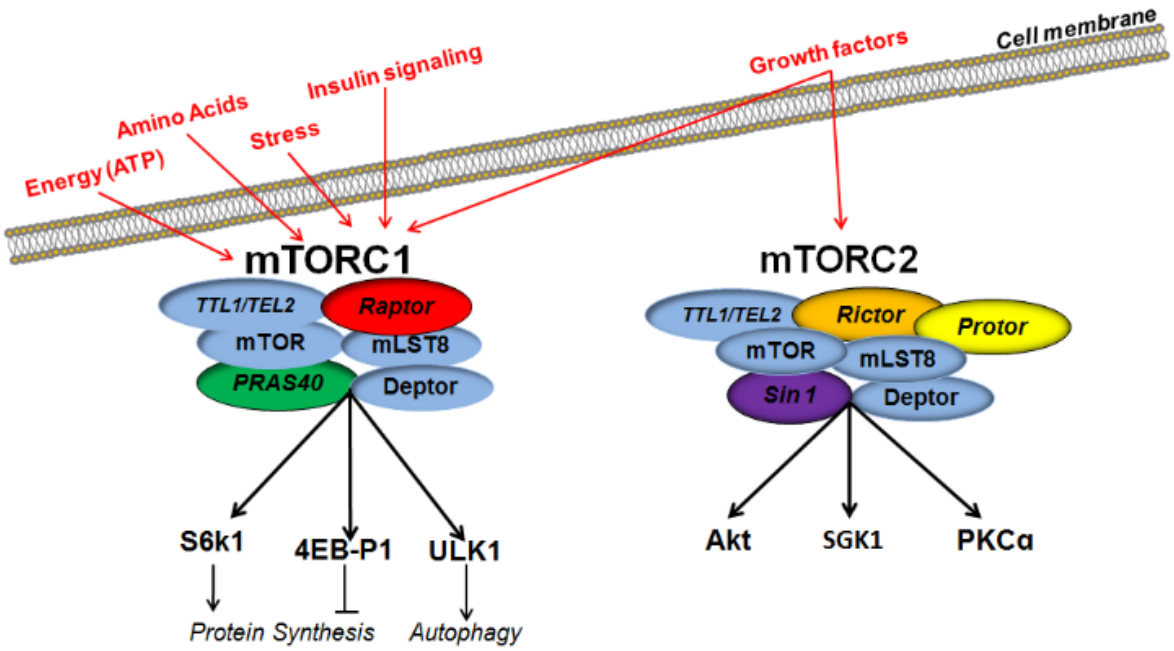

Figure 3. The mTORC1 vs. mTORC2 have distinct constituent proteins and regulate different downstream targets. Both mTORC1 and mTORC2 share the catalytic mTOR subunit, the mammalian lethal with sec-13 protein 8 (mLST8), the Tti1 and Tel2 complex, and the DEP domain containing mTOR-interacting protein (deptor), all depicted in blue. The mTORC1 contains the rapamycin sensitive raptor subunit (depicted in red) and the proline-rich Akt substrate 40 KDa (PRAS40; depicted in green). Downstream effectors ribosomal protein S6 kinase beta-1 (S6K1) and eukaryotic translation initiation factor 4E-binding protein 1 (4EBP1) play a critical role in protein translation by regulating the activation of initiation factors. Inhibition of mTORC1 decreases the phosphorylation of ULK1, which initiates the sequential activation of several autophagy-related proteins, culminating in the formation of AVs. In contrast, the mTORC2 contains the rictor subunit (depicted in orange), the protor component (depicted in yellow), and the mammalian stress-activated map kinase-interacting protein 1 (sin1; depicted in purple). Downstream effectors of mTORC2 are involved in regulating longevity, cellular stress response and cytoskeletal dynamics. The mTORC1 receives signals from growth factors, glucose, inflammatory cell signaling proteins and extracellular amino acids. The mTORC2 receives signals primarily from growth factors.

mTORC1 consist of mTOR, raptor, the mammalian lethal with sec-18 protein 8 (mLSTR8), the Dep domain containing mTOR interacting protein (Deptor), the Tti1/Tel2 complex, and the proline-rich Akt substrate 40 KDa (PRAS40) (Wullschleger et al., 2006). mTORC2 consist of mTOR, rictor, mLSTR8, deptor, Tti1/Tel2, and mammalian stress-activated map kinase-interacting protein 1 (Gingras et al., 1999). mTORC1 is regulated by signaling from insulin, growth factors, amino acids, and oxidative stress (Hay and Sonenberg, 2004). It promotes cell growth and proliferation (by facilitating mRNA translation and protein synthesis), lipid biogenesis, regulates mitochondrial metabolism, and modulates autophagy (Kim and Guan, 2015; Perluigi et al., 2015; Wang and Proud, 2006). In contrast, mTORC2 appears to be strictly under control of growth factors and it is thought to function primarily in cytoskeleton assembly and cell size (Frias et al., 2006; Graber et al., 2013). Both mTORC1 and mTORC2 are involved the regulation of longevity (Hay and Sonenberg, 2004; Johnson et al., 2013).

mTORC1 regulates protein translation mainly by controlling the activity of ribosomal protein S6 kinase-1 (S6K1) and eukaryotic initiation factor 4E binding protein 1 (4EBP1), which directly control the activity of several initiation factors (Gingras et al., 1999; Hands et al., 2009; Hay and Sonenberg, 2004; Ruvinsky and Meyuhas, 2006). Malnutrition, stress, insulin, growth factors, and various other signaling pathways that converge on mTOR may differentially activate/inhibit protein synthesis (Gingras et al., 1999; Hay and Sonenberg, 2004).

1.2.1 mTOR in aging

The first evidence of TOR's involvement in aging came from work conducted in *S. cerevisiae*. Deletion of the gene encoding the yeast orthologue of S6K1 resulted in a doubling of the chronological lifespan(Fabrizio et al., 2001). Shortly after, inhibition of raptor or S6K1 was shown to extend lifespan in *C. elegans* (Jia et al., 2004; Vellai et al., 2003). These initial studies have been confirmed and expanded to other species (Johnson et al., 2013; Kapahi et al., 2004). To

this end, a landmark report showed that rapamycin, an mTOR inhibitor, fed to genetically heterogeneous mice, increased their lifespan (Harrison et al., 2009). The involvement of mTOR in regulating lifespan in mammals has also been shown using two independent genetic approaches. The first one highlighted that deletion of S6K1, a downstream target of mTOR, extends lifespan and healthspan in both male and female mice by ~9% (Selman et al., 2009). The second report found that mice with two hypomorphic alleles that reduce mTOR expression by 25% compared to wild type levels showed an ~20% increased the median lifespan (Wu et al., 2013). Notably, complete inhibition of TOR signaling during development leads to premature lethality (Montagne et al., 1999; Murakami et al., 2004; Oldham et al., 2000), indicating that TOR signaling is an important and evolutionarily conserved regulator of longevity, which operates within a narrow range in order to maintain homeostasis and health. The role of mTOR in aging has been extensively discussed elsewhere (Johnson et al., 2013; Richardson et al., 2014).

1.2.2 mTOR, cognition, and brain aging

mTOR is highly expressed throughout the brain, primarily in neurons, but it is also found in astrocytes (Li et al., 2015; Meijer et al., 2014). In addition to regulating brain energy levels, mTOR is linked to synaptic plasticity and cognition (Graber et al., 2013; Perluigi et al., 2015; Tang et al., 2002). For example, mTOR activity is necessary for the expression of the late-phase of long-term potentiation (LTP) in the hippocampus, by modulating *de novo* protein synthesis after LTP induction (Cammalleri et al., 2003; Tang et al., 2002). In addition, mTOR coordinates the timing and location for the synthesis of new proteins (Cammalleri et al., 2003; Tang et al., 2002). A critical role for mTOR in cognition has also been shown by conditionally removing rictor, and therefore mTORC2 activity, from excitatory neurons in limbic and cortical regions after development (Huang et al., 2013). These conditional rictor knockout mice, which still have a fully functional mTORC1, are incapable of establishing LTP and consequently show cognitive deficits

(Huang et al., 2013). There deficits appear mediated by alterations in actin-dynamics which are known to regulate the growth of dendritic spines necessary for memory formation (Huang et al., 2013).

While mTOR activity is necessary for normal cognition, mTOR hyperactivity is also detrimental to brain function. The primary evidence comes from clinical cases of tuberous sclerosis (TSC), in which mTOR hyperactivity leads to cognitive deficits (Ehninger et al., 2009). Consistent with these observations, mTOR hyperactivity in mouse models of TSC is linked to synaptic and cognitive deficits (Ehninger et al., 2008). Mechanistically, the cognitive deficits in these mice are mediated by an inability to maintain late-phase LTP, which is regulated by mTOR activity (Cammalleri et al., 2003; Tang et al., 2002). Interestingly, reducing mTOR activity via a two-week administration of rapamycin ameliorates synaptic and cognitive deficits in TSC mice (Ehninger et al., 2008). The link between hyperactive mTOR signaling and cognitive dysfunction has been widely confirmed by others (Costa-Mattioli and Monteggia, 2013; Ricciardi et al., 2011). Currently, there are ongoing clinical trials aimed at determining whether reducing mTOR activity with everolimus and sirolimus (two rapamycin analogs) ameliorates different aspects of TSC symptoms, including brain mTOR hyperactivity and cortical hyperexcitability (ClinicalTrials.gov Identifiers**:** NCT02451696 and NCT00490789). mTOR is also hyperactive in developmental disorders, such as Down syndrome, Rett syndrome, and fragile X syndrome (Troca-Marin et al., 2012)

mTOR also plays a role in cognitive decline associated with aging. To this end, life-long rapamycin administration ameliorates age-dependent spatial memory deficits in C57Bl/6 mice (Majumder et al., 2012). These rapamycin-mediated improvements were associated with decreased mTOR signaling and brain inflammation, as well as increased hippocampal NMDA signaling (Majumder et al., 2012). Notably, in the same study, mice that were given rapamycin at 15 months of age for three months show no detectable changes in cognitive functions (Majumder et al., 2012). These

findings have been confirmed by independent studies, which suggest that in addition to cognition, rapamycin also improves anxiety-related behaviors (Halloran et al., 2012; Kolosova et al., 2013). Further, the age-dependent decrease in autophagy function may lead to increased protein accumulation, which may interfere with normal brain funciton (Hands et al., 2009; Jung et al., 2010; Martinez-Lopez et al., 2015; Rubinsztein et al., 2011). Inhibition of mTOR increases autophagy induciton, which presumably maintains cellular function during aging by counteracting the age-dependent protein accumulation. Given the role of mTOR in several signaling pathways, it is plausible that multiple molecular mechanisms might link the reduction of mTOR signaling to improvements in age-dependent cognitive function. Future studies are necessary to establish why reducing mTOR signaling in older mice has no effects on cognition. It is tempting to speculate that there is a critical period of time before, but not after which, changes in brain function that occur during aging can be mitigated by reducing mTOR. Identifying why some age-dependent changes in brain function are reversible and others are not, may have long-lasting effects on the field's understanding of age-dependent cognitive deficits.

1.3 mTOR and Alzheimer's disease

1.3.1 mTOR signaling in AD brains. Disruption of mTOR signaling in the brain affects multiple pathways including glucose metabolism, cell growth and autophagy, all crucial players in age-related cognitive disorders such as Alzheimer disease. Studies done with postmortem human AD brains show that the levels of phospho-mTOR and two of its downstream targets, p70S6K and the eukaryotic translation factor 4E (eIF4E) are increased compared to age-matched control cases, suggesting that mTOR is hyperactive in AD (Oddo, 2012). Immunohistochemical and biochemical study of postmortem AD brain showed that phosphorylated p70S6K levels were significantly higher in AD brains and correlated with Braak's stage and the levels of total and PHF-tau. Interestingly the levels of activated p70S6K are higher in neurons that are known to later develop NFTs (Pei and Hugon, 2008). In addition, phosphorylated eIF4E levels were found to be

100-fold higher in AD brains compared to age-matched controls. These study highlighted increase in mTOR could mediate an up-regulation of tau and mTOR activity is elevated in AD brains. In another study from the same group, it has been reported that there is a 3-fold increase in phosphorylated mTOR in the medial temporal cortex of AD cases compared to control cases (Li et al., 2005), which correlates with increased mTOR activity. These studies show that mTOR signaling is augmented in AD brains, and these conclusions are further supported by other studies of human brains (Chang et al., 2002; Onuki et al., 2004; Peel and Bredesen, 2003), and in animal models (Caccamo et al., 2010b; Caccamo et al., 2011b; Khurana et al., 2006; Lin et al., 2013).

1.3.2 Aβ and mTOR. The relationship between Aβ and mTOR has been extensively studied *in vitro* and *in vivo* and a complex picture has emerged. Early *in vitro* reports showed that exposure of mouse neuroblastoma cells to 20 μM Aβ42 for 24 hours was sufficient to decrease mTOR signaling (Lafay-Chebassier et al., 2005). However, when applied at lower and more physiological concentrations, Aβ has the opposite effects on mTOR signaling. For example, mTOR is upregulated in Chinese hamster ovary (CHO) cells and mouse neuroblastoma cells (N2A) stably transfected with mutant APP (Caccamo et al., 2010a; Zhou et al., 2008). mTOR hyperactivity was also induced in wild type N2A cells by application of Aβ25-35 (Zhou et al., 2008). In mutant CHO cells, which are known to secrete low concentration of low molecular weight Aβ oligomers(Koo and Squazzo, 1994), the effects on mTOR were prevented by blocking Aβ production(Caccamo et al., 2010a). Consistent with these findings, intrahippocampal injection of naturally secreted Aβ oligomers was sufficient to increase mTOR signaling in the brains of wild type mice (Caccamo et al., 2011a).

Work in transgenic mice has also generated conflicting results. To this end, it has been reported that 12-month-old APP/PS1 mice have lower mTOR signaling than age-matched wild type mice (Lafay-Chebassier et al., 2005), which directly contradicts an earlier report showing hyperactive mTOR signaling in 9-month-old APP/PS1 mice (Zhou et al., 2008). In Tg2576 mice, mTOR signaling is down-regulated in young pre-pathological mice. In contrast, in aged Tg2575 mice with established Aβ pathology, mTOR activity is similar to age-matched wild type mice (Ma et al., 2010). We have shown an age- and regional-dependent increase in mTOR signaling in 3xTg-AD mice (Caccamo et al., 2010a; Caccamo et al., 2011a). Notably, genetically or immunologically preventing Aβ accumulation was sufficient to reduce mTOR signaling to wild type levels, indicating that mTOR hyperactivity was due to Aβ accumulation (Caccamo et al., 2011a). The results in the 3xTg-AD mice are in agreement with studies in postmortem human AD brains, which consistently show an upregulation of mTOR signaling (An et al., 2003; Chang et al., 2002; Griffin et al., 2005; Onuki et al., 2004; Pei et al., 2008; Tramutola et al., 2015).

While the mechanisms by which Aβ alters mTOR activity remain elusive, confocal microscopy data showed a direct interaction between intraneuronal $A\beta_{42}$ and mTOR (Ma et al., 2010). Furthermore, the Aβ-mediated increase in mTOR activity can be prevented by blocking the phosphorylation of PRAS40, suggesting that the build-up of Aβ may facilitate PRAS40 phosphorylation (Caccamo et al., 2011a). Consistent with this observation, the steady-state levels of phosphorylated PRAS40 were significantly higher in the brains of 3xTg-AD mice (Caccamo et al., 2011a). In summary, a large body of evidence suggests a direct or indirect interaction between Aβ and mTOR; however, this picture is complex as both *in vivo* and *in vitro* work have often revealed opposite effects. While it is hard to dissect the causes explaining these divergent effects, strain and age of the mice, as well as different levels of Aβ can have differential effects on mTOR. For example, mTOR hyperactivity in 3xTg-AD mice precedes the formation of Aβ plaques and it is most likely due to high soluble Aβ levels (Caccamo et al., 2010a). In contrast, in APP/PS1 mice

mTOR hyperactivity has been reported when the mice have widespread Aβ plaque deposits throughout the brain (Lafay-Chebassier et al., 2005).

Recent evidence suggests that, just as Aβ affects mTOR, mTOR also affects Aβ (Oddo, 2012), indicating that the two proteins interact closely with one another. Elucidating the mechanism(s) of this interaction may reveal previously unknown aspects of AD pathogenesis. The first *in vivo* evidence indicating that modulation of mTOR signaling had a direct effect on Aβ pathology came from pharmacological studies using 3xTg-AD mice. Specifically, 3xTg-AD and wild type mice were given rapamycin starting at the onset of cognitive deficits, for 10 weeks (Caccamo et al., 2010a). Rapamycin restored the hyperactive mTOR signaling in 3xTg-AD mice to control levels, rescued cognitive deficits, and decreased Aβ and tau pathology (Caccamo et al., 2010a). This study highlighted a crosstalk between Aβ and mTOR as it demonstrated that reducing high levels of mTOR activity reduced Aβ deposition, just as the application of Aβ increase mTOR activity. Consistent with this finding, reducing mTOR signaling by rapamycin or temsirolimus, ameliorated AD-like pathology and cognitive deficits in hAPP(J20) mice or in APP/PS1 mice, respectively (Jiang et al., 2014; Spilman et al., 2010). Further, rapamycin also reduced the formation of Aβ plaques and tangles when administered prior to their formation (Majumder et al., 2011). Conversely, administration of rapamycin to 15-month-old 3xTg-AD mice, with established AD-like neuropathology, had no effect on cognitive deficits or plaque and tangle load (Majumder et al., 2011). The rapamycin-mediated reduction in AD neuropathology was linked to an increase in autophagy induction (Caccamo et al., 2010a; Majumder et al., 2011), which may explain why rapamycin administration to mice with established pathology does not decrease Aβ or tau pathology. To this end, elegant work by the Nixon laboratory has shown that AVs accumulate in human AD brains as well as in a mouse model of AD, suggesting a deficit in their clearance (Boland et al., 2008; Yu et al., 2005). Consistent with this theory, inducing autophagy after the deficit in autophagy flux occurs (most likely following AD-like neuropathology) would simply

increase AV formation, which would fail to fuse to lysosomes for content degradation (Nixon and Yang, 2011a; Oddo, 2012). Indeed, compelling evidence suggests that substrate-filled AVs drastically accumulate in AD and animal models (Boland et al., 2008; Majumder et al., 2011; Yu et al., 2005). Thus, increasing autophagy induction (e.g., by rapamycin) may further lead to the accumulation of AVs, which may exacerbate AD pathogenesis as Aβ can be generated in and released from these vesicles (Nixon and Yang, 2011a).

1.3.3 Tau and mTOR. The evidence linking mTOR to tau is less controversial and several laboratories have consistently shown that hyperactive mTOR contributes to tau pathology. In postmortem human AD brains, hyperactive mTOR signaling was found in neurons that were predicted to develop tau pathology (An et al., 2003). Work in animal models has confirmed and expanded on this initial observation. Hyperactive TOR in *Drosophila* facilitates the development of tau pathology and the associated neurodegeneration (Khurana et al., 2006). Consistent with these observations, blocking TOR signaling rescued tau-induced toxicity, while genetically increasing TOR signaling enhanced tau-induced toxicity in *Drosophila* (Steinhilb et al., 2007). We have reported that mice with hyperactive mTOR also have increased brain levels of total and phosphorylated tau (Caccamo et al., 2013). Conversely, reducing mTOR has beneficial effects on tau pathology. To this end, reducing mTOR with rapamcyin in a transgenic mouse expressing mutant human tau decreased tau pathology and improved the associated motor deficits (Caccamo et al., 2013). Similar to these observations, chronic treatment with the rapamycin ester CCI-779/Temsirolimus in Tg30 mutant tau mice, decreased mTOR signaling, stimulated autophagy, reduced tau levels and NFT density, which led to an attenution of motor deficits (Frederick et al., 2014).

The mechanism underlying these observations is likely multifactorial. For example, hyperactive mTOR signaling decreased autophagy turnover, which is a known degradation pathway for tau (Lee et al., 2013; Wang and Mandelkow, 2012). mTOR can also regulate tau levels by increasing translation of its mRNA. Indeed, direct evidence from primary hippocampal neurons showed that inhibition of mTOR by rapamycin suppresses tau translation, while constitutively active mTOR signaling increased tau translation (Morita and Sobue, 2009). In addition, mTOR can directly regulate tau phosphorylation. To this end, mTOR and S6K1 phosphorylate tau at multiple residues (Pei et al., 2006; Tang et al., 2013; Tang et al., 2015). mTOR also suppresses the activity of the protein phosphatase 2A, an enzyme known to remove phosphate groups from tau (Liu and Gotz, 2013; Wullschleger et al., 2006). One startling implication of these observations is that long-term exposure to hyperactive mTOR might increase tau translation and decrease its degradation/turnover, while concomitantly increasing tau phosphorylation. Collectively, these studies highlight multiple pathways by which mTOR signaling contributes to tau pathology.

1.3.4 Autophagy, mTOR and AD. The autophagic system is a conserved intracellular system designed for the degradation of long-lived proteins and organelles in lysosomes (Cuervo, 2004; Jung et al., 2009; Klionsky and Emr, 2000). Three types of autophagy have been described: macroautophagy, microautophagy, and chaperon-mediated autophagy (CMA). While macro- and microautophagy involve the “in bulk” degradation of regions of the cytosol, CMA is a more selective pathway, and only proteins with a lysosomal targeting sequence are degraded (Cuervo, 2004; Klionsky and Emr, 2000; Majeski and Dice, 2004). Cumulative evidence suggests that an age-dependent decrease in the autophagy/lysosome system may account for the accumulation of abnormal proteins during aging (Cuervo et al., 2005).

Macroautophagy (herein referred to as autophagy) is induced when an isolation membrane is generated surrounding cytosolic components, forming an autophagic vacuole that will eventually

fuse with lysosomes for protein/organelle degradation (Cuervo, 2004). Although the molecular mechanisms underlying autophagy induction are not completely understood, an important step in the autophagosome formation is the activation of LC3-I. After its activation, LC3-I is lipidated to form membrane-associated LC3-II, which is incorporated in the growing autophagosome membrane and is often used as a marker of autophagy induction (Kabeya et al., 2000; Tanida et al., 2005). Overall, mTOR negatively regulates autophagy by interfering with its induction (Diaz-Troya et al., 2008).

Several neurodegenerative disorders are characterized by the abnormal accumulation of aggregated proteins and are collectively known as proteinopathies. Based on this premise, it has been suggested that alterations in the cellular quality control system, such autophagy, may be involved in disease pathogenesis (Caccamo et al., 2009; Li et al., 2008; McCray and Taylor, 2008; Nedelsky et al., 2008; Oddo, 2008; Rubinsztein, 2006). Furthermore, the autophagy function decreases with age (the major risk factor for AD and other neurodegenerative disorders), suggesting therefore that the age-dependent decrease in the autophagy function may contribute to the chronic buildup of aggregates in neurons (Cuervo et al., 2005; Martinez-Vicente and Cuervo, 2007). Indeed, genetically reducing autophagy induction leads to profound neurodegeneration and cell loss associated with the accumulation of ubiquitinated inclusions (Hara et al., 2006; Komatsu et al., 2006; Komatsu et al., 2007). Consequently, it has been proposed that inducing autophagy may have beneficial effects in a variety of neurodegenerative disorders (e.g., Berger et al., 2006; Fornai et al., 2008; Ouellet et al., 2009; Pandey et al., 2007; Ravikumar et al., 2004; Rubinsztein, 2006; Shao and Diamond, 2007; Yu et al., 2009).

The role of autophagy in AD is not well understood and contradicting reports have been published. For example, it has been reported that autophagic vacuoles accumulate in AD brains and in APP/PS1 transgenic mice, and this vacuoles maybe a source of Aβ production, suggesting that

an increase in autophagy induction may lead to a further accumulation of Aβ (Boland et al., 2008; Lafay-Chebassier et al., 2005; Yu et al., 2005). In contrast, other reports show that autophagy protects neurons from Aβ toxicity (Caccamo et al., 2010b; Hung et al., 2009; Ling and Salvaterra, 2009; Ling et al., 2009; Pickford et al., 2008; Spilman et al., 2010). Along these lines, Wyss-Coray and colleagues showed that beclin-1 levels, a key protein involved in autophagy induction, were decreased in AD patients (Pickford et al., 2008). Furthermore, using complementary genetic approaches, the authors showed that decreasing beclin-1 expression in a transgenic mouse model of AD, decreased autophagy induction and increased Aβ accumulation (Pickford et al., 2008). In contrast, increasing beclin-1 expression in the same mice, increased autophagy induction and reduced intracellular and extracellular Aβ pathology (Pickford et al., 2008), clearly indicating that increasing autophagy induction may be beneficial in AD. More recently, it has been shown that parkin mediates the beclin-dependent autophagic clearance of Aβ (Khandelwal et al., 2011).

We have shown that pharmacologically reducing mTOR hyperactivity in the brains of the 3xTg-AD mice led to a reduction in soluble Aβ and tau levels (Caccamo et al., 2010b). The effects of rapamycin appear to be mediated by an increase in autophagy induction as we showed that in the brains of rapamycin-treated 3xTg-AD mice there was a significant increase in LC3II and other autophagy related proteins, including Atg5, Atg7 and Atg12 (Caccamo et al., 2010b). Supporting this view, autophagy induction correlated with the decrease in Aβ levels in another mouse model of AD (Spilman et al., 2010). Furthermore, in cell culture experiments, we directly showed that autophagy induction was necessary for the rapamycin-mediated decrease in Aβ levels (Caccamo et al., 2010b). A recent report by Paul Greengard's group shows that inducing autophagy by small-molecule enhancer of rapamycin in immortalized cell lines and primary neurons led to an 80% reduction in $Abeta_{40}$ and $Abeta_{42}$ levels (Tian et al., 2011). These data were further supported by recent work showing that genetically increasing autophagic protein turnover ameliorates Aβ

pathology and the associated cognitive decline in a mouse model of AD (Yang et al., 2011). There is an apparent contradiction between the data reported by Nixon and colleagues, who showed that autophagic vacuoles accumulates in AD due to impaired clearance, suggesting that further increase in autophagy may exacerbate the pathology (Yu et al., 2005), and what we and others recently reported, increasing autophagy induction has beneficial effects on AD-like pathology in different animal model of AD (Caccamo et al., 2010b; Pickford et al., 2008; Spilman et al., 2010; Tian et al., 2011). Although the basis of this apparent inconsistency remains to be established, it is tempting to speculate that the relationship between autophagy and Aβ may change with the progression of the disease. At earlier stages of Aβ accumulation, induction of autophagy may facilitate its clearance. As the disease progresses, deficiencies in the clearance of autophagic vacuoles may occur and thus further increasing autophagy may exacerbate the AD phenotype. Indeed, the majority of the studies showing that increasing autophagy induction reduces Aβ and tau accumulation were done in animals with early stages pathology. Thus, when considering the role of mTOR in Aβ and tau pathology and the role of mTOR in autophagy induction, it will be important to determine the effect of increasing autophagy function in mice with established plaques and tangles.

2 AIM OF THE WORK

The lack of effective cures or treatments for Alzheimer's disease (AD) is alarming considering the number of people currently affected by this disorder and the projected increase in incidence and prevalence over the next two decades. Aging is the major risk factor associated with the development of AD; thus, it is plausible that alterations in selective pathways associated with aging may facilitate the development of this insidious disorder (Moll et al., 2014). Overwhelming evidence shows that reducing the activity of the mammalian target of rapamycin (mTOR) increases lifespan and health-span in several genetically different species (Lamming et al., 2013). mTOR is a ubiquitously expressed protein kinase that plays a key role in regulating protein synthesis and cell growth by phosphorylating downstream proteins such as p70 S6 kinase and eukaryotic initiation factor eIF4E binding protein (4E-BP Wullschleger et al., 2006). mTOR also is a negative regulator of autophagy induction (Wullschleger et al., 2006). By simultaneously regulating protein synthesis and degradation, mTOR is key in controlling protein homeostasis, a process that is altered in AD and other proteinopathies (Lee et al., 2013). **The Aim of this work is to fully dissect the role of mTOR in the pathogenesis of AD.** Specifically, we will test the hypothesis that hyperactive mTOR further contributes to the buildup of Aβ and tau, thereby exacerbating cognitive decline. To test this hypothesis, we employed multidisciplinary approaches in order to identify the mechanistic links between mTOR signaling, Aβ and tau accumulation, and cognitive decline. Overall our results highlight the mTOR/S6K1 pathway as a previously unidentified signaling cascade that plays a key role in AD pathogenesis and offers a potential therapeutic target for this insidious disorder.

3 RESULTS

3.1 Genetic reduction of mTOR ameliorates Alzheimer's disease-like cognitive and pathological deficits by restoring hippocampal gene expression signature

Alzheimer's disease (AD) is the most common neurodegenerative disorder and the 6th leading cause of death in the United States. Currently, it is estimated that 26 million people worldwide are living with AD and by 2050 the number of people with this disorder can reach 100 million (Thies et al., 2013). AD is characterized by progressive cognitive deficits associated with the build-up of amyloid-β (Aβ) and neurofibrillary tangles. The majority (>95%) of AD cases are sporadic and of unknown causes, while the remaining cases are caused by mutations in one of three genes, presenilin 1 and 2 and amyloid precursor protein (Querfurth and LaFerla, 2010). The single major risk factor for AD is aging; however, little is known as to how the aging process facilitates the development of AD. Nevertheless, molecular changes that occur in the brain as a function of age may facilitate the development of AD.

Overwhelming evidence shows that reducing the activity of the mammalian target of rapamycin (mTOR) increases lifespan and health-span in several genetically different species (Lamming et al., 2013). mTOR is a ubiquitously expressed protein kinase that plays a key role in regulating protein synthesis and cell growth by phosphorylating downstream proteins such as p70 S6 kinase and eukaryotic initiation factor eIF4E binding protein (4E-BP) (Wullschleger et al., 2006). mTOR also is a negative regulator of autophagy induction(Wullschleger et al., 2006). By simultaneously regulating protein synthesis and degradation, mTOR is key in controlling protein homeostasis, a process that is altered in AD and other proteinopathies (Lee et al., 2013). Another known function of mTOR signaling is the regulation of synaptic plasticity and function (Hoeffer and Klann, 2010;

Hoeffer et al., 2008; Santini et al., 2014; Tang et al., 2002). Toward this end, mTOR activity is necessary for memory consolidation (Parsons et al., 2006; Tang et al., 2002); however, mTOR hyperactivity is detrimental and causes cognitive deficits in animals and people (Ehninger, 2013; Ehninger et al., 2008; Puighermanal et al., 2009).

Several laboratories have shown that mTOR signaling is upregulated in AD patients and animal models (An et al., 2003; Caccamo et al., 2010b; Oddo, 2012). Thus, one might expect that lifestyle choices known to increase mTOR signaling, such as a high sugar or high fat diet increase the risk of developing AD. Toward this end, we and others have shown that diabetes increases the risk of developing AD by and mTOR-dependent mechanism (Ma et al., 2013b; Orr et al., 2013). In contrast, some of the beneficial effects of caloric restrictions on brain function might be mediated by reduction in mTOR signaling (Speakman and Mitchell, 2011). To fully dissect the role of mTOR in the pathogenesis of AD, we used a genetic approach and selectively ablated one mTOR gene from the forebrain of an animal model of AD. Our results highlight a previously unidentified signaling pathway as a key player in AD pathogenesis and offer a potential therapeutic target for this insidious disorder.

3.1.1 Removing one copy of the mTOR gene, decreases hippocampal mTOR signaling

To study the role of mTOR in AD, we genetically and selectively removed one mTOR allele from the brains of the Tg2576 mice, a mouse model of AD (Hsiao et al., 1996). This was accomplished by taking advantage of the Cre-Lox site-specific recombination. Precisely, to obtain brain specific mTOR knockout mice, we first bred hemizygous Tg2576 mice ($Tg2576^{+/0}$) with homozygous transgenic mice overexpressing the Cre recombinase enzyme under the control of the neuronal specific CamKII promoter ($CRE^{+/+}$). As expected ~50% of the offspring had the following genotype: $Tg2576^{+/0}$;$Cre^{+/0}$ (Fig. 4). These mice were bred with homozygous mTOR floxed mice ($mTOR^{fl/fl}$) (Carr et al., 2012; Lang et al., 2010). From these crosses, we obtained mice with four

genotypes: (1) $Tg2576^{+/0}$;$mTOR^{fl/wt}$;$Cre^{+/0}$; (2) $Tg2576^{0/0}$;$mTOR^{fl/wt}$;$Cre^{+/0}$; (3) $Tg2576^{+/0}$;$mTOR^{fl/wt}$;$Cre^{0/0}$; (4) $Tg2576^{0/0}$;$mTOR^{fl/wt}$;$Cre^{0/0}$ (Fig. 4). Notably, all four groups of mice are littermates, thereby reducing the genetic background effects on the phenotype. Using this breeding strategy, we removed a single copy of the mTOR gene in the forebrain of the Tg2576 mice. For simplicity, herein the mice with the $Tg2576^{+/0}$;$mTOR^{fl/wt}$;$Cre^{+/0}$ genotype are referred to as APP/$mTOR^{+/-}$ mice, the mice with the $Tg2576^{0/0}$;$mTOR^{fl/wt}$;$Cre^{+/0}$ genotype as $mTOR^{+/-}$ mice, the mice with the $Tg2576^{+/0}$;$mTOR^{fl/wt}$;$Cre^{0/0}$ genotype as APP mice, and the mice with the $Tg2576^{0/0}$;$mTOR^{fl/wt}$; $Cre^{0/0}$ genotype as CTL mice.

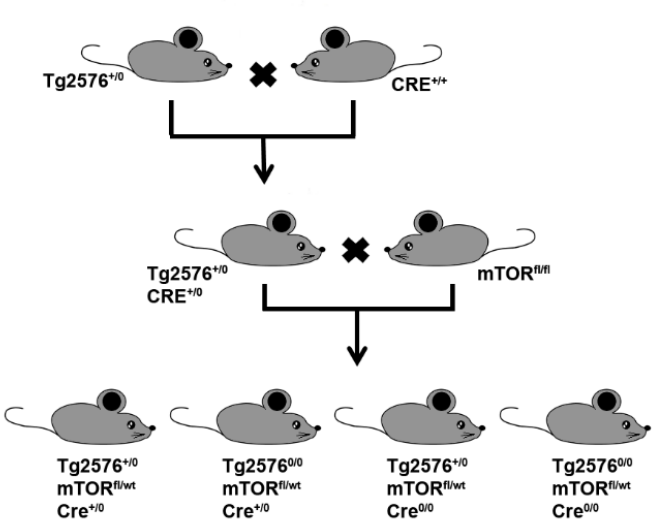

Figure 4. Schematic representation of the breeding strategy used to remove one copy of the mTOR gene from the forebrain of the Tg2576 mice. Abbreviations: "+" indicates the presence of a transgene (APP or CRE). "0" indicates the lack of such transgene. "fl" indicates the presence of a floxed allele. "wt" indicates the presence of a wild type allele.

To determine whether removing one copy of the mTOR gene was sufficient to reduce brain mTOR levels and signaling, we measured mTOR levels by Western blots in the hippocampi of 2- and 12-month-old mice (n = 5/genotype/age). We found that in 2-month-old mice, mTOR levels were significantly different among the four genotypes ($p = 0.01$; Fig. 5A-B). Specifically, mTOR levels

were 47 ± 6% and 52 ± 6% lower in the APP/mTOR$^{+/-}$ and mTOR$^{+/-}$ mice compared to the CTL mice, respectively. 4EBP-1 and p70S6K are two proteins downstream of mTOR, which directly phosphorylates them at Thr389 and Ser65; the levels of phosphorylated 4EBP-1 and p70S6K are used as an indication of activated mTOR signaling (Guertin and Sabatini, 2007; Hay and Sonenberg, 2004). In the hippocampi of 2-month-old mice, the total levels of p70S6K and 4EBP-1 were similar among the four groups. In contrast, we found that the levels of p70S6K phosphorylated at Thr389 and 4EBP-1 phosphorylated at Ser65 were significantly different among the four genotypes as indicated by one-way ANOVA ($p < 0.001$ for both; Fig. 5A-F). A *post hoc* test with Bonferroni correction showed that the phosphorylation levels of p70S6K and 4EBP-1 were significantly reduced in the APP/mTOR$^{+/-}$ and mTOR$^{+/-}$ mice compared to CTL and APP mice (Fig. 5D, F). To determine whether the changes in mTOR levels and signaling were maintained in older mice, we repeated these measurements in 12-month-old mice (n = 5/genotype). We found that mTOR levels were 37% and 40% lower in the hippocampi of the APP/mTOR$^{+/-}$ and mTOR$^{+/-}$ mice compared to CTL mice, respectively (Fig. 5G). While these changes did not affect total p70S6K and 4EBP-1 (Fig. 5 G, I-K), one-way ANOVA indicated that p70S6K levels phosphorylated at Thr389 and 4EBP-1 levels phosphorylated at Ser65 were significantly different among the four groups ($p = 0.0003$ and 0.0029, respectively). A *post hoc* test with Bonferroni correction showed that phosphorylated levels of p70S6K were significantly higher in the APP mice compared to CTL mice ($p < 0.01$). However, the phosphorylated levels of p70S6K in the hippocampi of the APP/mTOR$^{+/-}$ were not statistically different than CTL mice and were significantly reduced compared to the APP mice ($p < 0.01$; Fig. 5J). Similarly, the phosphorylated levels of 4EBP-1 were significantly reduced in the APP/mTOR$^{+/-}$ mice compared to the APP mice ($p < 0.05$; Fig. 5L). These data clearly show that removing one copy of the

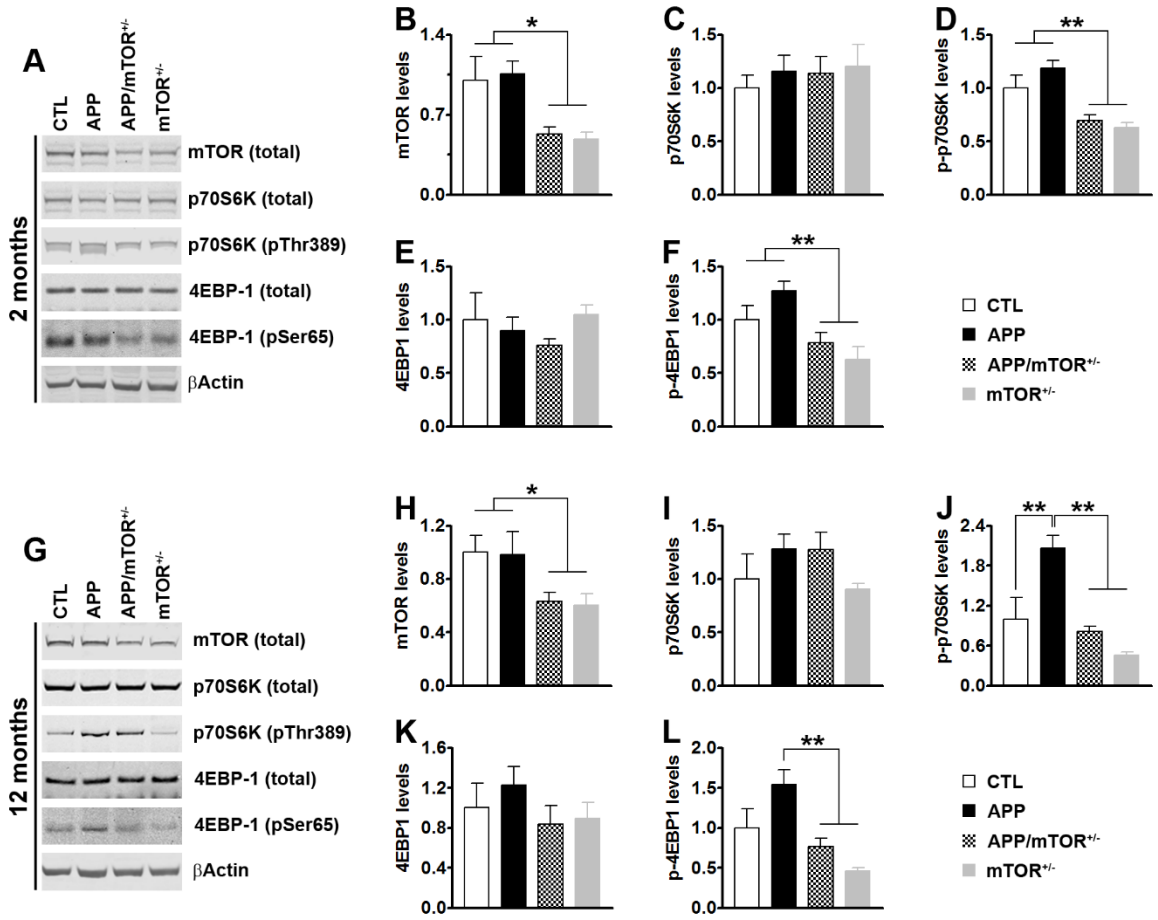

Figure 5. Removing one copy of the mTOR gene decreases mTOR levels and signaling. (A) Representative Western blots of proteins extracted from the hippocampi of 2-month-old mice probed with the indicated antibodies. **(B-F)** Quantification of the indicated proteins (n = 5 / genotype) showed that mTOR levels and the levels of phosphorylated p70S6K and 4EBP1 were significantly decreased in the hippocampi of mice lacking one copy of the mTOR gene. **(G)** Representative Western blots of proteins extracted from the hippocampi of 12-month-old mice probed with the indicated antibodies. **(H-L)** Quantification of the indicated proteins (n = 5 /genotype) showed that even as the mice age, mTOR levels and signaling were significantly lower in mice lacking one copy of the mTOR gene. Data were generated by normalizing the levels of the protein of interest to β-actin loading control. Results presented as means ± SEM and analyzed by one-way ANOVA with Bonferroni's correction. * $p < 0.05$; ** $p < 0.005$.

mTOR gene in the brain is sufficient to reduce mTOR levels and signaling. Notably, this approach restored the elevated levels of phospho-p70S6K of the APP mice to CTL levels.

3.1.2 Reducing mTOR signaling rescues cognitive deficits in Tg2576 mice

To evaluate the effects of removing one copy of the gene encoding mTOR from the brains of the Tg2576 mice, we tested 2- and 12-month-old mice in the spatial version of the Morris water maze (MWM), using two independent cohorts of mice. Mice received 4 training trials per day for 5 consecutive days to learn the location of a hidden platform using extra maze cues. Their performance was analyzed using a mixed-model, repeated-measures ANOVA, with genotype as the categorically fixed effects, days as the numeric covariate, animals as the random effect, and escape latency as the dependent variable. At two months of age, we found a significant effect for days ($p < 0.0001$), indicating that the mice learned the task across sessions (Fig. 6A). However, we found a non-significant genotype/day interaction ($p > 0.05$), indicating that there was no difference in the pace of learning among the four different groups (Fig. 6A). Twenty-four hours after the last training trial, we tested spatial memory by measuring the time mice spent in the target quadrant, the latency to reach the platform location, and the number of platform location crosses over a 60-second probe trial. We found no statistically significant changes in these three measurements among the four different genotypes (Fig. 6B-D). To determine whether the physical performance of the mice may have confounded these results, we measured their swim speed during the probe trials and found that it was not statistically different among the four genotypes (Fig. 6E). This is consistent with data in the literature showing that at this age, the Tg2576 mice are not cognitively impaired (Westerman et al., 2002).

As the Tg2576 mice age, they develop progressive cognitive deficits in several behavioral tests, including the MWM (Westerman et al., 2002). At 12 months of age, we found a significant effect for days ($p < 0.0001$) and genotype ($p = 0.0009$; Fig. 6F). The day effect indicates that the mice significantly improve their performance across sessions whereas the genotype effect indicates that one or more genotypes are different from each other. A *post hoc* test with Bonferroni correction showed that at day 4 and 5, the APP mice performed significantly worse than the other

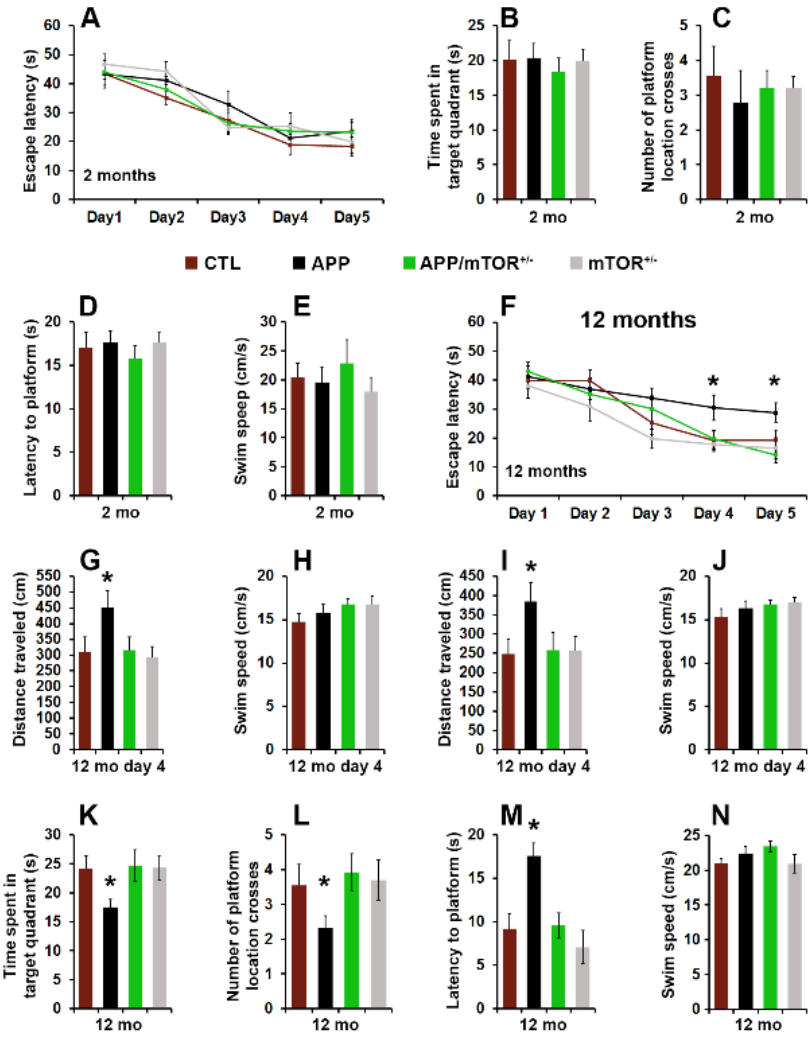

Figure 6. Decreasing mTOR signaling rescues learning and memory deficits. (A) Learning curve of 2-month-old mice trained in the spatial reference version of the MWM. Mice were trained to swim to a hidden platform in a tank using extramazal visual cues. All genotypes showed significant improvements over the 5 days of training. Each day represents the average of four training trials. **(B-D)** Reference memory, tested 24 h after the last training trial was not statistically different among the four groups. **(E)** Average swim speed during the probe trials. **(F)** Learning curve of 12-month-old mice in the MWM. All genotypes significantly learned the task; however, at day 4 and 5 the APP mice needed significantly more time to find the hidden platform than the other three genotypes. **(G-H)** Average distance traveled and swim speed of 12-month-old mice during day 4 of training. **(I-J)** Average distance traveled and swim speed of 12-month-old mice during day 5 of training. **(K-M)** Reference memory, tested 24 h after the last training trial was significantly impaired in the APP mice compared to the other three genotypes. Notably, the APP/mTOR$^{+/-}$ mice performed as well as the CTL mice and significantly better than the APP mice. **(N)** Average swim speed during the probe trials was not statistically different among the four genotypes. n = 10/genotype at 2 months of age; n = 14/genotype at 12 months of age. Data are presented as means ± SEM and were analyzed by two-way ANOVA with Bonferroni's correction. * $p < 0.05$.

three groups ($p = 0.039$ and 0.009, respectively; Fig. 6F). Notably, the APP/mTOR$^{+/-}$ mice

performed as well as the CTL mice across the 5 days of training. To determine whether differences in physical performance could account for the changes in escape latency on days 4 and 5, we measured the average distance traveled and the swim speed of the four groups of mice. Consistent with the escape latency data, the APP mice traveled longer to find the platform than the other groups for both days ($p < 0.05$; Fig. 6G and I). In contrast, the average swim speed was similar among the different groups for both days (Fig. 6H and J). Twenty-four hours after the last training trial, we conducted probe trials to measure spatial memory. In every measurement, APP mice performed significantly worse than the other three groups ($p < 0.01$ as calculated by one-way ANOVA; Fig. 6G-I). The swim speed of 12-month-old mice was not statistically significant among the four genotypes (Fig. 6J), clearly indicating that the genotype effects on learning and memory are independent of physical performance. These findings indicate that removing one copy of the mTOR gene from the brains of the Tg2576 mice is sufficient to rescue cognitive deficits.

3.1.3 Reducing mTOR signaling decreases Aβ levels and burden and increases synaptophysin levels

At the end of the behavioral tests, mice were sacrificed and their brains further analyzed. We initially focused on Aβ pathology, as this is the major neuropathological feature of the Tg2576 mice (Kawarabayashi et al., 2001). We immunostained sections from APP and APP/mTOR$^{+/-}$ mice with an $A\beta_{42}$ specific antibody and found that the $A_{\beta 42}$ immunoreactivity was significantly reduced in the APP/mTOR$^{+/-}$ mice compared to the APP mice (Fig. 7A-B). Quantitative analysis of the overall Aβ load indicated a decrease of 46.77%, which was highly significant ($p = 0.0004$). We next measured Aβ levels by sandwich ELISA and found that soluble $A\beta_{40}$ and $A\beta_{42}$ levels were significantly lower in the hippocampi of the APP/mTOR$^{+/-}$ mice compared to APP mice ($p < 0.0001$ and $p = 0.0024$, respectively; Fig. 7D-E). Similarly, insoluble $A\beta_{40}$ and $A\beta_{42}$ levels were

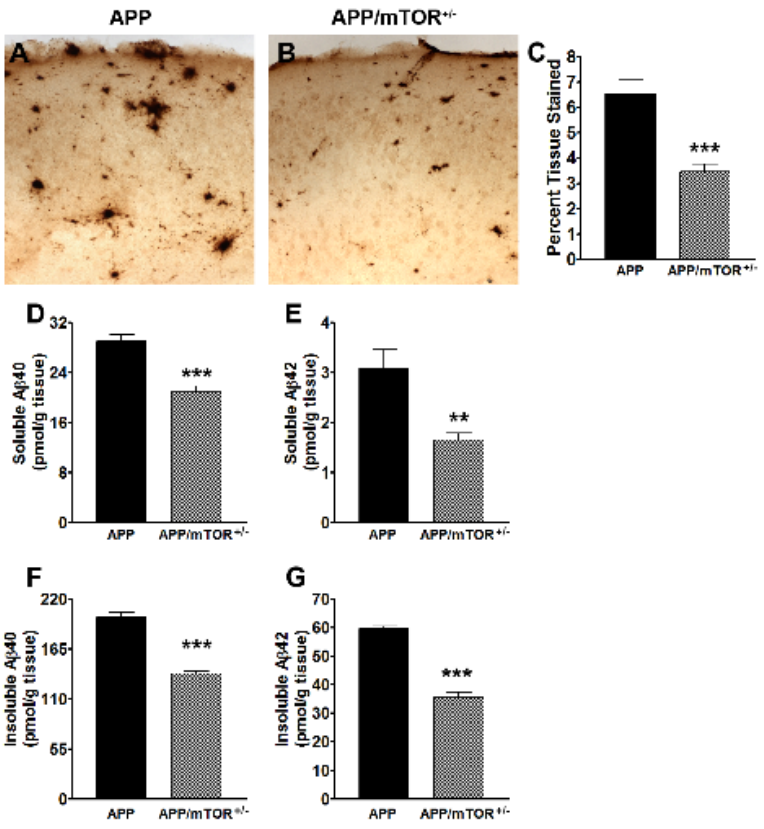

Figure 7. APP/mTOR$^{+/-}$ mice have less Aβ pathology than APP mice. (A-B) Representative microphotographs of brain section immunostained with an $A\beta_{42}$ specific antibody. **(C)** Quantitative analysis of the Aβ immunohistochemistry showed a significant decrease in Aβ load following removal of one copy of the mTOR gene (n = 7/genotype). **(D-E)** Soluble levels of $A\beta_{40}$ and $A\beta_{42}$ extracted from frozen hippocampi and measured by sandwich ELISA (n = 8/genotype). **(F-G)** Insoluble levels of $A\beta_{40}$ and $A\beta_{42}$ extracted from frozen hippocampi and measured by sandwich ELISA (n = 8/genotype). Data are presented as means ± SEM and were analyzed by t-test. ** p = 0.002; *** p < 0.0001.

significantly lower in the hippocampi of the APP/mTOR$^{+/-}$ mice compared to the APP mice ($p < 0.0001$ for both Aβ species; Fig. 7F-G).

To determine whether alterations in APP processing could account for the changes in Aβ levels between the APP and the APP/mTOR$^{+/-}$ mice, we measured the levels of full-length APP and its two major C-terminal fragments, C99 and C83 in the hippocampi of 2- and 12-month-old mice.

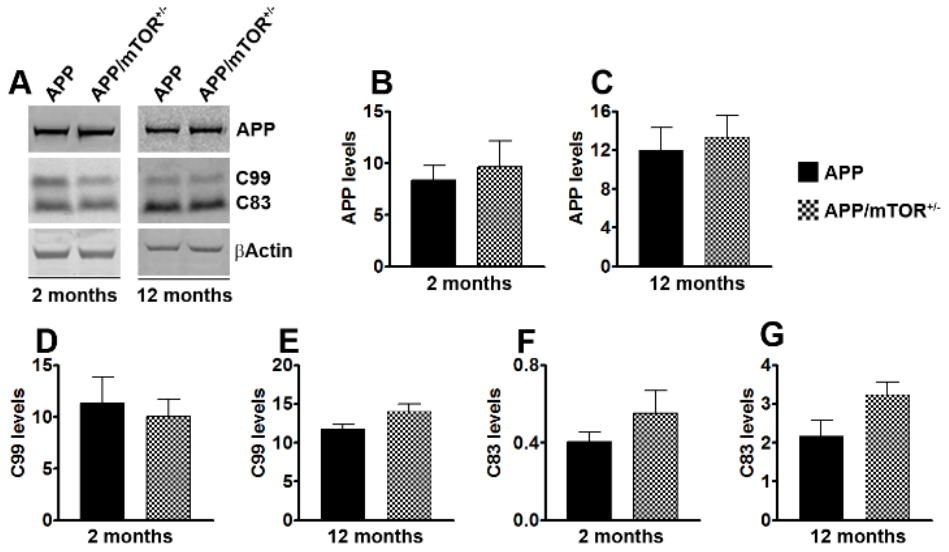

Figure 8. APP processing is not changed between APP and APP/mTOR$^{+/-}$ mice. **(A)** Representative Western blots of proteins extracted from frozen hippocampi of 2- and 12-month-old mice and probed with the indicated antibodies. **(B-G)** Quantification of the blots shows that the levels of APP, C99 and C83 were not statistically significant between APP/mTOR$^{+/-}$ and APP mice, at any of the age analyzed (n = 5/genotype/time point). Data are presented as means ± SEM and were analyzed by t-test.

We found that at both ages, full-length APP levels were not different between the two groups (Fig. 8A-C). Similarly, C99 and C83 levels were comparable between APP and APP/mTOR$^{+/-}$ mice at both ages (Fig. 8A, D-G). These results suggest that removing one copy of the mTOR gene is sufficient to reduce Aβ burden and levels without altering APP processing.

Synaptic dysfunction is a strong correlate of cognitive deficits in AD and, at least in mouse models, correlates with changes in Aβ. To determine whether the changes in Aβ pathology in the APP/mTOR$^{+/-}$ mice were followed by changes in synaptic markers, we measured the steady-state levels of synaptophysin and PSD95, two commonly used pre- and postsynaptic markers, respectively. We found that synaptophysin levels were significantly different among the three groups ($p = 0.025$ by one-way ANOVA; Fig. 9A-B). Bonferroni's post hoc analysis showed that synaptophysin levels were significantly higher in the APP/mTOR$^{+/-}$ mice compared to APP mice.

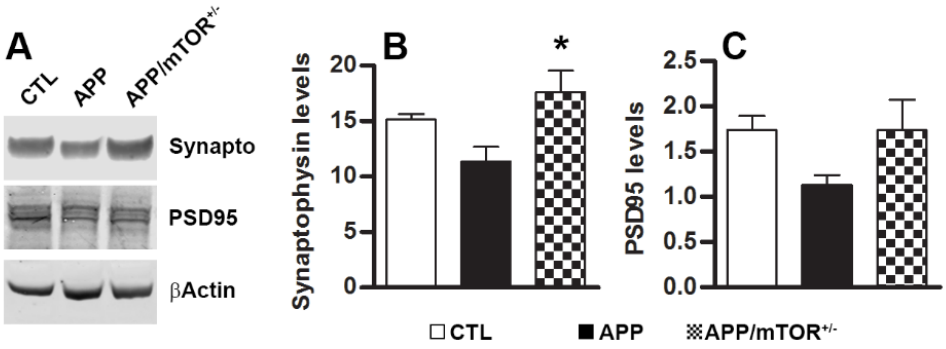

Figure 9. Increased synaptophysin levels in APP/mTOR$^{+/-}$ mice. (A) Representative Western blots of protein extracted from 12-month-old CTL, APP and APP/mTOR$^{+/-}$ mice. Blots were probed with the indicated antibodies. **(B-C)** Quantification of the blots shows that synaptophysin levels were restored to CTL levels in the APP/mTOR$^{+/-}$ mice. While the same trend was apparent for PSD95, the changes were not statistically significant. Data are presented as means ± SEM and were analyzed by one-way ANOVA with Bonferroni correction. * $p < 0.05$.

Notably, synaptophysin levels were similar between CTL and APP/mTOR$^{+/-}$ mice, suggesting that removing one copy of the mTOR gene was sufficient to rescue hippocampal synaptophysin levels. We found a similar trend for PSD95, although the changes did not reach significance (Fig. 9A, C).

3.1.4 Reducing brain mTOR signaling increases autophagy induction

To mechanistically link the reduction in mTOR signaling to cognitive improvements and the decrease in Aβ pathology, we analyzed the two major pathways downstream of mTOR. Specifically, when cell energy levels are high, mTOR facilitates protein translation and transcription; in contrast, when cell energy levels are low, mTOR facilitates autophagy for protein turnover (Wullschleger et al., 2006). Dysregulation in both of these processes has been linked to AD (Caldeira et al., 2013; Nixon and Yang, 2011b; Orr and Oddo, 2013). We first measured the levels of four key autophagy related proteins (Atgs), which have been shown to be critical in

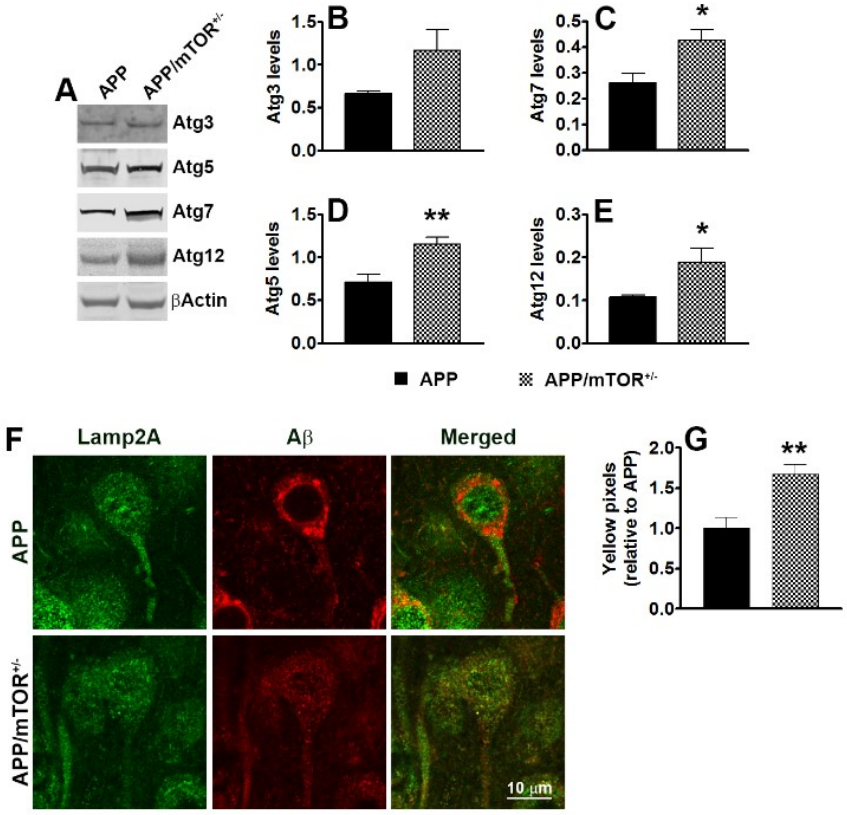

Figure 10. Decreasing mTOR signaling increases autophagy induction. **(A)** Representative Western blots of protein extracted from 12-month-old APP and APP/mTOR$^{+/-}$ mice. Blots were probed with the indicated antibodies. **(B-E)** Quantification of the blots shows that the levels of Atg3, Atg5, Atg7 and Atg12 were significantly higher in the APP/mTOR$^{+/-}$ than APP mice (n = 5/genotype). **(F)** Representative microphotographs of hippocampal sections immunostained with the indicated antibodies. **(G)** Semi-quantitative analysis showed that the number of yellow pixels (indicating a co-localization between Aβ and the lysosomal protein Lamp2A) was significantly higher in APP/mTOR+/- mice compared to APP mice (n = 7 / genotype). Data are presented as means ± SEM and were analyzed by t-test. * $p < 0.01$; ** $p < 0.001$.

autophagy induction (Komatsu et al., 2007; Mizushima et al., 1998). We found that Atg3 levels were increased by 75.6% in the hippocampi of APP/mTOR$^{+/-}$ mice compared to APP mice (Fig. 10A-B); however, this change was not statistically significant ($p = 0.0509$) likely due to the variability within the APP/mTOR$^{+/-}$ mice. In contrast, Atg5 levels were increased by 62.61% in the hippocampi of APP/mTOR$^{+/-}$ mice compared to APP mice ($p < 0.006$; Fig. 10A, D). Similarly, we found an increase of 62.76% and 76.36% in Atg7 and Atg12 levels, respectively, following the

removal of a copy of the mTOR gene ($p = 0.01$ and $p = 0.03$ for Atg7 and Atg12, respectively; Fig. 10A, C,E). In the autophagy pathway, once the autophagosomes are formed, they fuse with the lysosomes where their cargo is digested (Tanida, 2011). To assess whether increasing autophagy induction was sufficient to facilitate Aβ turnover by the lysosomes, we double labeled hippocampal sections from APP and APP/mTOR$^{+/-}$ mice with an $A\beta_{42}$-specific antibody and with Lamp2A, a lysosomal marker. Confocal imaging showed very little co-localization between Aβ and Lamp2A in the APP mice (Fig. 10F). In contrast, the APP/mTOR$^{+/-}$ mice showed a clear and robust co-localization between Aβ and Lamp2A (Fig. 10F), suggesting that upon autophagy induction, Aβ was delivered to the lysosomes for degradation. To better the degree of this change, we quantified the number of yellow pixels in a visual field and found a significant 67% increase in the APP/mTOR$^{+/-}$ than the APP mice (Fig. 10G). These data suggest an increase in autophagy induction in the hippocampi of the APP/mTOR$^{+/-}$ mice compared to APP mice.

3.1.5 Reducing mTOR signaling restores the gene expression profile of the Tg2576 mice to CTL levels

We next examined global gene expression in the hippocampi of 12-month-old CTL, APP, APP/mTOR$^{+/-}$ and CTL mice (n= 6 /genotype) and found that the expression of 266 transcripts was significantly changed among the four groups of mice (one-way ANOVA, $p < 0.05$; Fig.11A). A post-hoc analysis with Bonferroni correction revealed that 227 of these genes were differentially expressed between APP and APP/mTOR$^{+/-}$ mice (Fig. 11A). The top 20 transcripts showing greatest change in expression between APP and APP/mTOR$^{+/-}$ are summarized in Table 1.

To further evaluate the overall structure of the transcriptional changes, we performed a cluster analysis of gene expression levels by clustering all transcripts in an unbiased fashion to create a hierarchical tree. We found that 38 transcripts clustered according to genotype; specifically,

ProbeID	Symbol	Definition	ANOVA p values (among the four groups)	FC in APP/mTOR$^{+/-}$ relative to APP	Regulation	FC in APP relative to CTL	Regulation
2900154	Dctn1	Dynactin 1	0.00105	4.66475	up	2.91486	down
240025	Isl2	Immunoglobulin superfamily containing leucine-rich repeat 2	0.00539	2.37943	up	1.59996	down
2750066	Rn18s	18S RNA (Rn18s), non-coding RNA	0.00001	2.3704	up	2.0421	down
6510615	A130022A09Rik	RIKEN cDNA A130022A09	0.02492	2.36581	down	1.60222	up
7050673	Zxda	Zinc finger, X-linked, duplicated A, non-coding RNA	0.00042	2.13611	down	1.83545	up
5080064	Slc8a2	Solute carrier family 8 (sodium/calcium exchanger), member 2	0.00106	2.0633	up	1.67871	down
6130482	C230078M08Rik	RIKEN cDNA C230078M08 gene	0.00636	1.9872	up	1.55682	down
840224	2610301N02Rik	RIKEN cDNA 2610301N02 gene	0.00868	1.97983	down	1.37266	up
3520240	Rn18s	18S RNA (Rn18s), non-coding RNA	0.00001	1.971	up	1.7302	down
6480044	Arl4c	ADP-ribosylation factor-like 4C	0.01214	1.96944	down	1.75136	up
3870132	6330415B21Rik	RIKEN cDNA 6330415B21 gene	0.0343	1.9576	down	1.1986	up
1780707	9530053J19Rik	RIKEN cDNA 9530053J19 gene	0.02255	1.93924	down	1.44845	up
4890670	Iqsec2	IQ motif and Sec7 domain 2, transcript variant 2	0.00452	1.93587	up	1.2717	down
1710735	LOC381219	hypothetical LOC381219	0.00735	1.93024	down	1.33752	up
650189	3632431M01Rik	transmembrane and coiled coil domains 1	0.04541	1.92024	down	1.05674	up
5570097	5330431K02Rik	RIKEN cDNA 5330431K02 gene	0.02922	1.91527	down	1.3845	up
1780037	BC030476	cDNA sequence BC030476	0.01214	1.91476	down	1.52354	up
1940356	6030424L16Rik	RIKEN cDNA 6030424L16 gene	0.01271	1.91042	down	1.59773	up
4040768	Rn18s	18S RNA (Rn18s), non-coding RNA	0.00004	1.90669	up	1.68662	down
4540102	BC030499	cDNA sequence BC030499	0.01747	1.90504	down	1.53121	up

Table 1. Top 20 transcripts showing greatest change in expression between APP and APP/mTOR$^{+/-}$. Abbreviations: FC, fold change.

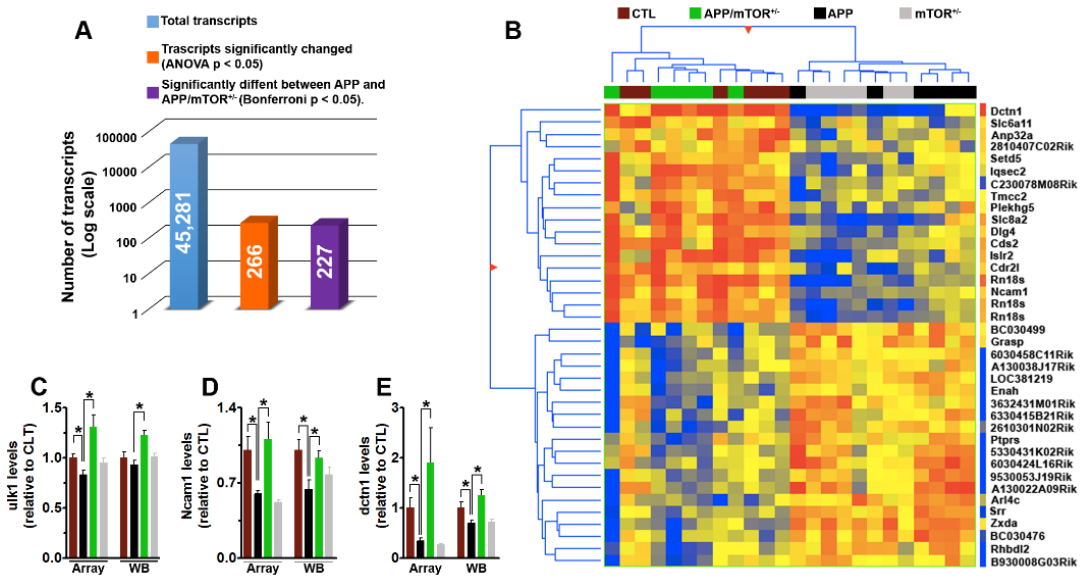

Figure 11. Removing one copy of the mTOR gene restores the hippocampal expression profiles of the APP mice to the CTL levels. **(A)** The graph summarizes the expression analysis results from transcripts isolated from frozen hippocampi (n = 6/genotype), indicating the number of genes measured, how many of those were differentially expressed among the four genotypes, and how many of those were differentially expressed between APP and APP/mTOR$^{+/-}$ mice. **(B)** Cluster analysis of samples from all genotypes with a fold change ≥ 1.8 fold when comparing CLT to APP mice. Each column represents a single sample, whose genotype is color labeled above the cluster diagram. Each raw represents a specific transcript, whose identity is listed to the right of the cluster diagram. **(C-E)** Validation of microarray results of three random genes by Western blot. Each graph shows the expression levels of each transcript (relative to CTL) as found by microarray and Western blots. For the Western blots (n = 6/genotype). Data are presented as means ± SEM and were analyzed by one way ANOVA. * $p < 0.05$.

APP/mTOR$^{+/-}$ and CTL mice cluster together, which highlights how reducing mTOR signaling restored the hippocampal gene expression signature of the APP mice to CTL levels (Fig. 11B). To validate the microarray data, we randomly selected three transcripts and measured their equivalent protein levels by Western blots. In all three cases we found that the microarray data closely reflected the Western blots results (Fig. 11C-E). Overall these results clearly indicate that the expression profile of APP mice is altered compared to CTL mice; notably, removing one copy of the mTOR gene was sufficient to reverse the expression of many of the genes altered in the APP mice to CTL levels.

3.1.6 Discussion

Several laboratories have reported that mTOR hyperactivity is increased in post-mortem human brains compared to age-matched controls (An et al., 2003; Chang et al., 2002; Griffin et al., 2005; Peel and Bredesen, 2003; Pei et al., 2008; Pei and Hugon, 2008). Consistently, we have shown that soluble Aβ accumulation is sufficient to increase mTOR activity and signaling *in vivo* (Caccamo et al., 2011b). Along these lines, here we show that mTOR is hyperactive in the hippocampi of 12-month-old CTL mice, which are characterized by widespread Aβ accumulation. Notably, mTOR hyperactivity has been linked to increased tau levels and phosphorylation in drosophila and mice (Caccamo et al., 2013; Khurana et al., 2006; Tang et al., 2013). Thus, mTOR might represent a molecular link between Aβ accumulation and tau pathology. Further, overwhelming evidence shows that reducing mTOR signaling increases lifespan and health-span in a variety of organisms, including mammals (Harrison et al., 2009; Selman et al., 2009). Given that aging is by far the strongest risk factor for AD, we hypothesize that one way by which aging facilitates the development of AD is by altering mTOR activity. Consistent with this hypothesis, we and others have shown that rapamycin, an mTOR inhibitor, increases lifespan in genetically-heterogeneous mice and decreases AD-like pathology in two independent animal models of AD (Caccamo et al., 2010b; Harrison et al., 2009; Majumder et al., 2011; Spilman et al., 2010).

In adult brains, mTOR regulates several protein-dependent events that are critical for learning and memory (Graber et al., 2013; Hoeffer and Klann, 2010; Hoeffer et al., 2008; Klann and Sweatt, 2008). However, strong evidence also shows that mTOR hyperactivity is detrimental for normal brain function (Cao et al., 2009; Ehninger, 2013; Ehninger et al., 2008; Puighermanal et al., 2009; Zeng et al., 2009). For example, clinical mutations in the tuberous sclerosis complex lead to mTOR hyperactivity and learning disabilities in affected patients (Ehninger, 2013). These findings have been replicated in animal models (Ehninger et al., 2008). Consistently, low doses of

rapamycin rescue memory deficits associated with cannabinoids consumption (Puighermanal et al., 2009). Overall, there might be a window for mTOR signaling that is optimal for learning and memory and that alterations leading to an excessive increase or decrease in mTOR signaling outside such optimal window may have detrimental effects on learning and memory (Cao et al., 2009; Inoki et al., 2005; Zeng et al., 2009). Given the above mentioned evidence, our experiments were purposely designed to remove only one copy of the mTOR gene from the brain of APP mice. Notably, we showed that this approach reduced but not abolished mTOR signaling. Indeed, at 12 months of age, mTOR signaling was similar between APP/mTOR$^{+/-}$ and CTL mice; in other words, we successfully reduced the hyperactive mTOR signaling of the APP mice to CTL levels. We postulate that major reductions in brain mTOR signaling might have detrimental effects on learning and memory.

It is not surprising that the transcriptome of AD patients is altered compared to age-matched controls (Caldeira et al., 2013). Nevertheless, detailed analyses of these experiments have led to critical insights into the disease pathogenesis. Some of the transcriptome changes seen in AD brains have been replicated in mouse models. Along these lines, the transcriptome of the Tg2576 mice has also been found to be significantly altered compared to age-matched control mice (George et al., 2010; Reddy et al., 2004; Tan et al., 2013). Here we show that reducing mTOR signaling restored the expression pattern of 227 transcripts. Importantly, the expression of these transcripts was altered in the APP brains compared to CTL but was restored to CTL levels when one copy of the mTOR gene was removed from the hippocampi of the APP mice. It is tempting to speculate that these changes in the hippocampal transcriptome significantly contribute to the cognitive improvement seen in the APP/mTOR$^{+/-}$ mice. These results are highly consistent with a recent report showing that reducing the activity of the eukaryotic initiation factor 2 α-subunit (eIF2α) ameliorates AD-like pathology and memory deficits associated with Aβ accumulation (Ma

et al., 2013a). Notably, eIF2α is a downstream effector of mTOR (Tuval-Kochen et al., 2013). Together these results argue that reducing mTOR signaling might be beneficial for AD.

To summarize, we provide compelling evidence clearly indicating a primary role of mTOR in AD pathogenesis and suggest a possible way by which aging increases the development of this disorder. Further, the data presented here point to mTOR as a potential therapeutic target for this disorder. The clinical implication of these findings is profound as there are several known compounds, some FDA-approved, known to reduce mTOR signaling.

3.2 Reducing ribosomal protein S6 kinase 1 expression improves spatial memory and synaptic plasticity in a mouse model of Alzheimer's disease

The lack of effective cures or treatments for Alzheimer's disease (AD) is alarming considering the number of people currently affected by this disorder and the projected increase in incidence and prevalence over the next two decades (Alzheimer's, 2014). The buildup of amyloid-β (Aβ) and tau is an invariable feature of AD and is believed to contribute to the progressive cognitive deficits associated with this disorder (Querfurth and LaFerla, 2010). Aβ is generated from the amyloid precursor protein (APP), which is sequentially cleaved by the β-site APP cleaving enzymes 1 (BACE-1) and the γ-secretase complex to liberate Aβ. Given the role of BACE-1 in the generation of Aβ, major efforts are underway to develop BACE-1 inhibitors as a possible treatment for AD. Another key event in AD is synaptic dysfunction, which appears to be an early event in disease pathogenesis and precedes neuronal loss (Sheng et al., 2012). Supporting this view, synaptic loss has been reported in the cortex of people with mild cognitive impairment (MCI) and early AD (Masliah et al., 2001).

Aging is the major risk factor associated with the development of AD; thus, it is plausible that alterations in selective pathways associated with aging may facilitate the development of this insidious disorder (Moll et al., 2014). The ribosomal protein S6 kinase 1 (S6K1) is a ubiquitously expressed protein involved in several cellular processes, including protein translation and glucose homeostasis (Fenton and Gout, 2011), both of which are altered in AD (Dineley et al., 2014). Overwhelming evidence shows S6K1 as a key regulator of lifespan and healthspan. For example, dominant negative *dS6K* increases lifespan in drosophila (Kapahi et al., 2004) while deletion of *S6K1* in mice is sufficient to increase lifespan and decrease the incident of age-dependent motor dysfunction and insulin sensitivity (Selman et al., 2009). Similarly, lack of S6K1 protects mice against age-induced obesity (Um et al., 2004). Given the role of S6K1 in aging and age-related

diseases, in this study we sought to determine whether decreasing S6K1 levels could prevent AD-like phenotype developed by the 3xTg-AD mice, a widely used mouse model of AD (Oddo et al., 2003b). Specifically, we used a genetic approach to selectively ablate one copy of the *S6K1* gene in 3xTg-AD mice. Our results reveal a previously unidentified signaling pathway as a key player in AD pathogenesis and offer a potential therapeutic target for this devastating disorder.

3.2.1 Reducing S6K1 levels prevents synaptic deficits in 3xTg-AD mice

The S6K1 gene encodes two proteins, the p70S6K1 and the p85S6K1 (Reinhard et al., 1992).

Table 2. Cases statistics. Aβ levels were measured by sandwich ELISA and tau levels were measured by western blot in the tissue used for the experiments described here. *$p < 0.05$.

	Cognitively Normal (*n* or *M* ± *SEM*)	**Alzheimer's Disease (*n* or *M* ± *SEM*)**	***N or df***	***t***	**Cohen's *d***
Male and female cases	11-***Male*** & 6-***Female***	8-***Male*** & 10-***Female***	35		
Cases per Braak stage	5-***I*** and 12-***II***	8-***V*** and 10-***VI***	35		
Expired age	82.12 ± 1.55	81.78 ± 1.95	33	-0.34	-0.05
PMI	3.05 ± 0.19	3.05 ± 0.26	16	< 0.00	< 0.00
MMSE	27.06 ± 1.54	12.11 ± 2.27	33	-5.39	-1.88*
Soluble $A\beta_{42}$ (pg/µl)	89.01 ± 26.75	306.01 ± 32.86	33	9.68	1.77*
Insoluble $A\beta_{42}$ (pg/µl)	8.93 ± 2.27	1483.99 ± 148	33	11.35	3.37*
Total $A\beta_{42}$ (pg/µl)	97.94 ± 28.35	1789.99 ± 142.21	33	11.35	3.95*
Tau-PHF1 (% Cognitively Normal)	8.05 ± 1.28	33.69 ± 9.39	33	2.63	0.91*

The former is the most predominant species, which is mainly localized in the cytoplasm; the latter is less abundant and is mainly localized in the nucleus (Fenton and Gout, 2011; Reinhard et al., 1992). Given the role of S6K1 in aging and age-related diseases (Kapahi et al., 2004; Rajapakse et al., 2011; Selman et al., 2009; Um et al., 2004), we first measured the total and phosphorylated

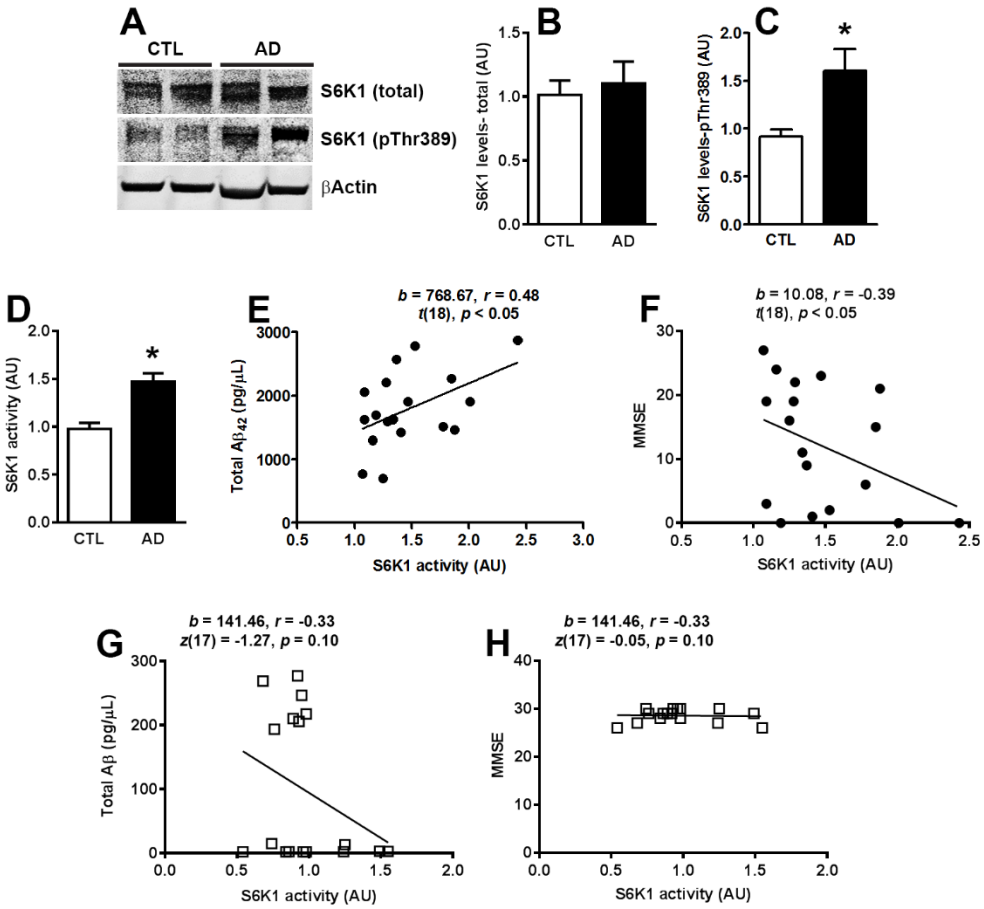

Figure 12. S6K1 activity correlate with Aβ levels and MMSE scores. **(A)** Western blots of proteins extracted from the inferior frontal gyrus of AD and control (CTL) cases. The blots were probed with the indicated antibodies. **(B-C)** Quantitative analyses of the arbitrary fluorescent units of the blots indicated that total S6K1 levels were similar between AD and CTL cases [t(33) = 0.42, p > 0.05). In contrast, the levels of S6K1-pThr389 were significantly higher in AD compared to CTL cases [$t(33) = 2.81$, $p = 0.008$]. **(D)** S6K1 enzymatic activity was significantly higher in AD brains compared to CTL cases [$t(33) = 4.48$, $p < 0.0001$]. **(E-H)** Scatter plots analyzed by linear regression displaying the correlation between S6K1 activity and total $A\beta_{42}$ levels and between S6K1 activity and MMSE scores in AD and CTL cases. Higher S6K1 activity positively correlated with higher levels of total $A\beta_{42}$ in AD but not in CLT brains. A negative correlation was also evident between S6K1 activity and MMSE scores in AD but not in CTL brains. Western blot data were obtained by normalizing the arbitrary fluorescent unit of the protein of interest to β-actin. Data in panels B-D were analyzed by unpaired t-test. For each experiment shown, $n = 17$ brains for CTL and $n = 18$ brains for AD cases. Error bars represent mean ± s.e.m

S6K1 levels in the inferior frontal gyrus of human AD and control brains (Table 2). While the levels of total S6K1 were similar between these two groups (Fig. 12A-B), we found that the levels of S6K1 phosphorylated at Thr389 (S6K1-Thr389), indicative of the activated state of the protein (Pearson et al., 1995), were 68.75 ± 24.42% higher in AD patients compared to control cases (*p*

= 0.008; Fig. 12A, C). We also measured S6K1 enzymatic activity and found that it was significantly higher in AD brains when compared to control cases ($p < 0.0001$; Fig. 12D). We then sought to determine whether S6K1 activity correlated with Aβ levels as well as the Mini Mental State Examination (MMSE) score, a commonly used test to assess cognitive impairments (Pangman et al., 2000). Given that S6K1 levels and activity were obtained from proteins extracted from 0.1 grams of inferior frontal gyrus, we used the same protein homogenate to measure Aβ levels (Table 2), and did not rely on the Aβ load throughout the whole brain. As expected, the levels of Aβ were significantly higher in AD cases compared to control cases (Table 2). We found a significant positive correlation between S6K1 activity and total Aβ levels in AD cases ($r = 0.48$, $p < 0.05$; Fig. 12E). In addition, in AD brains, we found an inverse correlation between S6K1 activity and the MMSE scores ($r = -0.39$, $p < 0.05$; Fig. 12G). In contrast, in control brains, there was no correlation between S6K1 activity and total $A\beta_{42}$ levels and MMSE (Fig. 12G-H). These findings indicate that the buildup of Aβ may contribute to an increase in S6K1 activity, which is consistent with our earlier report showing that naturally-secreted Aβ oligomers were sufficient to increase S6K1 phosphorylation in wild type mice (Caccamo et al., 2011b).

To study the role of S6K1 in the pathogenesis of AD, we crossed 3xTg-AD mice with S6K1 knockout mice to obtain and study mice with the following four genotypes: (1) 3xTg-AD; (2) 3xTg-AD;S6K1$^{+/-}$; (3) S6K1$^{+/-}$; and (4) NonTg. We first measured S6K1 activity in 15-month-old mice and found that it was significantly different among the four genotypes ($p < 0.0001$; Fig. 13A). A *post hoc* test with Bonferroni correction showed that S6K1 activity was higher in 3xTg-AD mice compared to all the other genotypes. S6K1 activity was similar between NonTg and 3xTg-AD/S6K1$^{+/-}$, while in S6K1$^{+/-}$ mice had the lowest S6K1 activity among the four groups. These data indicate that removing one copy of the S6K1 gene restored S6K1 activity in 3xTg-AD mice to NonTg levels. Consistent with these findings, we previously reported that S6K1 signaling was also increased in the brains of 3xTg-AD mice (Caccamo et al., 2014; Caccamo et al., 2010b). To

further assess changes in S6K1 function, we measured the levels of total and phosphorylated S6K1 (at Thr389), by western blot. We found that total S6K1 levels were significantly lower in the two groups lacking one copy of the S6K1 gene ($p < 0.0001$; Fig. 13B-C). The levels of S6K1 phosphorylated at Thr389 were also significantly different among the four groups ($p < 0.0001$; Fig. 13B, D). A *post hoc* test with Bonferroni correction showed that the levels of phosphorylated S6K1 were higher in 3xTg-AD mice compared to all the other genotypes. While phosphorylated S6K1 levels in S6K1$^{+/-}$ mice were the lowest among the all the groups, they were similar between NonTg and 3xTg-AD/S6K1$^{+/-}$.

The primary role of S6K1 is to regulate protein synthesis; several downstream effectors of S6K1 mediate its function(Magnuson et al., 2012). For example, S6K1 directly phosphorylates the eukaryotic elongation faction-2 kinase (eEF2K) at Ser366. Additionally, S6K1 phosphorylates the ribosomal protein S6 (rpS6), at Ser235/236 (Magnuson et al., 2012). eEF2K and rpS6 are known to regulate translation elongation and ribosomal biogenesis, respectively (Magnuson et al., 2012). To determine whether reducing S6K1 levels alters downstream pathways, we measured the levels of total and phosphorylated eEF2K and rpS6. Total eEF2K levels were not statistically different among the four groups (Fig. 13B, E). In contrast, we found that the levels of eEF2K phosphorylated at Ser366 were significantly different among the groups ($p < 0.0001$; Fig. 13B, G). A *post hoc* test with Bonferroni correction indicated that these changes mirrored the changes in S6K1 activity, with the 3xTg-AD mice having the highest levels and the S6K1$^{+/-}$ mice the lowest. Furthermore, total rpS6 levels were similar among the four groups (Fig. 13B, G). However, the levels of rpS6 phosphorylated at Thr235/236 were significantly different among the four groups ($p < 0.0001$; Fig. 13B, H). A *post hoc* test with Bonferroni correction indicated that the phosphorylated levels of rpS6 were significantly different in 3xTg-AD mice compared to all the other groups. Notably, no differences were found between NonTg and 3xTg-AD/S6K1$^{+/-}$ mice, and between NonTg and S6K1$^{+/-}$ mice.

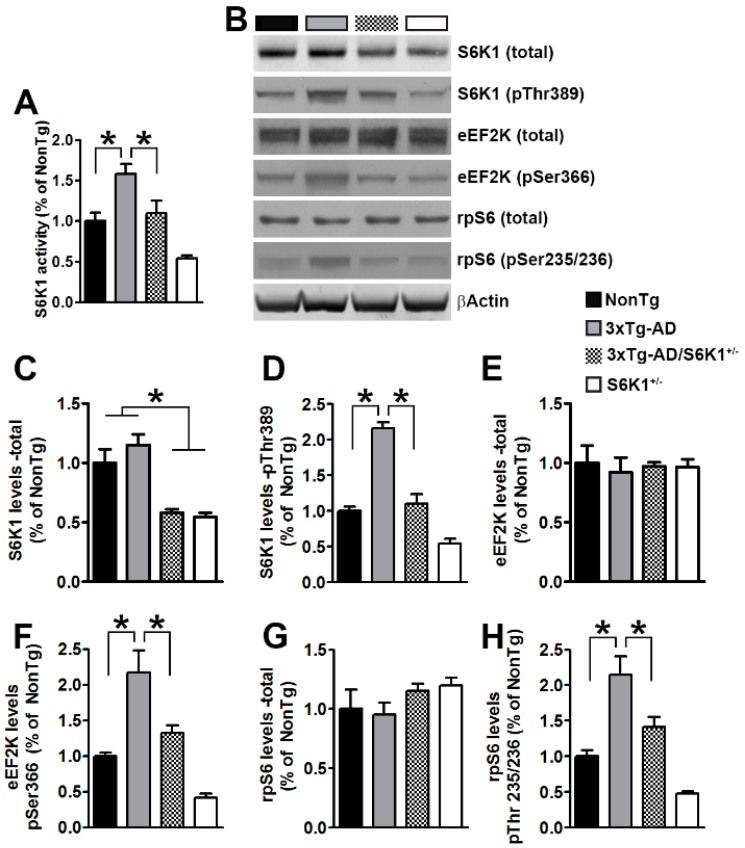

Figure 13. Reduced S6K1 signaling in 3xTg-AD/S6K1$^{+/-}$ mice. **(A)** S6K1 activity across the four groups [$p < 0.001$; $F(3, 28) = 14.15$]. *Post hoc* tests indicated that S6K1 activity in 3xTg-AD mice was significantly different from NonTg mice ($p < 0.01$, $t = 3.63$) and 3xTg-AD/S6K1$^{+/-}$ mice ($p < 0.05$, $t = 3.03$). Further, S6K1 activity in NonTg mice was similar to 3xTg-AD/S6K1$^{+/-}$ mice ($p > 0.05$, $t = 0.60$). **(B)** Western blots probed with the indicated antibodies. **(C)** Quantitative analyses of the blots probed for total S6K1 [$p < 0.0001$; $F(3, 28) = 15.01$]. *Post hoc* tests indicated that total S6K1 levels in NonTg mice were significantly different than 3xTg-AD/S6K1$^{+/-}$ ($p < 0.01$, $t = 3.80$. In contrast, no difference was found between NonTg and 3xTg-AD mice ($p > 0.05$, $t = 1.37$). Total S6K1 levels in 3xTg-AD mice were significantly different than 3xTg-AD/S6K1$^{+/-}$ mice ($p < 0.01$, $t = 5.18$). **(D)** The levels of S6K1 phosphorylated at Thr389 (pThr389) were significantly different among the four groups [$p < 0.0001$; $F(3, 28) = 57.48$]. *Post hoc* tests indicated that S6K1-pThr389 levels in 3xTg-AD mice were significantly different from NonTg mice ($p < 0.01$, $t = 9.11$), 3xTg-AD/S6K1$^{+/-}$ mice ($p < 0.01$, $t = 8.30$). S6K1-pThr389 levels in NonTg mice were similar to those of 3xTg-AD/S6K1$^{+/-}$ mice ($p > 0.05$, $t = 0.81$). **(E)** Total levels of eEF2K [$p > 0.05$; $F(3, 28) = 0.10$]. **(F)** eEF2K levels phosphorylated at Ser366 (eEF2K-pSer366) [$p < 0.0001$; $F(3, 28) = 19.66$]. *Post hoc* tests indicated that the eEF2K-pSer366 levels in NonTg mice were significantly different from 3xT-AD mice ($p < 0.01$, $t = 5.03$), but not from 3xTg-AD/S6K1$^{+/-}$ ($p > 0.05$, $t = 1.38$). In 3xTg-AD mice, the eEF2K-pSer366 levels were significantly different compared to 3xTg-AD/S6K1$^{+/-}$ ($p < 0.01$, $t = 3.65$). **(G)** Total levels of rpS6 [$p > 0.05$; $F(3, 28) = 1.24$]. **(H)** rpS6 levels phosphorylated at Thr235/236 (pThr235/236), [$p < 0.0001$; $F(3, 28) = 20.29$]. *Post hoc* tests indicated that the rpS6-pThr235/236 levels in NonTg mice were significantly different compared to 3xTg-AD mice ($p < 0.01$, $t = 5.17$), but not when compared to 3xTg-AD/S6K1$^{+/-}$ ($p > 0.05$, $t = 1.86$). rpS6-pThr235/236 levels in 3xTg-AD mice were significantly different compared to 3xTg-AD/S6K1$^{+/-}$ ($p < 0.05$, $t = 3.30$). Western blot data were obtained by normalizing the arbitrary fluorescent unit of the protein of interest to β-actin. Data were analyzed by one-way ANOVA followed by Bonferroni *post hoc* tests. For each experiment shown, $n = 8$ mice/genotype. Error bars represent mean ± s.e.m.

Given that mTOR/S6K1 signaling is necessary for proper learning and memory and hyperactive mTOR is detrimental, we designed our breeding strategy to reduce S6K1 activity in the 3xTg-AD mice in order to mitigate but not abolish S6K1 activity. Indeed, S6K1 activity and signaling in 3xTg-AD/S6K1$^{+/-}$ mice was similar to NonTg mice. To investigate basal synaptic transmission, we generated input/output (I/O) curves by measuring field excitatory postsynaptic potentials (fEPSPs) elicited in CA1 by stimulation of the Schaffer collaterals at increasing stimulus intensities. We found a statistically significant change in the I/O curves of the four groups ($p <$ 000.1; Fig. 14A). Tukey's *post hoc* tests revealed the I/O curves of NonTg and S6K1$^{+/-}$ mice were similar between each other but significantly different from the I/O curves of 3xTg-AD and 3xTg-AD/S6K1$^{+/-}$ mice. We next investigated paired-pulse facilitation (PPF), a measure of short-term plasticity. We found a significant difference in the amount of facilitation among the four groups ($p < 0.05$; Fig. 14B). A *post hoc* test with Bonferroni correction indicated that only the 3xTg-AD and S6K1$^{+/-}$ groups were significantly different from each other. Together, these data highlight a dissociation between basic synaptic transmission and S6K1 activity.

We examined long-term potentiation (LTP), a form of plasticity thought to underlie learning and memory, in Schaffer collateral-CA1 synapses using hippocampal slices. We found that LTP was significantly impaired in 3xTg-AD mice compared to NonTg mice ($p < 0.001$; Fig. 14C). Notably, removing one copy of the *S6K1* gene from the 3xTg-AD mice was sufficient to rescue the LTP deficits (Fig. 14C). Indeed, LTP in 3xTg-AD/S6K1$^{+/-}$mice was similar to NonTg mice and significantly different from 3xTg-AD mice ($p < 0.01$). We also found that S6K1$^{+/-}$ mice demonstrated a similar level of LTP to NonTg and 3xTg-AD/S6K1$^{+/-}$ mice. The mean fEPSP slopes (normalized to baseline) 5 minutes after tetanic stimulation was 1.69 ± 0.08, 1.29 ± 0.04, 1.64 ± 0.06, and 1.65 ± 0.09 for NonTg, 3xTg-AD, 3xTg-AD/S6K1$^{+/-}$, and S6K1$^{+/-}$ mice, respectively (Fig. 14D).

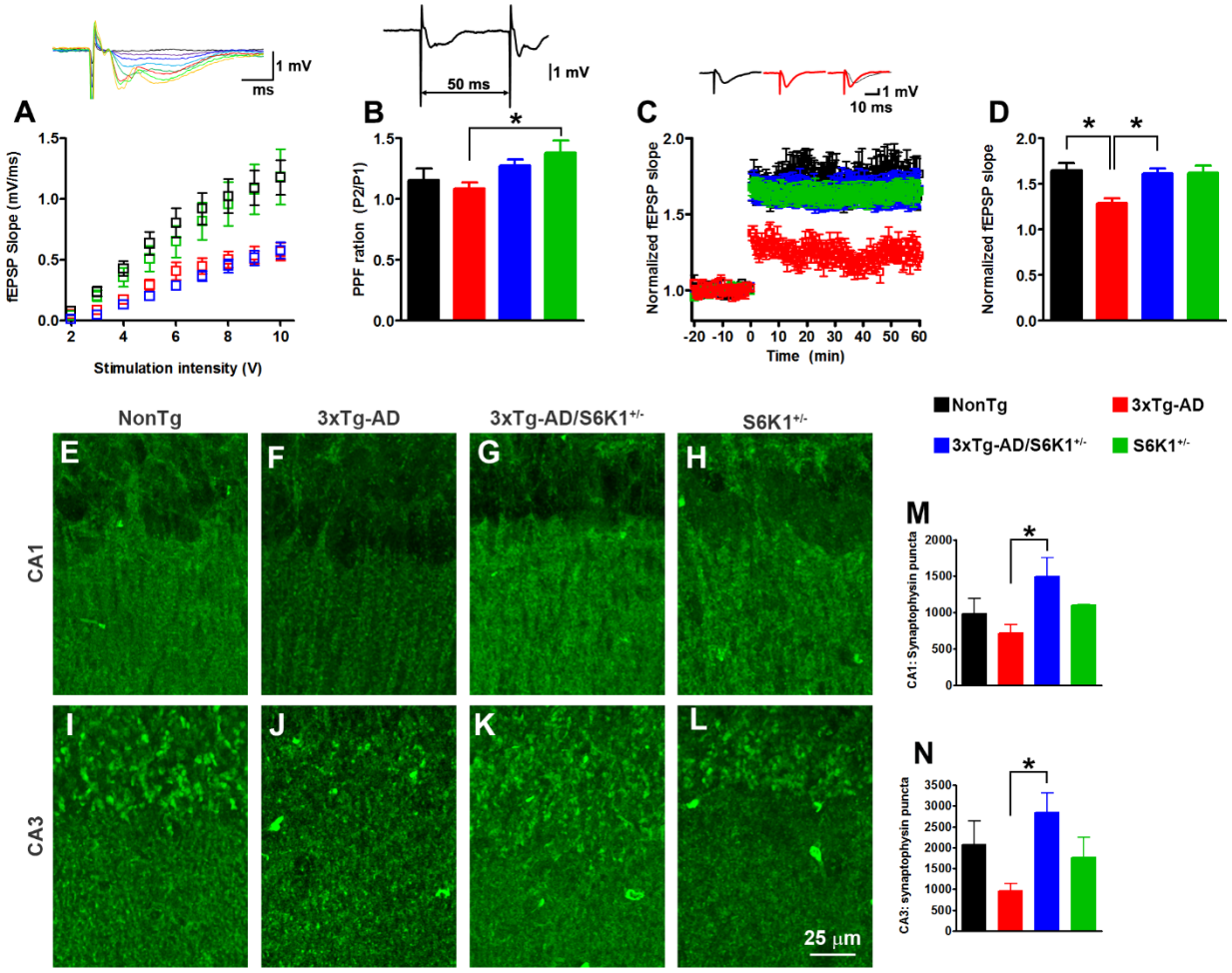

Figure 14. Reduced S6K1 signaling rescued synaptic deficits in 3xTg-AD mice. (A) Input/output (I/O) curves were obtained by measuring field excitatory postsynaptic potentials (fEPSPs) elicited in CA1 by stimulation of the Schaffer collaterals at increasing stimulus intensities. We analyzed the slope of each curve and found that they were statistically different from each other [F (3, 28) = 51.40; p < 0.0001]. *Post hoc* tests indicated that the I/O curves of NonTg mice were statistically significant from 3xTg-AD mice (p < 0.01, q = 12.39) and 3xTg-AD/S6K1$^{+/-}$ mice (p < 0.01, q = 11.68). The I/O curves of 3xTg-AD mice were not statistically significant compared to those of 3xTg-AD/S6K1$^{+/-}$ mice (p > 0.05, q = 0.71). Lastly, the I/O curves of 3xTg-AD/S6K1$^{+/-}$ and S6K1$^{+/-}$ were significantly different from each other (p < 0.01, q = 12.40). **(B)** PPF across the four groups [F (3, 56) = 3.05; p = 0.036]. *Post hoc* tests indicated that the only statistically significant difference was between 3xTg-AD and S6K1$^{+/-}$ mice (p < 0.05, q = 3.96). **(C)** Hippocampal LTP measured from 3xTg-AD, 3xTg-AD/S6K1$^{+/-}$, S6K1$^{+/-}$, and NonTg mice. **(D)** Cumulative data analyzed by one-way ANOVA showing the mean fEPSP slope 5 minutes after tetanic stimulation. Compared to NonTg mice, 3xTg-AD mice showed significant reduction of LTP [p < 0.001; F(3, 50) = 8.06]. In addition, LTP in 3xTg-AD;S6K1$^{+/-}$ mice was significantly higher than 3xTg-AD mice (p < 0.01), and it was similar to LTP from NonTg mice (p > 0.05). Data were recorded from NonTg (n = 13 slices from 5 mice), 3xTg-AD (n = 15 slices from 6 mice), 3xTg-AD/S6K1$^{+/-}$ (n = 16 slices from 5 mice), and S6K1$^{+/-}$ (n = 10 from 5 mice). **(E-L)** Confocal microphotographs of CA1 and CA3 sections from NonTg (n = 3 mice), 3xTg-AD, (n = 6 mice), 3xTg-AD/S6K1$^{+/-}$ (n = 6 mice), and S6K1$^{+/-}$ (n = 3 mice) stained with an anti-synaptophysin antibody. **(M-N)** Synaptophysin immunoreactivity was significantly different among the four groups CA1: p = 0.05; F(3, 14) = 3.21. CA3: p = 0.017; F(3, 14) 4.80. *Post hoc* tests indicated that in both hippocampal subregions the only statistically significant difference was between 3xTg-AD and 3xTg-AD/S6K1$^{+/-}$ mice (CA1: p < 0.05; t = 3.07. CA3: p < 0.05; t = 3.77). Error bars represent mean ± s.e.m.

To determine whether the LTP improvement corresponded to changes in synaptic markers, we measured synaptophysin immunoreactivity in CA1 and CA3 (Fig. 14E-N). To better quantify these changes, we analyzed 5 images per each section, per brain region (3-6 mice/genotype). We found that the total number of synaptophysin puncta was significantly different among the four groups ($p < 0.05$ in both CA1 and CA3; Fig. 14M-N). A *post hoc* test with Bonferroni correction indicated that in both CA1 and CA3, the 3xTg-AD/S6K1$^{+/-}$ mice had significantly more synaptophysin puncta when compared to 3xTg-AD mice. While our data are not meant to suggest a causal relation between synaptophysin levels and LTP deficits, these results implicate S6K1 as a key protein in the hippocampal synaptic deficit found in 3xTg-AD mice.

3.2.2 Reducing S6K1 levels rescue spatial memory deficits in 3xTg-AD mice

To determine the effect of removing one copy of the *S6K1* gene on spatial memory deficits developed by the 3xTg-AD mice, we tested 15-month-old mice on the spatial version of the Morris water maze (MWM). We gave mice four training trials per day for five consecutive days to learn the location of a hidden platform using distal extra maze cues. The distance traveled and the escape latency to find the platform across the training trials are indicators of mouse learning, with less distance and less time interpreted as better performance. Using a mixed ANOVA, we found that for the distance travelled there was a significant effect for days ($p < 0.0001$) and genotype ($p < 0.0001$) as well as a significant genotype x day interaction ($p < 0.002$; Fig 15A). The effect of day indicated that all mice learned the task across days whereas the effect of genotype indicated that one or more genotypes had a different pace of learning from each other. A *post hoc* test with Bonferroni correction showed that 3xTg-AD/S6K1$^{+/-}$ mice performed significantly better than 3xTg-AD mice on day 5 ($p < 0.01$; Fig. 15A). Notably, the 3xTg-AD/S6K1$^{+/-}$ mice after three, four, and five days of training performed as well as NonTg and S6K1$^{+/-}$ mice. We obtained similar results when we analyzed the escape latency as we found a significant effect for days ($p < 0.0001$) and genotype ($p = 0.008$; Fig. 15B). A *post hoc* test with Bonferroni correction showed that 3xTg-

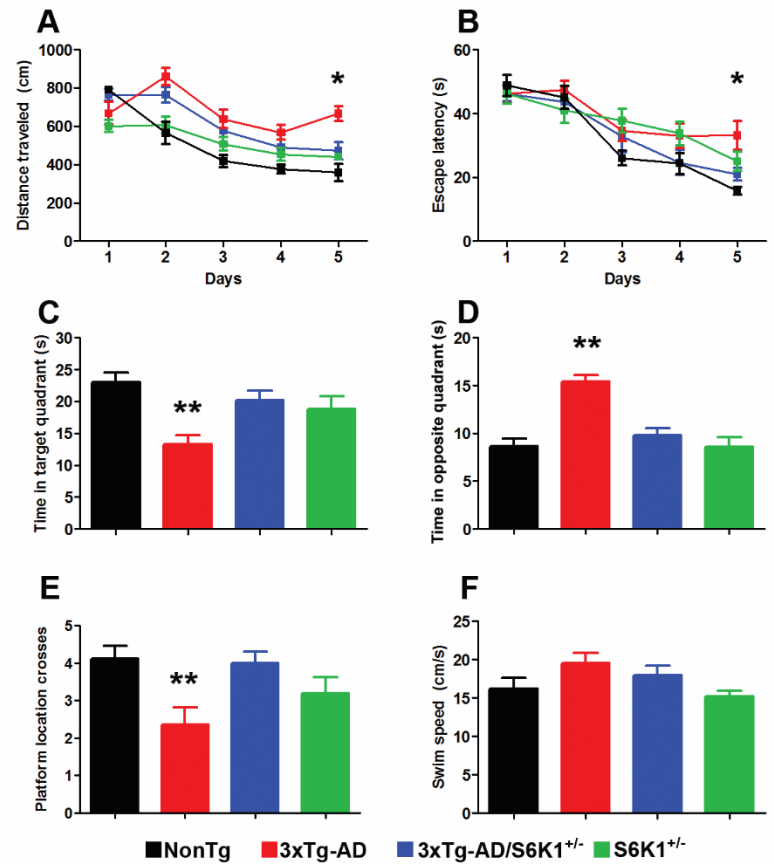

Figure 15. Reducing S6K1 levels improves spatial learning and memory deficits in 3xTg-AD mice. **(A-B)** Learning curve of mice trained in the spatial reference version of the Morris water maze (MWM). NonTg, n = 10 mice; S6K1$^{+/-}$, n = 10 mice; 3xTg-AD, n = 14 mice; 3xTg-AD/S6K1$^{+/-}$ n = 14 mice. The distance traveled and the escape latency to find the hidden platform was plotted against the days of training. The values for each day represent the average of four training trails. For the distance traveled, we found a significant effects for day [$p < 0.0001$; $F(3, 43) = 23.81$], genotype [$p < 0.0001$; $F(3, 43) = 15.99$] and genotype x day interaction [$p = 0.0018$; $F(12, 172) = 2.74$]. For the escape latency, we found a significant effect for day [$p < 0.0001$; $F(3, 43) = 32.19$], genotype [$p = 0.008$; $F(3, 43) = 4.01$]. *Post hoc* tests indicated that the distance traveled was higher in 3xTg-AD mice compared to NonTg mice on day 2 ($p < 0.001$, $t = 4.38$), day 3 ($p < 0.01$, $t = 3.27$), day 4 ($p < 0.05$, $t = 2.85$), and day 5 ($p < 0.001$, $t = 4.57$). However, the 3xTg-AD/S6K1$^{+/-}$ mice performed significantly worse than NonTg mice only on day 2 ($p < 0.05$, $t = 2.91$). Further, the distance traveled between 3xTg-AD and 3xTg-AD/S6K1$^{+/-}$ was significantly different on day 5 ($p < 0.01$; $t = 3.20$). The escape latency of NonTg mice was significantly different compared to 3xTg-AD mice at day 5 ($p < 0.01$, $t = 3.47$). However, 3xTg-AD/S6K1$^{+/-}$ mice performed as well as NonTg mice (day 5: $p > 0.05$; $t = 1.03$). **(C)** Time mice spent in the target quadrant during a single 60-second trial [$p = 0.001$; $F(3, 43) = 6.52$]. P*ost hoc* tests showed that 3xTg-AD mice performed significantly worse when compared to NonTg mice ($p < 0.05$; $t = 4.14$). More importantly, the 3xTg-AD/S6K1$^{+/-}$ mice performed significantly better than 3xTg-AD mice ($p < 0.05$; $t = 3.30$) and as well as NonTg mice ($p > 0.05$; $t = 2.42$). **(D)** Time mice spent in the opposite quadrant during a single 60-second trial [$p < 0.0001$; $F(3, 43) = 18.06$]. *Post hoc* tests showed that 3xTg-AD mice performed significantly worse when compared to NonTg mice ($p < 0.05$; $t = 5.80$), while 3xTg-AD/S6K1$^{+/-}$ mice performed significantly better than 3xTg-AD mice ($p < 0.05$; $t = 5.46$) and as well as NonTg mice ($p > 0.05$; $t = 0.98$). **(E)** Number of platform location crosses during a single 60-second probe trial [$p = 0.007$; $F(3, 43) = 4.52$]. *Post hoc* tests showed that 3xTg-AD mice performed significantly worse than NonTg mice ($p < 0.05$; $t = 3.01$). 3xTg-AD/S6K1$^{+/-}$ mice performed significantly better than 3xTg-AD mice ($p < 0.05$; $t = 3.19$) and as well as NonTg mice ($p > 0.05$; $t = 0.19$). **(F)** Swim speed was similar among the four different groups [$p > 0.05$; $F(3, 43) = 2.38$]. Learning data were analyzed by two-way ANOVA; probe trials were analyzed by one-way ANOVA. Bonferroni's was used for *post hoc* tests. * indicates a significant difference between 3xTg-AD and 3xTg-AD/S6K1+/- mice. Error bars represent mean ± s.e.m.

AD mice were significantly impaired on day 5 compared to NonTg mice ($p < 0.01$; Fig. 15B). Most notably, on day 5, the 3xTg-AD/S6K1$^{+/-}$ mice performed significantly better than 3xTg-AD mice ($p < 0.05$) and as well as NonTg mice ($p > 0.05$; Fig. 15B).

Twenty-four hours after the last training trial, we conducted probe trials to measure spatial reference memory. Specifically, we measured the time mice spent in the target and opposite quadrants as well as the number of platform location crosses during a single 60-second trial. We found that 3xTg-AD mice spent significantly less time in the target quadrant and more time in the opposite quadrant compared to the other three genotypes ($p = 0.001$; Fig. 15C-D). For the number of platform location crosses, we found that 3xTg-AD mice performed significantly worse when compared to the other three groups ($p = 0.007$; Fig. 15E). In contrast, the swim speed was not statistically significant among the four genotypes (Fig. 15F), indicating that the genotype effects on learning and memory were independent of physical performance. Taken together, these findings indicate that removing one copy of the S6K1 gene from 3xTg-AD mice is sufficient to rescue spatial learning and memory deficits.

3.2.3 Removing one copy of the *S6K1* gene lowers Aβ and tau pathology in 3xTg-AD mice

A key neuropathological feature of AD is the accumulation of neurofibrillary tangles made of hyperphosphorylated tau, a microtubule binding protein (Querfurth and LaFerla, 2010). To determine the effects of removing one copy of the gene encoding S6K1 from the 3xTg-AD mice, we first immunostained sections from 3xTg-AD and 3xTg-AD/S6K$^{+/-}$ mice with CP13, an antibody that recognizes tau phosphorylated at Serine 202. We found that CP13 immunoreactivity was markedly reduced in 3xTg-AD/S6K1$^{+/-}$ compared to 3xTg-AD mice (Fig. 16A-C). To further assess the tau pathology, we measured tau levels by western blot using antibodies against total and phosphorylated tau (Fig. 16D). We found that the levels of total human and mouse tau (measured by the HT7 and tau 5, respectively), were significantly different among the four groups ($p < 0.0001$;

Fig. 16E). A *post hoc* test with Bonferroni correction indicated that human tau levels in all groups were significantly different from each other with the exception of the NonTg with the S6K1$^{+/-}$ mice. The levels of mouse tau were significantly higher in 3xTg-AD mice compared to the other three

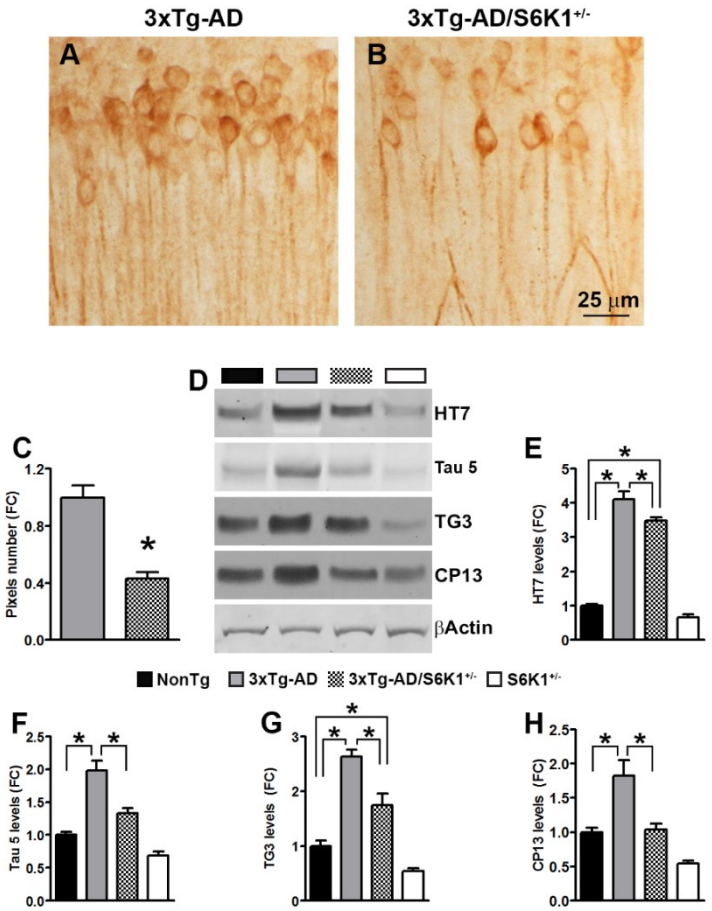

Figure 16. Reduced tau pathology in 3xTg-AD/S6K1$^{+/-}$ mice. (A-B) Microphotographs of CA1 neurons from 3xTg-AD and 3xTg-AD/S6K1$^{+/-}$ mice stained with the anti-tau antibody CP13, which recognizes tau phosphorylated at Ser202. **(C)** Quantitative analysis of the CP13 immunoreactivity by unpaired t-test [$t(14) = 5.96$; $p < 0.0001$]. **(D)** Western blots of protein extracted from NonTg, 3xTg-AD and 3xTg-AD/S6K1$^{+/-}$, and S6K1$^{+/-}$ mice. Blots were probed with the indicated antibodies. The HT7 antibody recognizes total human tau, the Tau 5 antibody recognizes total mouse tau, the TG3 antibody recognizes tau phosphorylated at Thr231. **(E-H)** Quantitative analyses of the blots obtained by normalizing the quantity of a specific protein with its loading control, β-actin. Data were analyzed by one-way ANOVA followed by a Bonferroni's multiple comparison test. For HT7: [$p < 0.0001$; $F(3, 28) = 166$]. *Post hoc* tests indicated that all groups were significantly different from each other with the exception of the NonTg with the S6K1$^{+/-}$ mice. For tau 5: [$p < 0.0001$; $F(3, 28) = 35.83$]. *Post hoc* tests indicated that the 3xTg-AD mice has significantly higher tau 5 levels than all the other three groups. Tau 5 levels in 3xTg-AD/S6K1$^{+/-}$ mice were higher than S6K1$^{+/-}$ mice, while no differences were observed between NonTg and 3xTg-AD/S6K1$^{+/-}$ and between NonTg and S6K1$^{+/-}$ mice. For TG3: [$p < 0.0001$; $F(3, 28) = 44.66$]. *Post hoc* tests indicated that all groups were significantly different from each other with the exception of the NonTg with the S6K1$^{+/-}$ mice. For CP13: [$p < 0.0001$; $F(3, 28) = 18.53$]. *Post hoc* tests indicated that all groups were significantly different from each other with the exception of the NonTg with the S6K1$^{+/-}$ mice. $n = 8$ mice/genotype. Error bars, represent mean ± s.e.m.

groups, including NonTg mice. Notably, mouse tau levels were not different between 3xTg-AD/S6K1$^{+/-}$ and NonTg mice nor were they different between NonTg and S6K1$^{+/-}$ mice. We also found that the levels of tau phosphorylated at Thr231 (measured by the TG3 antibody) and at Ser202 (measured by the CP13 antibody) were significantly different among the four groups (p < 0.0001; Fig. 16G-H). A *post hoc* test with Bonferroni correction indicated that TG3 levels in all groups were significantly different from each other with the exception of the NonTg with the S6K1$^{+/-}$ mice. CP13 levels were significantly higher in 3xTg-AD mice compared to the other three groups, including NonTg mice. Notably, CP13 levels were not different between 3xTg-AD/S6K1$^{+/-}$ and NonTg mice nor were they different between NonTg and S6K1$^{+/-}$ mice. Together, these results clearly indicate that removing one copy of the S6K1 gene is sufficient to ameliorate tau pathology in 3xTg-AD mice.

In addition to tau pathology, the accumulation of extracellular Aβ plaques is another hallmark of AD (Oddo et al., 2003b). Aβ peptides consist of 36 to 43 amino acids; $A\beta_{40}$ and $A\beta_{42}$ are the more abundant Aβ species, with the latter being more prone to aggregation and toxicity as compared to $A\beta_{40}$ (Querfurth and LaFerla, 2010). We immunostained sections from 3xTg-AD and 3xTg-AD/S6K1$^{+/-}$ mice with an $A\beta_{42}$ specific antibody and found that $A\beta_{42}$ immunoreactivity was significantly reduced in the brains of the 3xTg-AD mice lacking one copy of the S6K1 gene (Fig. 17A-D). Quantitative analysis of the overall Aβ load indicated a significant decrease of 64.32 ± 3.2% in the brain of 3xTg-AD/S6K1$^{+/-}$ compared to 3xTg-AD mice (p < 0.001). We next measured Aβ levels by sandwich enzyme-linked immunosorbent assay (ELISA) and found that soluble $A\beta_{42}$ and $A\beta_{40}$ levels were significantly lower in 3xTg-AD/S6K1$^{+/-}$ mice compared to 3xTg-AD mice (p = 0.01 and p = 0.03, respectively; Fig. 17E). We further found that while insoluble $A\beta_{40}$ levels were similar between the two groups, insoluble $A\beta_{42}$ levels were significantly lower in 3xTg-AD/S6K1$^{+/-}$ mice compared to 3xTg-AD mice (p = 0.02; Fig. 17F). To determine whether alterations in APP processing could account for the changes in Aβ levels, we measured the levels of full-length APP

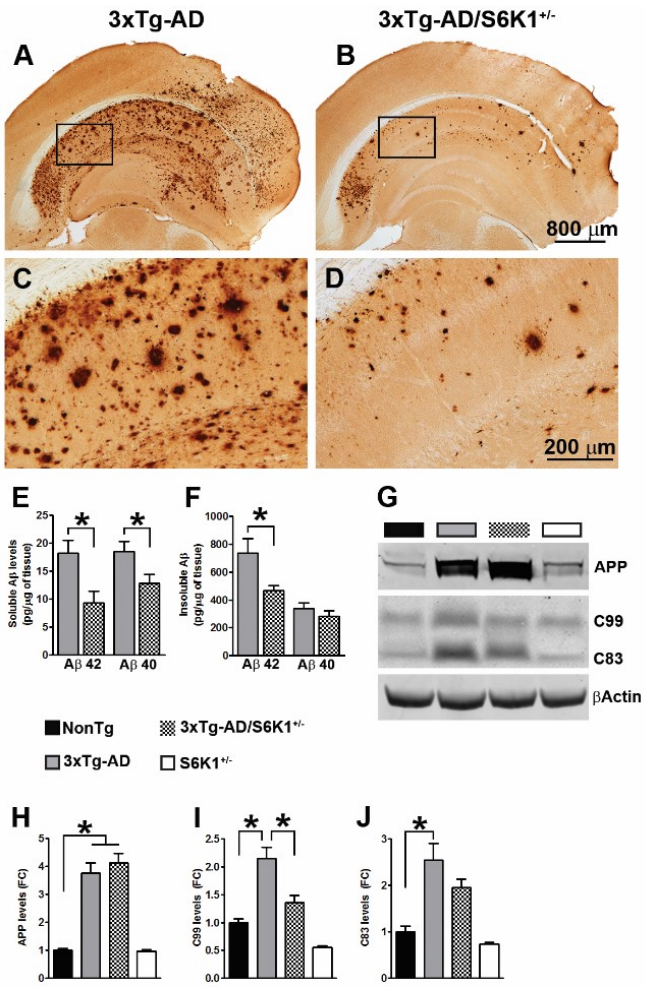

Figure 17. **Reduced Aβ pathology in 3xTg-AD/S6K1$^{+/-}$ mice.** (**A-D**) Photographs of brains sections stained with an anti-Aβ_{42} specific antibody. Panels c and d are high magnification images of the boxed areas in panels a and b, respectively. (**E**) ELISA measurements of soluble Aβ_{42} and Aβ_{40} levels. The levels of both peptides were significantly lower in mice lacking one copy of the S6K1 gene [t(14) = 2.31; p = 0.03 for Aβ_{40} and t(14) = 2.81; p = 0.01 for Aβ_{42}]. n = 8 mice/genotype. (**F**) ELISA measurements of insoluble Aβ_{42} and Aβ_{40} levels. While the levels of insoluble Aβ_{40} were similar between the two groups, the levels of insoluble Aβ_{42} were significantly lower in 3xTg-AD/S6K1$^{+/-}$ mice compared to 3xTg-AD mice [t(14) = 2.46; p = 0.02]. ELISA data were analyzed by student's t-test. (**G**) Western blots of protein extracted from NonTg, 3xTg-AD, 3xTg-AD/S6K1$^{+/-}$, and S6K1$^{+/-}$ mice. To identify full-length APP, blots were probed with 6E10. To identify C99 and C83, blots were probed with CT20, a C-terminal anti-APP antibody. **(H-J)** Quantitative analyses of the blots obtained by normalizing the quantity of a specific protein with its loading control, β-actin. Data were analyzed by one-way ANOVA followed by a Bonferroni's multiple comparison test (n = 8 mice/genotype). For APP: [p < 0.0001; F(3, 28) = 49.05]. *Post hoc* analysis indicated that APP levels were significantly higher in 3xTg-AD and 3xTg-AD/S6K1$^{+/-}$ compared to the other two groups. No differences were observed between 3xTg-AD and 3xTg-AD/S6K1$^{+/-}$ mice For C99: [p < 0.0001; F(3, 28) = 28.44]. *Post hoc* tests indicated that C99 levels were significantly higher in 3xTg-AD mice compared to the other three groups. No significant difference was found between NonTg and 3xTg-AD/S6K1$^{+/-}$ mice. For C83: [p < 0.0001; F(3, 28) = 15.90]. *Post hoc* tests indicated that C83 levels were significantly higher in 3xTg-AD and 3xTg-AD/S6K1$^{+/-}$ compared to the other two groups. No differences were observed between 3xTg-AD and 3xTg-AD/S6K1$^{+/-}$ mice. Error bars represent mean ± s.e.m.

and its two major C-terminal fragments, C99 and C83 in all four genotypes. We found that full-length APP levels were significantly different among the four groups ($p < 0.0001$; Fig. 17G-H). A *post hoc* test with Bonferroni correction indicated that 3xTg-AD and 3xTg-AD/S6K1$^{+/-}$ mice had higher APP levels than the other two groups, consistent with the presence of the APP transgene. Notably, APP levels were not statistically significant between 3xTg-AD and 3xTg-AD/S6K1$^{+/-}$ mice. For C99 and C83, we also found a significant change among the four groups ($p < 0.0001$; Fig. 17I-J). *A post hoc* test with Bonferroni correction indicated that C99 levels in 3xTg-AD mice were significantly different from the other three groups. However, removing one copy of the *S6K1* gene was sufficient to reduce C99 levels. To this end, C99 levels were similar between NonTg and 3xTg-AD/S6K1$^{+/-}$ mice. C83 levels were significantly different in the 3xTg-AD mice compared to NonTg and S6K1$^{+/-}$ mice; in contrast, they were similar between 3xTg-AD and 3xTg-AD/S6K1$^{+/-}$ mice. These results suggest that removing one copy of the *S6K1* gene is sufficient to reduce C99 levels together with Aβ burden and levels.

3.2.4 Low S6K1 signaling reduces BACE-1 and tau translation

Our data indicate that removing one copy of the S6K1 gene in 3xTg-AD mice is sufficient to ameliorate spatial learning and memory deficits. These changes were associated with an improvement in synaptic plasticity and a reduction in Aβ and tau pathology. To better understand the mechanisms underlying these changes, we first assess potential changes in autophagy induction and proteasome function. We focused on these systems as they represent the two major cellular protein degradation systems and are known to be involved in the turnover of Aβ and tau. First, we used the fluorogenic substrates Bz-VGR-AMC, Suc-LLVYAMC, and Z-LLE-AMC to measure trypsin-like, chymotrypsin-like, and caspase-like activities of the proteasome. For all three activities, we found an effect of time ($p < 0.0001$; Fig. 18A-C) but not genotype, indicating that proteasome function was similar among the four groups. Next, we assessed autophagy induction by measuring the levels of Atg3, Atg5, Atg7 and Atg12, and p62. These are key proteins

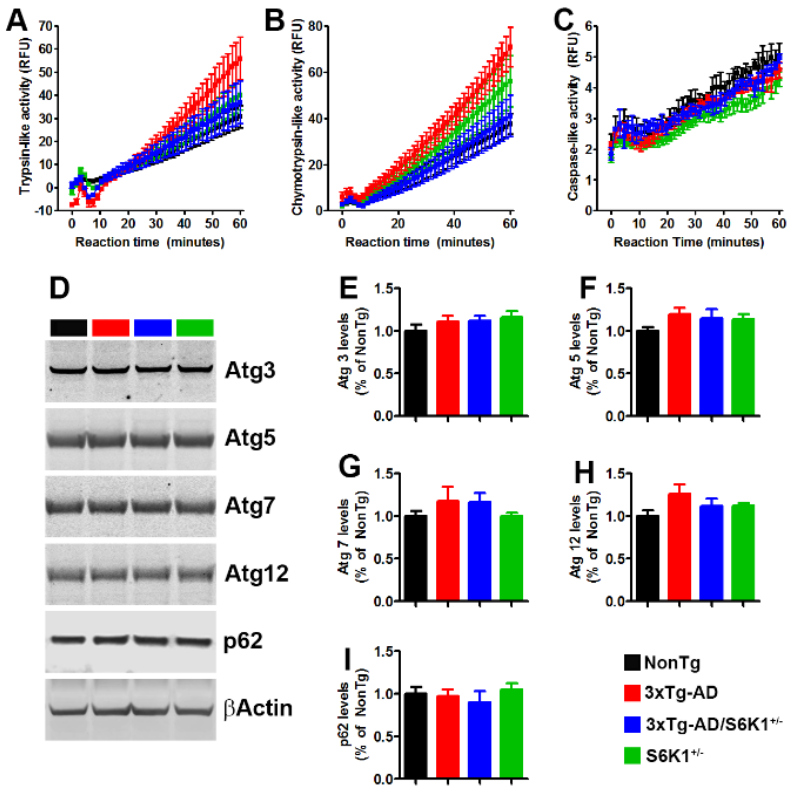

Figure 18. **Proteasome activity and autophagy induction are not affected by S6K1 signaling**. **(A-C)** Brain homogenates from NonTg, 3xTg-AD, 3xTg-AD/S6K1$^{+/-}$ and S6K1$^{+/-}$ mice were analyzed for proteasome activity (n = 4 mice/genotype). Data were analyzed by two-way ANOVA, which revealed no genotype effect of any of the three enzymatic activities measured. Panel a: [$p > 0.05$; $F(3, 12) = 0.77$]. Panel b: [$p > 0.05$; $F(3, 12) = 2.56$]. Panel c: [$p > 0.05$; $F(3, 12) = 2.87$]. **(D)** Representative western blots of protein extracted from the brains of NonTg, 3xTg-AD, 3xTg-AD/S6K1$^{+/-}$, and S6K1$^{+/-}$ mice (n = 8 mice/genotype). Blots were probed with the indicated antibodies. **(E-I)** Quantitative analyses of the blots were obtained by normalizing the protein of interest to β-Actin, used as a loading control. One-way ANOVA analyses indicated that none of these markers were statistically significant among the four groups. Panel b: [$p > 0.05$; $F(3, 28) = 0.43$]. Panel c: [$p > 0.05$; $F(3, 28) = 1.35$]. Panel d: [$p > 0.05$; $F(3, 28) = 0.81$]. Panel e: [$p > 0.05$; $F(3, 28) = 1.82$]. Panel f: [$p > 0.05$; $F(3, 28) = 0.50$]. Error bars represent mean ± s.e.m.

in autophagy induction and are routinely used to monitor it (Mizushima, 2004) . We found that the levels of these autophagy-related proteins were similar among the four groups (Fig. 18D-I). Together, these data suggest that proteasome and autophagy are not likely involved in the S6K1-mediated changes in Aβ and tau levels.

We found that C99 levels were significantly lower in 3xTg-AD/S6K1$^{+/-}$ mice compared to 3xTg-AD

mice. C99 is liberated from APP by a proteolytic cleavage executed by BACE-1, which is then further cleaved by the γ-secretase complex to generate Aβ (Querfurth and LaFerla, 2010). Therefore, we measured PS1 and BACE-1 levels by western blot. While PS1 levels were similar among the four groups, we found a significant change in BACE-1 levels ($p = 0.0007$; Fig. 19A-C). Bonferroni *post hoc* tests indicated that BACE-1 levels were significantly different in 3xTg-AD mice when compared to the other three groups. No other pairwise comparisons were statistically significant. To better understand the involvement of BACE-1, we measured BACE-1 enzymatic activity and found a significant difference among the four groups ($p < 0.0001$; Fig. 19D). Bonferroni *post hoc* tests indicated that all the groups were significantly different from each other with the exception of NonTg and 3xTg-AD/S6K1$^{+/-}$ mice. To better understand the mechanisms underlying the changes in BACE-1 levels and activity, we measured BACE-1 mRNA by quantitative PCR (qPCR). We found that the mRNA levels of BACE-1 were similar among the four groups ($p = 0.08$; Fig. 19E). Given the role of S6K1 in protein synthesis and that BACE-1 mRNA levels were similar between 3xTg-AD and 3xTg-AD/S6K1$^{+/-}$ mice while BACE-1 proteins levels were lower in 3xTg-AD/S6K1$^{+/-}$ mice, we hypothesized that changes in translation of the BACE-1 mRNA may account for the reduced BACE-1 levels and activity. To test this hypothesis, we measured the amount of BACE-1 mRNA associated with heavy polysomes (i.e., actively translated) in the brains of 3xTg-AD/S6K1$^{+/-}$ and 3xTg-AD mice. To obtain a ribosome profiling, we used an established ribosome fractionation protocol on 10-50% linear sucrose gradient (Gandin et al., 2014). To assess the amount of BACE-1 actively translated, we compared the mean BACE-1 mRNA levels in the fractions containing the polysomes. We found that the levels of BACE-1 mRNA associated with polysomes were significantly different among the four groups ($p = 0.0027$; Fig. 19F). Bonferroni *post hoc* tests indicated that BACE-1 mRNA levels actively translated were higher in 3xTg-AD mice compared to all the other groups; however, no difference was found between NonTg and 3xTg-AD/S6K1$^{+/-}$ mice. Taken together, these data suggest that BACE-1 translation in 3xTg-AD mice is higher than NonTg mice but it is similar between NonTg and 3xTg-AD/S6K1$^{+/-}$ mice.

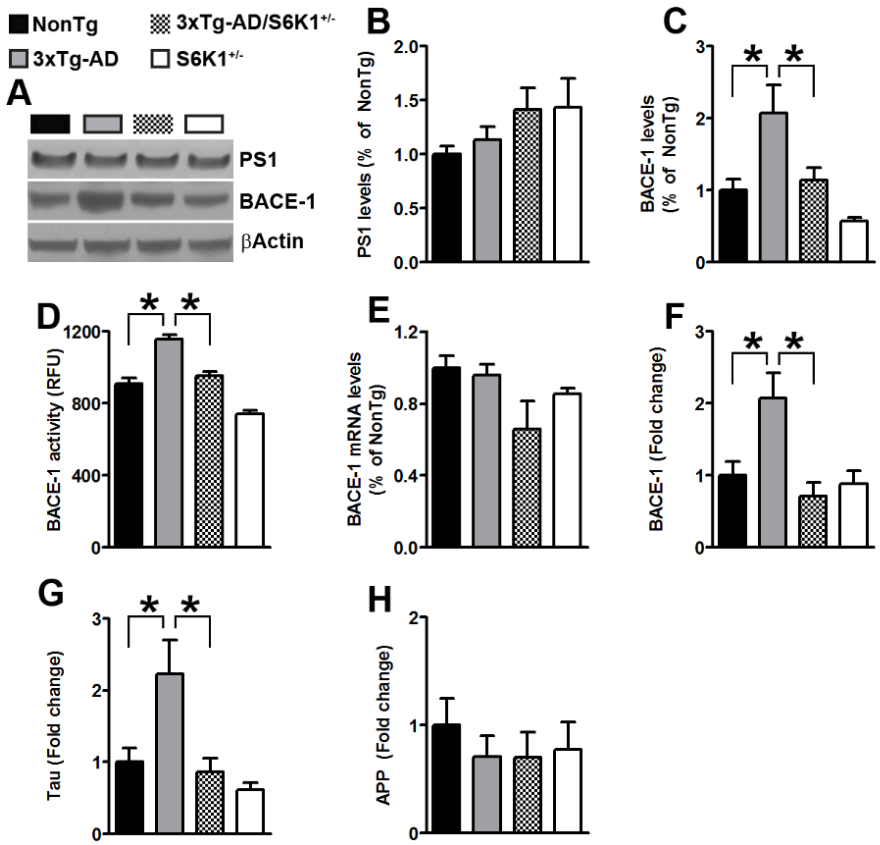

Figure 19. Removing one copy of the S6K1 gene reduces BACE-1 activity and translation and tau translation. **(A)** Western blot of protein extracted from NonTg, 3xTg-AD, 3xTg-AD/S6K1$^{+/-}$, and S6K1$^{+/-}$ mice (n = 8 mice) and probed with the indicated antibodies. **(B)** The graph shows the quantitative analyses of the PS1 blot. The values were similar among the four groups. **(C)** BACE-1 protein levels were significantly different among the four groups [$p = 0.0007$; $F(3, 28) = 7.62$]. *Post hoc* tests revealed that BACE-1 levels were significantly different between NonTg and 3xTg-AD mice ($p < 0.05$, $t = 3.31$). In contrast, BACE-1 levels in 3xTg-AD mice were significantly different than 3xTg-AD/S6K1$^{+/-}$ ($p < 0.05$, $t = 2.87$). **(D)** The graph shows BACE-1 enzymatic activity (n = 6 mice/genotype), which was significantly different among the four groups [$p < 0.0001$; $F(3, 20) = 7.62$]. Post hoc analyses revealed that BACE-1 activity in NonTg mice was significantly different than 3xTg-AD mice ($p < 0.01$, $t = 6.66$) but not from 3xTg-AD/S6K1$^{+/-}$ mice. BACE-1 activity in 3xTg-AD mice was significantly different compared to 3xTg-AD/S6K1$^{+/-}$ ($p < 0.01$, $t = 5.42$) mice. **(E)** The graph shows BACE-1 mRNA levels obtained by qPCR ($n = 4$ mice), which were not statistically different among the four groups. **(F)** The graph shows BACE-1 mRNA levels in the fractions containing heavy polysomes, which are expressed as fold change over NonTg. The levels of BACE-1 mRNA were significantly different among the four groups [$p = 0.0027$; $F(3, 20) = 6.66$]. *Post hoc* tests indicated that the 3xTg-AD mice were significantly different than the other three groups, while 3xTg-AD/S6K1$^{+/-}$ mice were similar to NonTg mice. **(G)** The levels of tau mRNA were significantly different among the four groups [$p = 0.002$; $F(3, 20) = 7.89$]. *Post hoc* tests indicated that the 3xTg-AD mice were significantly different than the other three groups, while 3xTg-AD/S6K1$^{+/-}$ mice were similar to NonTg mice. **(H)** The levels of APP mRNA were not significantly different among the four groups [$p = 0.78$; $F(3, 20) = 0.35$]. Quantitative analyses of the blots obtained by normalizing the quantity of a specific protein with its loading control, β-actin. Data were analyzed by one-way ANOVA followed by a Bonferroni's (panels b-e) or Tukey's (panels f-i) multiple comparison tests. Error bars represent mean ± s.e.m.

Previous data suggested that mTOR signaling is involved in the regulation of tau translation (Khurana et al., 2006). To test this hypothesis, we measured the levels of tau mRNA associated with heavy polysomes. We found a significant difference among the groups (p = 0.0019; Fig. 19G). Bonferroni *post hoc* tests indicated that tau mRNA levels associated with the polysome were higher in 3xTg-AD mice compared to the other groups; however, no difference was found between NonTg and 3xTg-AD/S6K1$^{+/-}$ mice. In contrast, APP mRNA levels were similar among the groups (Fig. 19H), suggesting that removing one copy of the *S6K1* gene does not alter global protein translation. This observation is consistent with previous reports (Garelick et al., 2013). Taken together, these data indicate that the lack of one copy of the S6K1 gene reduces BACE-1 and tau activities by decreasing translation of their mRNAs.

3.2.5 Discussion

Increasing evidence suggests that insulin resistance and concomitant elevated blood glucose is a key metabolic dysfunction contributing to AD (Cholerton et al., 2013). As mentioned above, S6K1 plays a key role in metabolic function and insulin resistance (Um et al., 2004). Thus, it is possible that the beneficial effects of S6K1 haploinsufficiency in the 3xTg-AD mice could be the result of reduced S6K1 activity in neurons or could instead be secondary to changes in peripheral energy metabolism. While we cannot directly distinguish between these two possibilities, our recent report argues for a central effect of S6K1 on AD-like pathology (Orr et al., 2014). To this end, we found that high sucrose intake induces obesity with changes in central and peripheral insulin signaling in 3xTg-AD mice. These changes were associated with increase in Aβ production and deposition as well as tau pathology. Notably, we showed that pharmacologically reducing the mTOR/S6K1 pathway with rapamycin prevented the detrimental effects of sucrose in the brain (e.g., central insulin signaling, Aβ and tau pathology), without changes in peripheral insulin resistance (Orr et al., 2014). Furthermore, chronic rapamycin administration ameliorates AD-like

phenotype in AD mouse models by reducing the mTOR/S6K1 pathway (Caccamo et al., 2010b; Majumder et al., 2011). These findings suggest that 3xTg-AD/S6K1$^{+/-}$ mice would be less responsive to rapamycin. Future studies are needed to directly evaluate this prediction.

Tau is a microtubule binding protein and a hallmark of several neurodegenerative disorders, collectively known as tauopathies (Querfurth and LaFerla, 2010). Pathological tau is hyperphosphorylated and it aggregates to form neurofibrillary tangles. Recently, there has been a growing appreciation of the role of tau in AD pathogenesis. To this end, reducing tau levels prevents cognitive deficits in transgenic mice characterized by the buildup of Aβ (Roberson et al., 2007). This and other reports support the hypothesis that reducing tau levels may represent a valid therapeutic approach for AD and other tauopathies (Frost et al., 2014; Iqbal et al., 2014). Here we show that removing one copy of the S6K1 gene reduces tau phosphorylation and accumulation at least in part by reducing translation of tau mRNA. Pathological tau is phosphorylated by several kinases including S6K1, which has been shown to directly phosphorylate tau at Serine 214, Serine 262 and Threonine 212 (Pei et al., 2006). Consistent with a direct interaction between S6K1 and tau are data from Drosophila and mice showing that the target of rapamycin, a protein kinase that activates S6K1, regulates tau levels and phosphorylation (Caccamo et al., 2013; Khurana et al., 2006). These data could explain the reduction in phosphorylated tau detected in 3xTg-AD/S6K1$^{+/-}$ mice. A direct interaction between S6K1 and tau may have profound implications for other tauopathies, such as frontotemporal degeneration, Pick's disease, and corticobasal degeneration. While further studies, in model of tau pathology are needed, our data promote S6K1 as a new therapeutic target for tauopathies. The tau pathology in 3xTg-AD mice is highly dependent on Aβ levels. For example, we have shown that genetic or immunological reduction of Aβ pathology significantly reduces tau deposition without altering the tau transgene levels (Oddo et al., 2008). The findings that Aβ can induce tau pathology have been recently showed *in vitro* as well (Choi et al., 2014). Therefore, it

is tempting to speculate that the S6K1-mediated decrease in tau may be linked, at least in part, to the reduced Aβ levels. Consistent with this theory, studies in neuroblastoma cells show that high Aβ levels concomitantly increase S6K1 and tau phosphorylation (Zhou et al., 2008). Overall, while the interaction between tau and S6K1 might be complex, the data presented here unambiguously demonstrate that reducing S6K1 levels ameliorates tau pathology.

Genetic and pharmacological manipulation of general protein synthesis have supported a key role for this process in long-term memory formation (Santini et al., 2014). The translation initiation factor eIF2 is a master regulator of general protein translation; indeed, its phosphorylation suppresses general protein translation (Donnelly et al., 2013). Consistent with the role of protein translation in memory formation, reducing the phosphorylation of eIF2 improves memory in wild type mice (Costa-Mattioli et al., 2007) and rescues memory deficits in a mouse model of AD (Ma et al., 2013a). However, there is growing appreciation that the relation between protein translation and memory formation is not as linear as originally thought. For example, there are several endogenous inhibitors of learning and memory, such as ATF4, and reducing translation of such proteins has beneficial effects on memory (Pavitt, 2013). Therefore, while the need for *de novo* protein synthesis during long-term memory formation of key proteins is undisputable, there is also strong evidence that reducing synthesis of selective proteins may benefit learning and memory (Pavitt, 2013). S6K1 controls several steps of protein synthesis. For example, it regulates ribosomal biogenesis by phosphorylating rpS6, which is located in mature ribosomes (Magnuson et al., 2012). The involvement of S6K1 in protein synthesis is further corroborated by studies showing its role in mRNA processing, translational initiation and elongation as well as protein folding (Magnuson et al., 2012). Early work using *post mortem* human brains suggested that alterations in protein translations may contribute to the pathogenesis of AD (Sajdel-Sulkowska and Marotta, 1984). Here we provide compelling evidence showing that reducing S6K1 levels decreases the translation of BACE-1, thereby affecting its protein levels and enzymatic activity.

In turn, the reduction in BACE-1 activity lowered C99 levels and Aβ production. Together, these finding further highlight a role of protein translation in AD and provide a new mechanisms by which S6K1 may affect AD pathogenesis.

The role of S6K1 in memory appears to be complex. For example, mice lacking both copies of the *S6K1* gene show contextual and spatial memory deficits (Antion et al., 2008). In contrast, mice lacking a copy of the tuberous sclerosis complex have high S6K1 signaling (Caccamo et al., 2013) as well as deficits in LTP and cognition (Ehninger et al., 2008). Notably, reducing mTOR/S6K1 signaling rescues LTP and cognitive deficits in these mice (Ehninger et al., 2008). Although the lack of S6K1 does not affect general protein synthesis (Garelick et al., 2013), our experiments were designed to reduce, but not eliminate, S6K1 activity in 3xTg-AD mice. Here we show that removing a single copy of S6K1 ameliorates the synaptic and spatial memory deficits associated with AD pathology. Our results support the notion that removing a single copy of the *S6K1* gene decreases the translation of BACE-1 and tau, two key proteins involved in AD pathogenesis.

Overall, our data provide compelling evidence indicating that reducing S6K1 levels improves the AD-like phenotype developed by the 3xTg-AD mice, including spatial memory deficits. Given the role of this protein kinase in aging, S6K1 may represent a molecular link between aging and AD. Aging is the major risk factor for most neurodegenerative diseases; thus, our results may have far-reaching implications into other diseases. Consequently, S6K1 may be a new therapeutic target for AD and other age-dependent diseases.

4. CONCLUDING REMARKS

The vast majority of AD cases (> 95%) are sporadic and of unknown etiology (Querfurth and LaFerla, 2010). Genetic and epidemiological studies have identified several risk factors that contribute to the pathogenesis of AD (Reitz and Mayeux, 2014). Aging is the single major risk factor for AD. In fact, even in the rare familial cases of AD, which are caused by autosomal dominant mutations, the disease develops as a function of age (Alzheimer's, 2014; Querfurth and LaFerla, 2010). Despite this wealth of information, little is known on how aging contributes to the pathogenesis of AD. Dissecting pathways that regulate the aging process may highlight new molecular mechanisms at the basis of AD pathogenesis. The mTOR/S6K1 pathway regulates cell growth and proliferation via different mechanisms, including by regulating gene expression and protein translation (Fenton and Gout, 2011). Notably, pharmacological reduction of mTOR improves lifespan in mice and other lower species (Richardson et al., 2015). Similarly, S6K1 knockout mice show an increased median and maximum lifespan, and a decrease in age-related diseases, including motor and immune dysfunction, insulin resistance, and obesity (Selman et al., 2009; Um et al., 2004). The data presented here unambiguously show that reduction of the mTOR/S6K1 signaling has beneficial effects on AD-like pathology developed by Tg2576 and 3xTg-AD mice. Indeed, we reported that APP/mTOR$^{+/-}$ mice performed significantly better than APP mice and as well as CTL mice in a spatial learning and memory task. Similarly, cognitive functions were restored in 3xTg-AD/S6K1$^{+/-}$ mice. These cognitive improvements were associated with a reduction in Aβ and tau pathology and profound changes in gene expression and protein translation. Our results link mTOR/S6K1 signaling, which is clearly tied to the aging process, to the pathogenesis of AD.

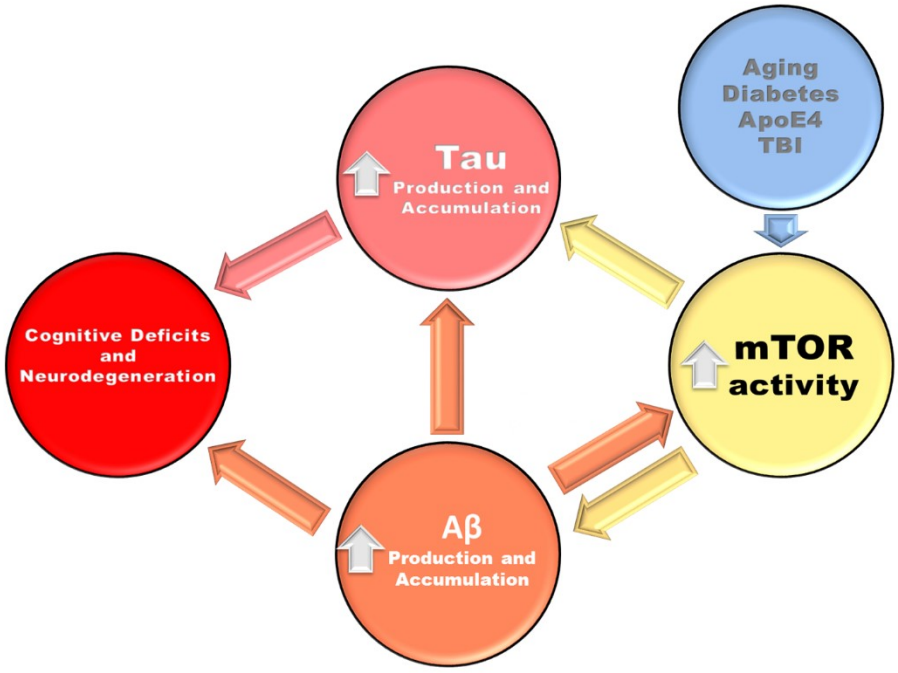

Figure 20. Diagram illustrating the proposed crosstalk among mTOR, Aβ, and tau. In AD, hyperactive mTOR increases Aβ and tau production, Aβ positively feedbacks on to mTOR further increasing mTOR's activity. Many factors including diabetes, traumatic brain injury, and ApoE4 may all influence the crosstalk of these proteins and the aberrant cycle they create leading to AD pathogenesis.

Overall, we propose a crosstalk between mTOR and the two neuropathological hallmarks of AD, Aβ and tau (Fig. 20). Specifically, Aβ accumulation increases mTOR signaling, which in turn further increase Aβ accumulation by decreasing autophagy induction. mTOR regulates tau pathology by controlling its phosphorylation and degradation (via autophagy). Further, mTOR directly increases overall tau levels by regulating translation of its mRNA. This model predicts that factors (e.g., environmental, genetics) known to increase mTOR may contribute to the development of AD. Consistent with this prediction, several AD risk factors, such as high fat diet, diabetes, traumatic brain injury, and the inheritance of the apolipoprotein E4 gene, also increase mTOR activity. In summary, mTOR plays a key role in aging and AD pathogenesis. Therefore,

modulating mTOR activity is an attractive avenue to discover new therapies to enhance healthy brain and body aging, as well as attenuating age-related disease progression and treating age-related diseases, including AD.

5. Methods

5.1 Mice

The Tg2576 and CamKII-CRE mice were purchased from the Jackson laboratory. The mTOR floxed mice [Mtortm1.1Clyn Mtor<tm1.1Clyn> Targeted Allele Detail MGI Mouse (MGI:4820819)] were a generous gift from Dr. Christopher Lynch, Penn State University College of Medicine. The generation of the 3xTg-AD and S6K1 knockout mice has been described previously (Oddo et al., 2003b; Shima et al., 1998). All mice were housed 4-5 to cage at 23 ºC, kept on a 12 hour light/dark cycle and were given *ad libitum* access to food and water. In our colony of 3xTg-AD mice, males show a large neuropathological variability, even between littermates. In contrast, female 3xTg-AD mice do not show such large variability and their phenotype changes as a function of age in a predictable manner. Therefore, only female mice were used for the experiments described here. All animal procedures were approved by The Institutional Animal Care and Use Committee of the Banner Sun Health Research Institute and the Institutional Animal Care and Use Committee at the Barrow Neurological Institute for electrophysiological recordings. Mice were assigned to a specific group based on their genotype after birth and there were no other factors that determined group selection. Mice did not receive any other type of treatment prior to the initiation of the experiments described here. All experiments were performed with the experimenters blinded to genotype and treatment.

5.2 Human tissue

The human tissue was obtained from the Brain and Body Donation Program at the Banner Sun Health Research Institute, a longitudinal clinicopathological study of normal aging and neurodegenerative disorders (Beach et al., 2008). Human cases were selected randomly by

personnel of the Brain and Body Donation program among the tissue available. Groups were matched based on their clinical and neuropathological phenotype.

5.3 Morris water maze

This test was performed in a circular plastic tank of 1.5 m diameter filled with water kept at 25 ºC. The water was made opaque with non-toxic white paint. A 14 cm wide platform, which was kept 1.5 cm under the surface of the water, was invisible to mice. Thus, mice were forced to use extramaze visual cues (located throughout the room) to find the escape platform. The location of the cues and platform were kept in the same place in space throughout the testing period. Mice received four training trials per day for five consecutive days. Mice were tested between 9:00AM and 3:00 PM. Before the first trial of the first day, mice were placed on the platform for 10 seconds, after which they were placed in the water. Mice were kept in the water until they reached the platform. If a mouse failed to find the platform in 60 seconds, it was gently guided to the platform location and allowed to stay on it for 20 seconds. At the end of each trial, mice were placed in a warm holding cage for 25 seconds before starting the next trial. Twenty-four hours after the last training trial, mice were placed in the pool for a final 60-second probe trial, during which the platform was removed from the water and mice were allowed to freely swim in the tank. Extreme care was taken to minimize animal stress during these procedures. A video camera recorded each mouse, and a tracking system (Ethovision 7.0, Noldus Information Technology, Wageningen, Netherlands) analyzed each mouse's path. The dependent variables for learning were escape latency and swim distance, with less time or swim distance interpreted as better learning. The dependent measures for the probe trials were time spent in the four quadrants and the number times a mouse crossed the location that previously contained the platform.

5.4 Protein extraction

Human and mouse proteins were prepared as previously described (Orr et al., 2014). Briefly, mice were sacrificed by CO_2 asphyxiation and their brains removed and cut in half along the medial longitudinal/sagittal fissure. One hemisphere of the brain was post-fixed in 4% paraformaldehyde for 48 hours and used for immunohistochemical evaluation. The other hemisphere was flash-frozen on dry ice and used for biochemical experiments and stored at -80 ºC. The frozen mouse hemispheres as well as 0.1 grams of human inferior frontal gyrus tissue were mechanically homogenized in ice-cold T-PER (Thermo Fisher Scientific, Waltham, MA) protein extraction buffer containing complete protease inhibitor (Roche) and phosphatase inhibitor (Life Technologies, Carlsbad, CA). Brain homogenates were ultracentrifuged at 100,000 g for 1 hour at 4 ºC. The supernatant was recovered and stored at -80 ºC until used for western blots and to measure soluble Aβ levels by ELISA. The pellet was resuspended in 70% formic acid, mechanically homogenized, and centrifuged as described above. The supernatant of this second centrifugation was recovered and stored at -80 ºC until used as the insoluble fraction for ELISA experiments.

5.5 Western Blot

Western blots were performed under reducing conditions using precast Novex gels (Life Technologies). Proteins were transferred to nitrocellulose membranes (iBlot, Life Technologies), which were then incubated for 60 minutes in 5% non-fat powdered milk (Great Value) in tris buffered saline with tween (TBST, 0.1M Tris, 0.15M NaCl, & 0.1% Tween-20). Primary antibodies specific to the experiment were then applied overnight at 4 ºC in TBST 5% milk. The next day, blots were washed in TBST three times for 10 minutes/wash and then incubated in the appropriate fluorescent secondary antibody(s) for 1 hour at room temperature (RT). The blots were then washed as describe above, and imaged/quantified using a LI-COR Odyssey CLx (LI-COR Biosciences, Lincoln, NE) attached to a Dell computer (OptiPlex 7010) running Windows 7 and Image Studio (version 1.0.11, LI-COR Biosciences).

5.6 Enzyme-linked immunosorbent assay (ELISA)

$A\beta_{40}$ and $A\beta_{42}$ levels were assessed via sandwich ELISA using commercially available kits from Life Technologies. Briefly, either the stored soluble or insoluble fractions of brain tissue homogenates were processed and read in a plate reader (BioTek, Winooski, VT) at 450 nm in pre-coated, flat-bottom 96 well plates according to the kit's instructions. The range of Aβ detection was between ~10 pg/mL and 1000 pg/mL. For each assay kit, cross-reactivity with other species of Aβ, APP, or tau was negligible when concentrations were < 10 ng/mL. The concentration of Aβ (pg/mL of sample) present in the homogenate was the dependent variable used for statistical analysis.

5.7 Immunohistochemistry

Fixed hemibrains were sliced into 50 µm thick free-floating sections using a vibratome. Sections were stored in 0.02% sodium azide in phosphate buffered saline at 4 ºC until use. On the day of the experiment, sections were washed twice with TBS (100 mM Tris pH 7.5; 150 mM NaCl) and incubated in 3% H_2O_2 for 30 minutes at 25 ºC to quench endogenous peroxidase activity. For $A\beta_{1-42}$ staining tissue was incubated for 7 minutes in 95% formic acid to retrieve the epitope. Next, sections were washed with TBS-A (100 mM Tris pH 7.5; 150 mM NaCl; 0.1% Triton X-100) and TBS-B (100 mM Tris pH 7.5; 150 mM NaCl; 0.1% Triton X-100; 2% BSA) for 15 and 30 minutes, respectively, to block non-specific binding. Sections were then incubated overnight at 4°C with the appropriate primary antibody. Subsequently, sections were washed in TBA-A and TBS-B to remove excess antibody and incubated in the suitable secondary antibody for 1h at 25°C. Signal was enhanced by incubating sections in the avidin-biotin complex (Thermo Scientific) for 1 hour at 25°C. Sections were then washed and developed with diaminobenzidine substrate using the avidin–biotin horseradish peroxidase system (Vector Labs, Burlingame, CA, USA). Images were obtained with a digital Zeiss camera and analyzed with ImageJ software. Quantification of

staining was achieved using pixilation detection acquired by ImageJ. A threshold is set using a positive control and a standard mean gray area function, which allows the set software to recognize positive staining and decrease error caused by background staining.

5.8 Microarray

The microarray experiments were performed by the genomic core at the University of Texas Health Science Center at San Antonio. RNA was extracted using the mirVana RNA Isolation kit (Life Technologies), following the manufacturer's instructions. To check for RNA integrity, 1 µl of RNA was run on the Agilent 2100 Bioanalyzer (using the RNA Nano Chip).

Average RIN values were between 8.3 and 9.3. cRNA probes (from 500 ng RNA) were made using the Ambion Illumina TotalPrep RNA Amplification Kit (Life Technologies) following the manufacture's protocol. We then measured cRNA concentration and prepared 150 ng/µl dilutions. Subsequently, we assessed the cRNA size distribution profiles by loading 1 µl onto the Agilent Bioanalyzer. We then loaded 1500ng cRNA onto 4 Illumina Mouse WG-6 v2 Gene Expression beadchips, hybridized 18hr overnight, washed and scanned on the Illumina iScan following the manufacturer's protocol. Data were then analyzed using GeneSpring.

5.9 Electrophysiology

Electrophysiological measurements were done in hippocampal slices as described previously (Kimura et al., 2012; Song et al., 2005). Briefly, mice were anesthetized with isoflurane and decapitated. Their brains were rapidly dissected and placed in iced, well oxygenated in artificial cerebrospinal fluid (ACSF), containing (in mM): NaCl 117; KCl 5.4; $NaHCO_3$ 26; $MgSO_4$ 1.3; NaH_2PO_4 1.2; $CaCl_2$ 2.5; glucose 10, continuously bubbled with 95% O_2 - 5% CO_2. Brain tissue was glued to a cryotome and several 400 µm transverse slices were cut through the hippocampal formation using a vibratome (Vibratome 1000 Plus, St. Louis, MO). After cutting, slices were

incubated in 35°C ACSF first for 30 min and stored in a pre-incubator (65-0076/BSC-PC, Harvard Apparatus Co, Holliston, MA) at room temperature for at least one hour before electophysiological recordings were started. Thereafter, one slice was transferred to a liquid-air interface chamber (Warner Instrument, LLC, Hamaden, CT) and suspended on a nylon net at the liquid-air interface in a bath of continuously-dripping oxygenated ACSF (2-2.5 mL/min). Humidified ACSF was passed along the upper surface of the slice and bath temperature was set at 30 ± 1°C.

Standard extracellular field potential recordings were performed in coronal hippocampal slice containing CA1 region. Evoked extracellular field potentials were recorded from stratum radiatum using a borosilicate glass capillary pulled to a tip diameter of ~1 μm, filled with 2 M sodium chloride. A bipolar platinum (0.03 μm diameter) stimulation electrode was placed in Schaffer-collateral-commissural fibers with 0.33 HZ stimulation. After verification of evoked field excitatory postsynaptic potential (fEPSP) stability for 20 min as the baseline, the experimental protocols were applied. For tetanically induced LTP, the theta-burst stimulation (TBS), which contains 15 burst trains at 5 Hz (each train contains 5 pulses at 100 Hz), were applied. Then, the continuous recordings were performed for 60 min using 0.03 Hz stimulation. All electrophysiological signals were recorded using two-channel amplifier (Axon-Clamp 2A) and data acquisition was performed using Clampex 9.2 (Molecular Devices, Sunnyvale, CA, USA) using an 8-pole Bessel filter and a 1 kHz low-pass filter, and stored on hard media for subsequent off-line analysis.

5.10 Quantitative real-time polymerase chain reaction

Total RNA was extracted from hippocampi of NonTg, 3xTg-AD, 3xTg-AD/S6K1$^{+/-}$, and S6K1$^{+/}$ using the RNeasy® Mini Kit (Qiagen, Valencia, CA) according to manufacturer's instruction. RNA (500 pg/sample) was reverse-transcribed with the Quantitect® Reverse Transcription Kit (Qiagen). After cDNA synthesis, qPCR was carried out using the SYBR Green Master Mix (Biorad, Hercules, CA) with the following gene-specific primers (0.3 pmol/μL): BACE-1 Fw 5'-

GGACAACCTGAGGGGAAAGT -3'; Rev 5'- CGGAGGTCTCGATATGTGCT -3'; β-actin, Fw 5'-GGCTCTTTTCCAGCCTTCCT-3' and Rev 5'- ATGCCTGGGTACATGGTGGT-3'. mAPP, Fw 5'-GTGATCTACGAGCGCATGAA-3' and Rev 5'-CGTCGTTTCCGTAGCTGATT-3'. mTau, Fw 5'-AGCCCTAAGACTCCTCCA-3' and Rev 5'-TGCTGTAGCCGCTTCGTTCT-3'. All primers were designed specifically for mouse mRNA, using the ensembl database (www.ensembl.org), validated by PCR and in silico PCR, which confirmed specificity for mouse but not human genes.

5.11 Polysome profiling

The polysome fractionation was performed as described previously(Gandin et al., 2014). Briefly, hippocampi from NonTg, 3xTg-AD, 3xTg-AD/S6K1$^{+/-}$, and S6K1$^{+/-}$ mice were homogenized in hypotonic buffer (5 mM Tris HCl pH 7.5, 2.5 mM $MgCl_2$, 1.5 mM KCl, protease inhibitor, 0.1 mg/ml cycloheximide, 2 mM DTT, 0.2 U/µl RNasin®, 0.5% Triton-X100, 0.5% sodium deoxycholate). The lysates were loaded onto a 10-50% sucrose gradient and centrifuged using a SW41Ti rotor at 36,000 rpm for 2 hours. RNA was extracted from each fraction using Trizol® (Life Technologies) according to manufacturer's instruction. RNA was then run on the Agilent 2100 Bioanalyzer (using the RNA nanochip) to evaluate RNA distribution. RNA (500 pg/sample) was reverse-transcribed with the Quantitect® Reverse Transcription Kit (Qiagen). After cDNA synthesis, qPCR was carried out as described above. C_T values of the gene of interest were normalized to the corresponding C_T values obtained from the input sample for the same animal. ΔC_T values were obtained by subtracting the C_T of the gene of interest to the C_T value of β-actin. $\Delta\Delta C_T$ values were obtained by subtracting the ΔC_T values of the gene of interest in 3xTg-AD, 3xTg-AD/S6K1$^{+/-}$, and S6K1$^{+/-}$ to the ΔC_T values of NonTg mice. Fold change represents 2 power (-ΔΔCT).

5.12 BACE-1 activity

BACE-1 enzymatic activity was measured using a kit from Abcam, Cambridge, UK, following the manufacturer's recommendations. All reagents used were provided with the kit. Briefly,

hippocampi were homogenized in 200 µl of extraction buffer. The homogenized tissue was left on ice for 10 minutes and centrifuged at 10,000 g, for 5m at 4 ºC. The supernatant was used to measure BACE-1 activity. 100 µg of protein per sample were loaded into each well of a 96-well plate (experiments were run in duplicates). Samples were incubated with 2 µl of BACE-1 substrate for one hour at 37 ºC in the dark. Plates were then read using a fluorescent plate reader with an excitation of 335 – 355 nm and emission of 495 – 510 nm.

5.13 S6K1 activity

S6K1 activity was measured using a kit from Enzo Life Sciences, Farmingdale, NY, following the manufacturer's specifications. All the buffers and reagents used were part of the kit. Briefly, frozen brains were homogenized as described in the western blot section. Samples were diluted in Dilution Buffer (mouse tissue 1:20, human tissue 1:10). 96-well plates, pre-coated with the S6K1 substrate, were soaked with 30 µl of kinase assay dilution buffer. After adding the samples to each well (in duplicate), reactions were started by 10 µl of ATP per each well. Plates were then incubated at 30 ºC for 60 minutes. After the incubation, plates were emptied and 40 µl of the phosphorylation-specific substrate antibody was added to each well. Plates were incubated an additional 60 minutes at room temperature. After this incubation, plates were washed four times with 1X Wash Buffer and incubated for 30 minutes at room temperature with anti-rabbit IgG HRP conjugate antibody. Subsequently, plates were washed four times in 1X Wash Buffer and incubated with 3, 3',5, 5'-tetramethylbenzidine (60 µl per well) at room temperature for 15 minutes. The chromogen reaction was terminated by the addition of Acid Stop Solution (20 µl per well). Absorbance was recorded at 450 nm.

5.14 Proteasome activity

Proteasome activity was assessed by incubating 10 µl of brain homogenate with proteasomal substrates Suc-LLVY-AMC, Bz-VGR-AMC and Z-LLE-AMC (Enzo Life Sciences), which probe

for chymotrypsin-like, trypsin-, and caspase-like activities, respectively. Reactions were carried out in 200 µ of assay buffer (25mM HEPES, pH 7.5, 0.5mM EDTA, 0.05% NP-40) using black 96-well plates. Substrates were added immediately prior to readings. Kinetic readings were taken at 37°C every 1.5 minutes for 60 min (excitation 360 nm, emission 460 nm) using the Synergy HT multi-mode microplate reader using the Gen5 software (BioTek, Winooski, VT). Readings were normalized to total protein concentrations assayed via a Coomassie Protein Assay Kit (Bradford, Thermo Scientific, Waltham, MA) following the manufacturer's instructions.

5.15 Antibodies

All of the antibodies used in these studies were validated by the manufacturers for use in mouse and/or human tissue (see manufacturers webpages). From Cell Signaling: Total p70S6K (1:1000), p70S6K Thr389 (1:1000), β-actin (1:10000), PSD95 (1:1000), eEF2K (1:000), rpS6 (1:1000), Atg3 (1:1000), Atg5 (1:1000), Atg7 (1:1000), Atg12 (1:1000), mTOR (1:1000), 4EBP1 (1:1000), 4EBP1 Ser65 (1:1000), ULK-1 (1:1000), and NCAM (1:1000). From Millipore: anti-Aβ42 (1:200), p62 (1:1000), CT20 (1:3000), and synaptophysin (1:1000). From BioLegend: 6E10 (1:3000). From Thermo Fisher Scientific: HT7 (1:3000). TG3 (1:1000) and CP13 (1:000) were a gift from Dr. Peter Davies. From Abcam: DCTN-1 (1:1000).

5.16 Statistical analyses

Examination of the data evaluated via mixed (repeated measures) ANOVAs revealed no violations of any assumptions that would warrant using a statistical test other than the ones described. Assumptions were tested via conventional methods using SPSS 18 (IBM Corporation, Armonk, NY). These included normality (Shapiro-Wilk, *p*s > 0.10), homogeneity of variance (Levene's Test, *p*s > 0.05), and sphericity (Mauchly's Test, *p*s > 0.26). LTP data were analyzed by a two-way mixed ANOVA followed by a *post hoc* multiple comparisons based on Holm-Sidak using SigmaStat V 3.5 (Systat Software, Inc, La Jolla, CA). Learning data were analyzed by a

two-way mixed ANOVA, followed by Bonferroni corrected *post hoc* tests using GraphPad Prism 5 (GraphPad Software, Inc.). Probe trials were analyzed by an omnibus one-way ANOVA, followed by Bonferroni corrected *post hoc* tests. Proteasome activity was analyzed by an omnibus two-way ANOVA. An omnibus one-way ANOVA followed by Bonferroni corrected or Tukey's *post hoc* tests were used to analyze select comparisons with more than two groups (e.g., western blots and S6K1 activity in mice), as specified in the results section. A two-tailed unpaired *t*-test was used to analyze select pairwise comparisons (e.g., western blots in human cases and histology), as specified in the results section. These analyses were performed using either SPSS 18 or GraphPad Prism 5. Relationships between bivariate data were assessed via one predictor linear regression and simple correlations (i.e., Pearson product-moment correlations). *A priori* power analyses were not performed but our sample sizes are similar to those reported in previously published papers (Caccamo et al., 2014; Ma et al., 2013a). Where representative images are shown, statistical analyses were performed on the entire sample as indicated in each figure legend.

6. References

Alvarez, A., Munoz, J.P., and Maccioni, R.B. (2001). A Cdk5-p35 stable complex is involved in the beta-amyloid-induced deregulation of Cdk5 activity in hippocampal neurons. Exp Cell Res *264*, 266-274.

Alvarez, A., Toro, R., Caceres, A., and Maccioni, R.B. (1999). Inhibition of tau phosphorylating protein kinase cdk5 prevents beta-amyloid-induced neuronal death. FEBS Lett *459*, 421-426.

Alzheimer's, A. (2014). 2014 Alzheimer's disease facts and figures. Alzheimer's & dementia : the journal of the Alzheimer's Association *10*, e47-92.

An, W.L., Cowburn, R.F., Li, L., Braak, H., Alafuzoff, I., Iqbal, K., Iqbal, I.G., Winblad, B., and Pei, J.J. (2003). Up-regulation of phosphorylated/activated p70 S6 kinase and its relationship to neurofibrillary pathology in Alzheimer's disease. The American journal of pathology *163*, 591-607.

Andorfer, C., Kress, Y., Espinoza, M., de Silva, R., Tucker, K.L., Barde, Y.A., Duff, K., and Davies, P. (2003). Hyperphosphorylation and aggregation of tau in mice expressing normal human tau isoforms. J Neurochem *86*, 582-590.

Antion, M.D., Merhav, M., Hoeffer, C.A., Reis, G., Kozma, S.C., Thomas, G., Schuman, E.M., Rosenblum, K., and Klann, E. (2008). Removal of S6K1 and S6K2 leads to divergent alterations in learning, memory, and synaptic plasticity. Learning & memory *15*, 29-38.

Artero, S., Tierney, M.C., Touchon, J., and Ritchie, K. (2003). Prediction of transition from cognitive impairment to senile dementia: a prospective, longitudinal study. Acta psychiatrica Scandinavica *107*, 390-393.

Beach, T.G., Sue, L.I., Walker, D.G., Roher, A.E., Lue, L., Vedders, L., Connor, D.J., Sabbagh, M.N., and Rogers, J. (2008). The Sun Health Research Institute Brain Donation Program: description and experience, 1987-2007. Cell and tissue banking *9*, 229-245.

Berger, Z., Ravikumar, B., Menzies, F.M., Oroz, L.G., Underwood, B.R., Pangalos, M.N., Schmitt, I., Wullner, U., Evert, B.O., O'Kane, C.J., *et al.* (2006). Rapamycin alleviates toxicity of different aggregate-prone proteins. Hum Mol Genet *15*, 433-442.

Billings, L.M., Oddo, S., Green, K.N., McGaugh, J.L., and LaFerla, F.M. (2005). Intraneuronal Abeta causes the onset of early Alzheimer's disease-related cognitive deficits in transgenic mice. Neuron *45*, 675-688.

Binder, L.I., Frankfurter, A., and Rebhun, L.I. (1985). The distribution of tau in the mammalian central nervous system. J Cell Biol *101*, 1371-1378.

Bird, T.D. (2008). Genetic aspects of Alzheimer disease. Genet Med *10*, 231-239.

Blanchard, V., Czech, C., Bonici, B., Clavel, N., Gohin, M., Dalet, K., Revah, F., Pradier, L., Imperato, A., and Moussaoui, S. (1997). Immunohistochemical analysis of presenilin 2 expression in the mouse brain: distribution pattern and co-localization with presenilin 1 protein. Brain Res *758*, 209-217.

Boland, B., Kumar, A., Lee, S., Platt, F.M., Wegiel, J., Yu, W.H., and Nixon, R.A. (2008). Autophagy induction and autophagosome clearance in neurons: relationship to autophagic pathology in Alzheimer's disease. The Journal of neuroscience : the official journal of the Society for Neuroscience *28*, 6926-6937.

Borchelt, D.R., Ratovitski, T., van Lare, J., Lee, M.K., Gonzales, V., Jenkins, N.A., Copeland, N.G., Price, D.L., and Sisodia, S.S. (1997). Accelerated amyloid deposition in the brains of transgenic mice coexpressing mutant presenilin 1 and amyloid precursor proteins. Neuron *19*, 939-945.

Busciglio, J., Lorenzo, A., Yeh, J., and Yankner, B.A. (1995). beta-amyloid fibrils induce tau phosphorylation and loss of microtubule binding. Neuron *14*, 879-888.

Busciglio, J., Yeh, J., and Yankner, B.A. (1993). beta-Amyloid neurotoxicity in human cortical culture is not mediated by excitotoxins. J Neurochem *61*, 1565-1568.

Caccamo, A., De Pinto, V., Messina, A., Branca, C., and Oddo, S. (2014). Genetic reduction of mammalian target of rapamycin ameliorates Alzheimer's disease-like cognitive and pathological deficits by restoring hippocampal gene expression signature. The Journal of neuroscience : the official journal of the Society for Neuroscience *34*, 7988-7998.

Caccamo, A., Magri, A., Medina, D.X., Wisely, E.V., Lopez-Aranda, M.F., Silva, A.J., and Oddo, S. (2013). mTOR regulates tau phosphorylation and degradation: implications for Alzheimer's disease and other tauopathies. Aging cell *12*, 370-380.

Caccamo, A., Majumder, S., Deng, J.J., Bai, Y., Thornton, F.B., and Oddo, S. (2009). Rapamycin rescues TDP-43 mislocalization and the associated low molecular weight neurofilament instability. The Journal of biological chemistry.

Caccamo, A., Majumder, S., Richardson, A., Strong, R., and Oddo, S. (2010a). Molecular interplay between mammalian target of rapamycin (mTOR), amyloid-beta, and Tau: effects on cognitive impairments. J Biol Chem *285*, 13107-13120.

Caccamo, A., Majumder, S., Richardson, A., Strong, R., and Oddo, S. (2010b). Molecular interplay between mammalian target of rapamycin (mTOR), amyloid-beta, and Tau: effects on cognitive impairments. The Journal of biological chemistry *285*, 13107-13120.

Caccamo, A., Maldonado, M.A., Majumder, S., Medina, D.X., Holbein, W., Magri, A., and Oddo, S. (2011a). Naturally secreted amyloid-beta increases mammalian target of rapamycin (mTOR) activity via a PRAS40-mediated mechanism. J Biol Chem *286*, 8924-8932.

Caccamo, A., Maldonado, M.A., Majumder, S., Medina, D.X., Holbein, W., Magri, A., and Oddo, S. (2011b). Naturally secreted amyloid-beta increases mammalian target of rapamycin (mTOR) activity via a PRAS40-mediated mechanism. The Journal of biological chemistry *286*, 8924-8932.

Caccamo, A., Oddo, S., Sugarman, M.C., Akbari, Y., and LaFerla, F.M. (2005). Age- and region-dependent alterations in Abeta-degrading enzymes: implications for Abeta-induced disorders. Neurobiol Aging *26*, 645-654.

Caldeira, G.L., Ferreira, I.L., and Rego, A.C. (2013). Impaired transcription in Alzheimer's disease: key role in mitochondrial dysfunction and oxidative stress. J Alzheimers Dis *34*, 115-131.

Calhoun, M.E., Burgermeister, P., Phinney, A.L., Stalder, M., Tolnay, M., Wiederhold, K.H., Abramowski, D., Sturchler-Pierrat, C., Sommer, B., Staufenbiel, M.*, et al.* (1999). Neuronal overexpression of mutant amyloid precursor protein results in prominent deposition of cerebrovascular amyloid. Proc Natl Acad Sci U S A *96*, 14088-14093.

Cammalleri, M., Lutjens, R., Berton, F., King, A.R., Simpson, C., Francesconi, W., and Sanna, P.P. (2003). Time-restricted role for dendritic activation of the mTOR-p70S6K pathway in the induction of late-phase long-term potentiation in the CA1. Proceedings of the National Academy of Sciences of the United States of America *100*, 14368-14373.

Cao, R., Li, A., and Cho, H.Y. (2009). mTOR signaling in epileptogenesis: too much of a good thing? The Journal of neuroscience : the official journal of the Society for Neuroscience *29*, 12372-12373.

Carr, T.D., DiGiovanni, J., Lynch, C.J., and Shantz, L.M. (2012). Inhibition of mTOR suppresses UVB-induced keratinocyte proliferation and survival. Cancer prevention research *5*, 1394-1404.

Chang, R.C., Wong, A.K., Ng, H.K., and Hugon, J. (2002). Phosphorylation of eukaryotic initiation factor-2alpha (eIF2alpha) is associated with neuronal degeneration in Alzheimer's disease. Neuroreport *13*, 2429-2432.

Chen, G., Chen, K.S., Knox, J., Inglis, J., Bernard, A., Martin, S.J., Justice, A., McConlogue, L., Games, D., Freedman, S.B.*, et al.* (2000). A learning deficit related to age and beta-amyloid plaques in a mouse model of Alzheimer's disease. Nature *408*, 975-979.

Chishti, M.A., Yang, D.S., Janus, C., Phinney, A.L., Horne, P., Pearson, J., Strome, R., Zuker, N., Loukides, J., French, J.*, et al.* (2001). Early-onset amyloid deposition and cognitive deficits in transgenic mice expressing a double mutant form of amyloid precursor protein 695. J Biol Chem *276*, 21562-21570.

Choi, S.H., Kim, Y.H., Hebisch, M., Sliwinski, C., Lee, S., D'Avanzo, C., Chen, H., Hooli, B., Asselin, C., Muffat, J.*, et al.* (2014). A three-dimensional human neural cell culture model of Alzheimer's disease. Nature.

Cholerton, B., Baker, L.D., and Craft, S. (2013). Insulin, cognition, and dementia. Eur J Pharmacol.

Chui, D.H., Tanahashi, H., Ozawa, K., Ikeda, S., Checler, F., Ueda, O., Suzuki, H., Araki, W., Inoue, H., Shirotani, K.*, et al.* (1999). Transgenic mice with Alzheimer presenilin 1 mutations show accelerated neurodegeneration without amyloid plaque formation. Nat Med *5*, 560-564.

Citron, M., Oltersdorf, T., Haass, C., McConlogue, L., Hung, A.Y., Seubert, P., Vigo-Pelfrey, C., Lieberburg, I., and Selkoe, D.J. (1992). Mutation of the beta-amyloid precursor protein in familial Alzheimer's disease increases beta-protein production. Nature *360*, 672-674.

Costa-Mattioli, M., Gobert, D., Stern, E., Gamache, K., Colina, R., Cuello, C., Sossin, W., Kaufman, R., Pelletier, J., Rosenblum, K.*, et al.* (2007). eIF2alpha phosphorylation bidirectionally regulates the switch from short- to long-term synaptic plasticity and memory. Cell *129*, 195-206.

Costa-Mattioli, M., and Monteggia, L.M. (2013). mTOR complexes in neurodevelopmental and neuropsychiatric disorders. Nature neuroscience *16*, 1537-1543.

Cruts, M., Hendriks, L., and Van Broeckhoven, C. (1996). The presenilin genes: a new gene family involved in Alzheimer disease pathology. Hum Mol Genet *5 Spec No*, 1449-1455.

Cuervo, A.M. (2004). Autophagy: many paths to the same end. Molecular and cellular biochemistry *263*, 55-72.

Cuervo, A.M., Bergamini, E., Brunk, U.T., Droge, W., Ffrench, M., and Terman, A. (2005). Autophagy and aging: the importance of maintaining "clean" cells. Autophagy *1*, 131-140.

Davis, J., Xu, F., Deane, R., Romanov, G., Previti, M., Zeigler, K., Zlokovic, B.V., and Van Nostrand, W.E. (2004). Early-onset and robust cerebral microvascular accumulation of

amyloid beta -protein in transgenic mice expressing low levels of a vasculotropic Dutch/Iowa mutant form of amyloid beta -protein precursor. J Biol Chem.

Diaz-Troya, S., Perez-Perez, M.E., Florencio, F.J., and Crespo, J.L. (2008). The role of TOR in autophagy regulation from yeast to plants and mammals. Autophagy *4*, 851-865.

Dineley, K.T., Jahrling, J.B., and Denner, L. (2014). Insulin resistance in Alzheimer's disease. Neurobiology of disease.

Dodart, J.C., Meziane, H., Mathis, C., Bales, K.R., Paul, S.M., and Ungerer, A. (1999). Behavioral disturbances in transgenic mice overexpressing the V717F beta-amyloid precursor protein. Behav Neurosci *113*, 982-990.

Donnelly, N., Gorman, A.M., Gupta, S., and Samali, A. (2013). The eIF2alpha kinases: their structures and functions. Cellular and molecular life sciences : CMLS *70*, 3493-3511.

Drechsel, D.N., Hyman, A.A., Cobb, M.H., and Kirschner, M.W. (1992). Modulation of the dynamic instability of tubulin assembly by the microtubule-associated protein tau. Mol Biol Cell *3*, 1141-1154.

Duff, K., Eckman, C., Zehr, C., Yu, X., Prada, C.M., Perez-tur, J., Hutton, M., Buee, L., Harigaya, Y., Yager, D.*, et al.* (1996). Increased amyloid-beta42(43) in brains of mice expressing mutant presenilin 1. Nature *383*, 710-713.

Ehninger, D. (2013). From genes to cognition in tuberous sclerosis: implications for mTOR inhibitor-based treatment approaches. Neuropharmacology *68*, 97-105.

Ehninger, D., de Vries, P.J., and Silva, A.J. (2009). From mTOR to cognition: molecular and cellular mechanisms of cognitive impairments in tuberous sclerosis. J Intellect Disabil Res *53*, 838-851.

Ehninger, D., Han, S., Shilyansky, C., Zhou, Y., Li, W., Kwiatkowski, D.J., Ramesh, V., and Silva, A.J. (2008). Reversal of learning deficits in a Tsc2+/- mouse model of tuberous sclerosis. Nature medicine *14*, 843-848.

Fabrizio, P., Pozza, F., Pletcher, S.D., Gendron, C.M., and Longo, V.D. (2001). Regulation of longevity and stress resistance by Sch9 in yeast. Science *292*, 288-290.

Fenton, T.R., and Gout, I.T. (2011). Functions and regulation of the 70kDa ribosomal S6 kinases. The international journal of biochemistry & cell biology *43*, 47-59.

Fornai, F., Longone, P., Cafaro, L., Kastsiuchenka, O., Ferrucci, M., Manca, M.L., Lazzeri, G., Spalloni, A., Bellio, N., Lenzi, P.*, et al.* (2008). Lithium delays progression of amyotrophic lateral sclerosis. Proceedings of the National Academy of Sciences of the United States of America *105*, 2052-2057.

Frederick, C., Ando, K., Leroy, K., Heraud, C., Suain, V., Buee, L., and Brion, J.P. (2014). Rapamycin Ester Analog CCI-779/Temsirolimus Alleviates Tau Pathology and Improves Motor Deficit in Mutant Tau Transgenic Mice. J Alzheimers Dis.

Frias, M.A., Thoreen, C.C., Jaffe, J.D., Schroder, W., Sculley, T., Carr, S.A., and Sabatini, D.M. (2006). mSin1 is necessary for Akt/PKB phosphorylation, and its isoforms define three distinct mTORC2s. Current biology : CB *16*, 1865-1870.

Frost, B., Gotz, J., and Feany, M.B. (2014). Connecting the dots between tau dysfunction and neurodegeneration. Trends in cell biology.

Gamblin, T.C., Chen, F., Zambrano, A., Abraha, A., Lagalwar, S., Guillozet, A.L., Lu, M., Fu, Y., Garcia-Sierra, F., LaPointe, N.*, et al.* (2003). Caspase cleavage of tau: linking amyloid and neurofibrillary tangles in Alzheimer's disease. Proc Natl Acad Sci U S A *100*, 10032-10037.

Games, D., Adams, D., Alessandrini, R., Barbour, R., Berthelette, P., Blackwell, C., Carr, T., Clemens, J., Donaldson, T., Gillespie, F.*, et al.* (1995). Alzheimer-type neuropathology in transgenic mice overexpressing V717F beta-amyloid precursor protein. Nature *373*, 523-527.

Gandin, V., Sikstrom, K., Alain, T., Morita, M., McLaughlan, S., Larsson, O., and Topisirovic, I. (2014). Polysome fractionation and analysis of mammalian translatomes on a genome-wide scale. Journal of visualized experiments : JoVE.

Garelick, M.G., Mackay, V.L., Yanagida, A., Academia, E.C., Schreiber, K.H., Ladiges, W.C., and Kennedy, B.K. (2013). Chronic rapamycin treatment or lack of S6K1 does not reduce ribosome activity in vivo. Cell cycle *12*, 2493-2504.

George, A.J., Gordon, L., Beissbarth, T., Koukoulas, I., Holsinger, R.M., Perreau, V., Cappai, R., Tan, S.S., Masters, C.L., Scott, H.S.*, et al.* (2010). A serial analysis of gene expression profile of the Alzheimer's disease Tg2576 mouse model. Neurotoxicity research *17*, 360-379.

Gervais, F.G., Xu, D., Robertson, G.S., Vaillancourt, J.P., Zhu, Y., Huang, J., LeBlanc, A., Smith, D., Rigby, M., Shearman, M.S.*, et al.* (1999). Involvement of caspases in proteolytic cleavage of Alzheimer's amyloid-beta precursor protein and amyloidogenic A beta peptide formation. Cell *97*, 395-406.

Gingras, A.C., Gygi, S.P., Raught, B., Polakiewicz, R.D., Abraham, R.T., Hoekstra, M.F., Aebersold, R., and Sonenberg, N. (1999). Regulation of 4E-BP1 phosphorylation: a novel two-step mechanism. Genes Dev *13*, 1422-1437.

Goate, A., Chartier-Harlin, M.C., Mullan, M., Brown, J., Crawford, F., Fidani, L., Giuffra, L., Haynes, A., Irving, N., James, L.*, et al.* (1991). Segregation of a missense mutation in the amyloid precursor protein gene with familial Alzheimer's disease. Nature *349*, 704-706.

Gotz, J., Chen, F., Barmettler, R., and Nitsch, R.M. (2001a). Tau filament formation in transgenic mice expressing P301L tau. J Biol Chem *276*, 529-534.

Gotz, J., Chen, F., van Dorpe, J., and Nitsch, R.M. (2001b). Formation of neurofibrillary tangles in P301l tau transgenic mice induced by Abeta 42 fibrils. Science *293*, 1491-1495.

Graber, T.E., McCamphill, P.K., and Sossin, W.S. (2013). A recollection of mTOR signaling in learning and memory. Learning & memory *20*, 518-530.

Griffin, R.J., Moloney, A., Kelliher, M., Johnston, J.A., Ravid, R., Dockery, P., O'Connor, R., and O'Neill, C. (2005). Activation of Akt/PKB, increased phosphorylation of Akt substrates and loss and altered distribution of Akt and PTEN are features of Alzheimer's disease pathology. J Neurochem *93*, 105-117.

Guertin, D.A., and Sabatini, D.M. (2007). Defining the role of mTOR in cancer. Cancer cell *12*, 9-22.

Guo, Q., Fu, W., Sopher, B.L., Miller, M.W., Ware, C.B., Martin, G.M., and Mattson, M.P. (1999). Increased vulnerability of hippocampal neurons to excitotoxic necrosis in presenilin-1 mutant knock-in mice. Nat Med *5*, 101-106.

Haass, C., and Selkoe, D.J. (1993). Cellular processing of beta-amyloid precursor protein and the genesis of amyloid beta-peptide. Cell *75*, 1039-1042.

Halloran, J., Hussong, S.A., Burbank, R., Podlutskaya, N., Fischer, K.E., Sloane, L.B., Austad, S.N., Strong, R., Richardson, A., Hart, M.J.*, et al.* (2012). Chronic inhibition of mammalian target of rapamycin by rapamycin modulates cognitive and non-cognitive components of behavior throughout lifespan in mice. Neuroscience *223*, 102-113.

Hands, S.L., Proud, C.G., and Wyttenbach, A. (2009). mTOR's role in ageing: protein synthesis or autophagy? Aging (Albany NY) *1*, 586-597.

Hara, T., Nakamura, K., Matsui, M., Yamamoto, A., Nakahara, Y., Suzuki-Migishima, R., Yokoyama, M., Mishima, K., Saito, I., Okano, H.*, et al.* (2006). Suppression of basal autophagy in neural cells causes neurodegenerative disease in mice. Nature *441*, 885-889.

Hardy, J. (2003). The relationship between amyloid and tau. J Mol Neurosci *20*, 203-206.

Hardy, J., and Selkoe, D.J. (2002). The amyloid hypothesis of Alzheimer's disease: progress and problems on the road to therapeutics. Science *297*, 353-356.

Hardy, J.A., and Higgins, G.A. (1992). Alzheimer's disease: the amyloid cascade hypothesis. Science *256*, 184-185.

Harrison, D.E., Strong, R., Sharp, Z.D., Nelson, J.F., Astle, C.M., Flurkey, K., Nadon, N.L., Wilkinson, J.E., Frenkel, K., Carter, C.S.*, et al.* (2009). Rapamycin fed late in life extends lifespan in genetically heterogeneous mice. Nature *460*, 392-395.

Hay, N., and Sonenberg, N. (2004). Upstream and downstream of mTOR. Genes Dev *18*, 1926-1945.

Higgins, L.S., Catalano, R., Quon, D., and Cordell, B. (1993). Transgenic mice expressing human beta-APP751, but not mice expressing beta-APP695, display early Alzheimer's disease-like histopathology. Ann N Y Acad Sci *695*, 224-227.

Hoeffer, C.A., and Klann, E. (2010). mTOR signaling: at the crossroads of plasticity, memory and disease. Trends Neurosci *33*, 67-75.

Hoeffer, C.A., Tang, W., Wong, H., Santillan, A., Patterson, R.J., Martinez, L.A., Tejada-Simon, M.V., Paylor, R., Hamilton, S.L., and Klann, E. (2008). Removal of FKBP12 enhances mTOR-Raptor interactions, LTP, memory, and perseverative/repetitive behavior. Neuron *60*, 832-845.

Holcomb, L., Gordon, M.N., McGowan, E., Yu, X., Benkovic, S., Jantzen, P., Wright, K., Saad, I., Mueller, R., Morgan, D*., et al.* (1998). Accelerated Alzheimer-type phenotype in transgenic mice carrying both mutant amyloid precursor protein and presenilin 1 transgenes. Nat Med *4*, 97-100.

Hoshi, M., Sato, M., Matsumoto, S., Noguchi, A., Yasutake, K., Yoshida, N., and Sato, K. (2003). Spherical aggregates of beta-amyloid (amylospheroid) show high neurotoxicity and activate tau protein kinase I/glycogen synthase kinase-3beta. Proc Natl Acad Sci U S A *100*, 6370-6375.

Hoshi, M., Takashima, A., Noguchi, K., Murayama, M., Sato, M., Kondo, S., Saitoh, Y., Ishiguro, K., Hoshino, T., and Imahori, K. (1996). Regulation of mitochondrial pyruvate dehydrogenase activity by tau protein kinase I/glycogen synthase kinase 3beta in brain. Proc Natl Acad Sci U S A *93*, 2719-2723.

Hsiao, K., Chapman, P., Nilsen, S., Eckman, C., Harigaya, Y., Younkin, S., Yang, F., and Cole, G. (1996). Correlative memory deficits, Abeta elevation, and amyloid plaques in transgenic mice. Science *274*, 99-102.

Huang, W., Zhu, P.J., Zhang, S., Zhou, H., Stoica, L., Galiano, M., Krnjevic, K., Roman, G., and Costa-Mattioli, M. (2013). mTORC2 controls actin polymerization required for consolidation of long-term memory. Nature neuroscience *16*, 441-448.

Hung, S.Y., Huang, W.P., Liou, H.C., and Fu, W.M. (2009). Autophagy protects neuron from Abeta-induced cytotoxicity. Autophagy *5*, 502-510.

Hutton, M., Lendon, C.L., Rizzu, P., Baker, M., Froelich, S., Houlden, H., Pickering-Brown, S., Chakraverty, S., Isaacs, A., Grover, A.*, et al.* (1998). Association of missense and 5'-splice-site mutations in tau with the inherited dementia FTDP-17. Nature *393*, 702-705.

Imahori, K., and Uchida, T. (1997). Physiology and pathology of tau protein kinases in relation to Alzheimer's disease. J Biochem (Tokyo) *121*, 179-188.

Inoki, K., Corradetti, M.N., and Guan, K.L. (2005). Dysregulation of the TSC-mTOR pathway in human disease. Nature genetics *37*, 19-24.

Iqbal, K., Gong, C.X., and Liu, F. (2014). Microtubule-associated protein tau as a therapeutic target in Alzheimer's disease. Expert opinion on therapeutic targets *18*, 307-318.

Ishiguro, K., Ihara, Y., Uchida, T., and Imahori, K. (1988). A novel tubulin-dependent protein kinase forming a paired helical filament epitope on tau. J Biochem (Tokyo) *104*, 319-321.

Ishiguro, K., Takamatsu, M., Tomizawa, K., Omori, A., Takahashi, M., Arioka, M., Uchida, T., and Imahori, K. (1992). Tau protein kinase I converts normal tau protein into A68-like component of paired helical filaments. J Biol Chem *267*, 10897-10901.

Jia, K., Chen, D., and Riddle, D.L. (2004). The TOR pathway interacts with the insulin signaling pathway to regulate C. elegans larval development, metabolism and life span. Development (Cambridge, England) *131*, 3897-3906.

Jiang, T., Yu, J.T., Zhu, X.C., Tan, M.S., Wang, H.F., Cao, L., Zhang, Q.Q., Shi, J.Q., Gao, L., Qin, H.*, et al.* (2014). Temsirolimus promotes autophagic clearance of amyloid-beta and provides protective effects in cellular and animal models of Alzheimer's disease.

Pharmacological research : the official journal of the Italian Pharmacological Society *81*, 54-63.

Johnson, S.C., Rabinovitch, P.S., and Kaeberlein, M. (2013). mTOR is a key modulator of ageing and age-related disease. Nature *493*, 338-345.

Jung, C.H., Jun, C.B., Ro, S.H., Kim, Y.M., Otto, N.M., Cao, J., Kundu, M., and Kim, D.H. (2009). ULK-Atg13-FIP200 complexes mediate mTOR signaling to the autophagy machinery. Molecular biology of the cell *20*, 1992-2003.

Jung, C.H., Ro, S.H., Cao, J., Otto, N.M., and Kim, D.H. (2010). mTOR regulation of autophagy. FEBS letters *584*, 1287-1295.

Kabeya, Y., Mizushima, N., Ueno, T., Yamamoto, A., Kirisako, T., Noda, T., Kominami, E., Ohsumi, Y., and Yoshimori, T. (2000). LC3, a mammalian homologue of yeast Apg8p, is localized in autophagosome membranes after processing. The EMBO journal *19*, 5720-5728.

Kapahi, P., Zid, B.M., Harper, T., Koslover, D., Sapin, V., and Benzer, S. (2004). Regulation of lifespan in Drosophila by modulation of genes in the TOR signaling pathway. Current biology : CB *14*, 885-890.

Kawarabayashi, T., Younkin, L.H., Saido, T.C., Shoji, M., Ashe, K.H., and Younkin, S.G. (2001). Age-dependent changes in brain, CSF, and plasma amyloid (beta) protein in the Tg2576 transgenic mouse model of Alzheimer's disease. The Journal of neuroscience : the official journal of the Society for Neuroscience *21*, 372-381.

Khandelwal, P.J., Herman, A.M., Hoe, H.S., Rebeck, G.W., and Moussa, C.E. (2011). Parkin mediates beclin-dependent autophagic clearance of defective mitochondria and ubiquitinated A{beta} in AD models. Hum Mol Genet.

Khurana, V., Lu, Y., Steinhilb, M.L., Oldham, S., Shulman, J.M., and Feany, M.B. (2006). TOR-mediated cell-cycle activation causes neurodegeneration in a Drosophila tauopathy model. Current biology : CB *16*, 230-241.

Kim, Y.C., and Guan, K.L. (2015). mTOR: a pharmacologic target for autophagy regulation. J Clin Invest *125*, 25-32.

Kimberly, W.T., Xia, W., Rahmati, T., Wolfe, M.S., and Selkoe, D.J. (2000). The transmembrane aspartates in presenilin 1 and 2 are obligatory for gamma-secretase activity and amyloid beta-protein generation. J Biol Chem *275*, 3173-3178.

Kimura, R., Ma, L.Y., Wu, C., Turner, D., Shen, J.X., Ellsworth, K., Wakui, M., Maalouf, M., and Wu, J. (2012). Acute exposure to the mitochondrial complex I toxin rotenone impairs synaptic long-term potentiation in rat hippocampal slices. CNS neuroscience & therapeutics *18*, 641-646.

Klann, E., and Sweatt, J.D. (2008). Altered protein synthesis is a trigger for long-term memory formation. Neurobiol Learn Mem *89*, 247-259.

Klionsky, D.J., and Emr, S.D. (2000). Autophagy as a regulated pathway of cellular degradation. Science *290*, 1717-1721.

Koffie, R.M., Hyman, B.T., and Spires-Jones, T.L. (2011). Alzheimer's disease: synapses gone cold. Mol Neurodegener *6*, 63.

Kolosova, N.G., Vitovtov, A.O., Muraleva, N.A., Akulov, A.E., Stefanova, N.A., and Blagosklonny, M.V. (2013). Rapamycin suppresses brain aging in senescence-accelerated OXYS rats. Aging (Albany NY) *5*, 474-484.

Komatsu, M., Waguri, S., Chiba, T., Murata, S., Iwata, J., Tanida, I., Ueno, T., Koike, M., Uchiyama, Y., Kominami, E.*, et al.* (2006). Loss of autophagy in the central nervous system causes neurodegeneration in mice. Nature *441*, 880-884.

Komatsu, M., Wang, Q.J., Holstein, G.R., Friedrich, V.L., Jr., Iwata, J., Kominami, E., Chait, B.T., Tanaka, K., and Yue, Z. (2007). Essential role for autophagy protein Atg7 in the maintenance of axonal homeostasis and the prevention of axonal degeneration. Proceedings of the National Academy of Sciences of the United States of America *104*, 14489-14494.

Koo, E.H., and Squazzo, S.L. (1994). Evidence that production and release of amyloid beta-protein involves the endocytic pathway. The Journal of biological chemistry *269*, 17386-17389.

Lafay-Chebassier, C., Paccalin, M., Page, G., Barc-Pain, S., Perault-Pochat, M.C., Gil, R., Pradier, L., and Hugon, J. (2005). mTOR/p70S6k signalling alteration by Abeta exposure as well as in APP-PS1 transgenic models and in patients with Alzheimer's disease. J Neurochem *94*, 215-225.

LaFerla, F.M. (2002). Calcium dyshomeostasis and intracellular signalling in Alzheimer's disease. Nat Rev Neurosci *3*, 862-872.

LaFerla, F.M., and Oddo, S. (2005). Alzheimer's disease: Abeta, tau and synaptic dysfunction. Trends Mol Med *11*, 170-176.

LaFerla, F.M., Tinkle, B.T., Bieberich, C.J., Haudenschild, C.C., and Jay, G. (1995). The Alzheimer's A beta peptide induces neurodegeneration and apoptotic cell death in transgenic mice. Nat Genet *9*, 21-30.

Lamming, D.W., Ye, L., Sabatini, D.M., and Baur, J.A. (2013). Rapalogs and mTOR inhibitors as anti-aging therapeutics. J Clin Invest *123*, 980-989.

Lang, C.H., Frost, R.A., Bronson, S.K., Lynch, C.J., and Vary, T.C. (2010). Skeletal muscle protein balance in mTOR heterozygous mice in response to inflammation and leucine. American journal of physiology Endocrinology and metabolism *298*, E1283-1294.

Lee, K.Y., Clark, A.W., Rosales, J.L., Chapman, K., Fung, T., and Johnston, R.N. (1999). Elevated neuronal Cdc2-like kinase activity in the Alzheimer disease brain. Neurosci Res *34*, 21-29.

Lee, M.J., Lee, J.H., and Rubinsztein, D.C. (2013). Tau degradation: the ubiquitin-proteasome system versus the autophagy-lysosome system. Progress in neurobiology *105*, 49-59.

Lee, M.S., Kwon, Y.T., Li, M., Peng, J., Friedlander, R.M., and Tsai, L.H. (2000). Neurotoxicity induces cleavage of p35 to p25 by calpain. Nature *405*, 360-364.

Leissring, M.A., LaFerla, F.M., Callamaras, N., and Parker, I. (2001). Subcellular mechanisms of presenilin-mediated enhancement of calcium signaling. Neurobiol Dis *8*, 469-478.

Leissring, M.A., Parker, I., and LaFerla, F.M. (1999a). Presenilin-2 mutations modulate amplitude and kinetics of inositol 1, 4,5-trisphosphate-mediated calcium signals. J Biol Chem *274*, 32535-32538.

Leissring, M.A., Paul, B.A., Parker, I., Cotman, C.W., and LaFerla, F.M. (1999b). Alzheimer's presenilin-1 mutation potentiates inositol 1,4,5-trisphosphate-mediated calcium signaling in Xenopus oocytes. J Neurochem *72*, 1061-1068.

Levy-Lahad, E., Wasco, W., Poorkaj, P., Romano, D.M., Oshima, J., Pettingell, W.H., Yu, C.E., Jondro, P.D., Schmidt, S.D., Wang, K.*, et al.* (1995). Candidate gene for the chromosome 1 familial Alzheimer's disease locus. Science *269*, 973-977.

Lewis, J., Dickson, D.W., Lin, W.L., Chisholm, L., Corral, A., Jones, G., Yen, S.H., Sahara, N., Skipper, L., Yager, D.*, et al.* (2001). Enhanced neurofibrillary degeneration in transgenic mice expressing mutant tau and APP. Science *293*, 1487-1491.

Lewis, J., McGowan, E., Rockwood, J., Melrose, H., Nacharaju, P., Van Slegtenhorst, M., Gwinn-Hardy, K., Paul Murphy, M., Baker, M., Yu, X.*, et al.* (2000). Neurofibrillary tangles, amyotrophy and progressive motor disturbance in mice expressing mutant (P301L) tau protein. Nat Genet *25*, 402-405.

Li, C.Y., Li, X., Liu, S.F., Qu, W.S., Wang, W., and Tian, D.S. (2015). Inhibition of mTOR pathway restrains astrocyte proliferation, migration and production of inflammatory mediators after oxygen-glucose deprivation and reoxygenation. Neurochem Int *83-84*, 9-18.

Li, X., Alafuzoff, I., Soininen, H., Winblad, B., and Pei, J.J. (2005). Levels of mTOR and its downstream targets 4E-BP1, eEF2, and eEF2 kinase in relationships with tau in Alzheimer's disease brain. The FEBS journal *272*, 4211-4220.

Li, X., Li, H., and Li, X.J. (2008). Intracellular degradation of misfolded proteins in polyglutamine neurodegenerative diseases. Brain research reviews *59*, 245-252.

Lin, A.L., Zheng, W., Halloran, J.J., Burbank, R.R., Hussong, S.A., Hart, M.J., Javors, M., Shih, Y.Y., Muir, E., Solano Fonseca, R.*, et al.* (2013). Chronic rapamycin restores brain vascular integrity and function through NO synthase activation and improves memory in symptomatic mice modeling Alzheimer's disease. Journal of cerebral blood flow and metabolism : official journal of the International Society of Cerebral Blood Flow and Metabolism *33*, 1412-1421.

Lindwall, G., and Cole, R.D. (1984). Phosphorylation affects the ability of tau protein to promote microtubule assembly. J Biol Chem *259*, 5301-5305.

Ling, D., and Salvaterra, P.M. (2009). A central role for autophagy in Alzheimer-type neurodegeneration. Autophagy *5*, 738-740.

Ling, D., Song, H.J., Garza, D., Neufeld, T.P., and Salvaterra, P.M. (2009). Abeta42-induced neurodegeneration via an age-dependent autophagic-lysosomal injury in Drosophila. PloS one *4*, e4201.

Liu, C., and Gotz, J. (2013). How it all started: tau and protein phosphatase 2A. J Alzheimers Dis *37*, 483-494.

LoPresti, P., Szuchet, S., Papasozomenos, S.C., Zinkowski, R.P., and Binder, L.I. (1995). Functional implications for the microtubule-associated protein tau: localization in oligodendrocytes. Proc Natl Acad Sci U S A *92*, 10369-10373.

Ma, T., Hoeffer, C.A., Capetillo-Zarate, E., Yu, F., Wong, H., Lin, M.T., Tampellini, D., Klann, E., Blitzer, R.D., and Gouras, G.K. (2010). Dysregulation of the mTOR pathway mediates impairment of synaptic plasticity in a mouse model of Alzheimer's disease. PloS one *5*.

Ma, T., Trinh, M.A., Wexler, A.J., Bourbon, C., Gatti, E., Pierre, P., Cavener, D.R., and Klann, E. (2013a). Suppression of eIF2alpha kinases alleviates Alzheimer's disease-related plasticity and memory deficits. Nature neuroscience *16*, 1299-1305.

Ma, Y.Q., Wu, D.K., and Liu, J.K. (2013b). mTOR and tau phosphorylated proteins in the hippocampal tissue of rats with type 2 diabetes and Alzheimer's disease. Molecular medicine reports *7*, 623-627.

Magnuson, B., Ekim, B., and Fingar, D.C. (2012). Regulation and function of ribosomal protein S6 kinase (S6K) within mTOR signalling networks. The Biochemical journal *441*, 1-21.

Majeski, A.E., and Dice, J.F. (2004). Mechanisms of chaperone-mediated autophagy. The international journal of biochemistry & cell biology *36*, 2435-2444.

Majumder, S., Caccamo, A., Medina, D.X., Benavides, A.D., Javors, M.A., Kraig, E., Strong, R., Richardson, A., and Oddo, S. (2012). Lifelong rapamycin administration ameliorates age-dependent cognitive deficits by reducing IL-1beta and enhancing NMDA signaling. Aging cell *11*, 326-335.

Majumder, S., Richardson, A., Strong, R., and Oddo, S. (2011). Inducing autophagy by rapamycin before, but not after, the formation of plaques and tangles ameliorates cognitive deficits. PloS one *6*, e25416.

Martinez-Lopez, N., Athonvarangkul, D., and Singh, R. (2015). Autophagy and aging. Adv Exp Med Biol *847*, 73-87.

Martinez-Vicente, M., and Cuervo, A.M. (2007). Autophagy and neurodegeneration: when the cleaning crew goes on strike. Lancet neurology *6*, 352-361.

Masliah, E., Mallory, M., Alford, M., DeTeresa, R., Hansen, L.A., McKeel, D.W., Jr., and Morris, J.C. (2001). Altered expression of synaptic proteins occurs early during progression of Alzheimer's disease. Neurology *56*, 127-129.

Mattson, M.P., Cheng, B., Davis, D., Bryant, K., Lieberburg, I., and Rydel, R.E. (1992). beta-Amyloid peptides destabilize calcium homeostasis and render human cortical neurons vulnerable to excitotoxicity. J Neurosci *12*, 376-389.

McCray, B.A., and Taylor, J.P. (2008). The role of autophagy in age-related neurodegeneration. Neuro-Signals *16*, 75-84.

Meijer, A.J., Lorin, S., Blommaart, E.F., and Codogno, P. (2014). Regulation of autophagy by amino acids and MTOR-dependent signal transduction. Amino Acids.

Mizushima, N. (2004). Methods for monitoring autophagy. The international journal of biochemistry & cell biology *36*, 2491-2502.

Mizushima, N., Noda, T., Yoshimori, T., Tanaka, Y., Ishii, T., George, M.D., Klionsky, D.J., Ohsumi, M., and Ohsumi, Y. (1998). A protein conjugation system essential for autophagy. Nature *395*, 395-398.

Moechars, D., Dewachter, I., Lorent, K., Reverse, D., Baekelandt, V., Naidu, A., Tesseur, I., Spittaels, K., Haute, C.V., Checler, F.*, et al.* (1999). Early phenotypic changes in transgenic mice that overexpress different mutants of amyloid precursor protein in brain. J Biol Chem *274*, 6483-6492.

Moll, L., El-Ami, T., and Cohen, E. (2014). Selective manipulation of aging: a novel strategy for the treatment of neurodegenerative disorders. Swiss medical weekly *144*, w13917.

Montagne, J., Stewart, M.J., Stocker, H., Hafen, E., Kozma, S.C., and Thomas, G. (1999). Drosophila S6 kinase: a regulator of cell size. Science *285*, 2126-2129.

Morita, T., and Sobue, K. (2009). Specification of neuronal polarity regulated by local translation of CRMP2 and Tau via the mTOR-p70S6K pathway. The Journal of biological chemistry *284*, 27734-27745.

Mucke, L., Masliah, E., Johnson, W.B., Ruppe, M.D., Alford, M., Rockenstein, E.M., Forss-Petter, S., Pietropaolo, M., Mallory, M., and Abraham, C.R. (1994). Synaptotrophic effects of human amyloid beta protein precursors in the cortex of transgenic mice. Brain Res *666*, 151-167.

Mucke, L., Masliah, E., Yu, G.Q., Mallory, M., Rockenstein, E.M., Tatsuno, G., Hu, K., Kholodenko, D., Johnson-Wood, K., and McConlogue, L. (2000). High-level neuronal expression of abeta 1-42 in wild-type human amyloid protein precursor transgenic mice: synaptotoxicity without plaque formation. J Neurosci *20*, 4050-4058.

Mullan, M., Crawford, F., Axelman, K., Houlden, H., Lilius, L., Winblad, B., and Lannfelt, L. (1992). A pathogenic mutation for probable Alzheimer's disease in the APP gene at the N-terminus of beta-amyloid. Nat Genet *1*, 345-347.

Murakami, M., Ichisaka, T., Maeda, M., Oshiro, N., Hara, K., Edenhofer, F., Kiyama, H., Yonezawa, K., and Yamanaka, S. (2004). mTOR is essential for growth and proliferation in early mouse embryos and embryonic stem cells. Molecular and cellular biology *24*, 6710-6718.

Nakagawa, T., Zhu, H., Morishima, N., Li, E., Xu, J., Yankner, B.A., and Yuan, J. (2000). Caspase-12 mediates endoplasmic-reticulum-specific apoptosis and cytotoxicity by amyloid-beta. Nature *403*, 98-103.

Nedelsky, N.B., Todd, P.K., and Taylor, J.P. (2008). Autophagy and the ubiquitin-proteasome system: collaborators in neuroprotection. Biochimica et biophysica acta *1782*, 691-699.

Nixon, R.A., and Yang, D.S. (2011a). Autophagy failure in Alzheimer's disease--locating the primary defect. Neurobiology of disease *43*, 38-45.

Nixon, R.A., and Yang, D.S. (2011b). Autophagy failure in Alzheimer's disease-locating the primary defect. Neurobiology of disease *43*, 38-45.

Novak, M., Kabat, J., and Wischik, C.M. (1993). Molecular characterization of the minimal protease resistant tau unit of the Alzheimer's disease paired helical filament. Embo J *12*, 365-370.

Oddo, S. (2008). The ubiquitin-proteasome system in Alzheimer's disease. Journal of cellular and molecular medicine *12*, 363-373.

Oddo, S. (2012). The role of mTOR signaling in Alzheimer disease. Front Biosci (Schol Ed) *4*, 941-952.

Oddo, S., Caccamo, A., Kitazawa, M., Tseng, B.P., and LaFerla, F.M. (2003a). Amyloid deposition precedes tangle formation in a triple transgenic model of Alzheimer's disease. Neurobiol Aging *24*, 1063-1070.

Oddo, S., Caccamo, A., Shepherd, J.D., Murphy, M.P., Golde, T.E., Kayed, R., Metherate, R., Mattson, M.P., Akbari, Y., and LaFerla, F.M. (2003b). Triple-transgenic model of Alzheimer's

disease with plaques and tangles: intracellular Abeta and synaptic dysfunction. Neuron *39*, 409-421.

Oddo, S., Caccamo, A., Tseng, B., Cheng, D., Vasilevko, V., Cribbs, D.H., and LaFerla, F.M. (2008). Blocking Abeta42 accumulation delays the onset and progression of tau pathology via the C terminus of heat shock protein70-interacting protein: a mechanistic link between Abeta and tau pathology. The Journal of neuroscience : the official journal of the Society for Neuroscience *28*, 12163-12175.

Oldham, S., Montagne, J., Radimerski, T., Thomas, G., and Hafen, E. (2000). Genetic and biochemical characterization of dTOR, the Drosophila homolog of the target of rapamycin. Genes Dev *14*, 2689-2694.

Onuki, R., Bando, Y., Suyama, E., Katayama, T., Kawasaki, H., Baba, T., Tohyama, M., and Taira, K. (2004). An RNA-dependent protein kinase is involved in tunicamycin-induced apoptosis and Alzheimer's disease. The EMBO journal *23*, 959-968.

Orr, M.E., and Oddo, S. (2013). Autophagic/lysosomal dysfunction in Alzheimer's disease. Alzheimer's research & therapy *5*, 53.

Orr, M.E., Salinas, A., Buffenstein, R., and Oddo, S. (2013). Mammalian target of rapamycin hyperactivity mediates the detrimental effects of a high sucrose diet on Alzheimer's disease pathology. Neurobiology of aging.

Orr, M.E., Salinas, A., Buffenstein, R., and Oddo, S. (2014). Mammalian target of rapamycin hyperactivity mediates the detrimental effects of a high sucrose diet on Alzheimer's disease pathology. Neurobiology of aging *35*, 1233-1242.

Ouellet, M., Emond, V., Chen, C.T., Julien, C., Bourasset, F., Oddo, S., LaFerla, F., Bazinet, R.P., and Calon, F. (2009). Diffusion of docosahexaenoic and eicosapentaenoic acids through the blood-brain barrier: An in situ cerebral perfusion study. Neurochem Int *55*, 476-482.

Palop, J.J., and Mucke, L. (2010). Amyloid-beta-induced neuronal dysfunction in Alzheimer's disease: from synapses toward neural networks. Nature neuroscience *13*, 812-818.

Pandey, U.B., Nie, Z., Batlevi, Y., McCray, B.A., Ritson, G.P., Nedelsky, N.B., Schwartz, S.L., DiProspero, N.A., Knight, M.A., Schuldiner, O., *et al.* (2007). HDAC6 rescues neurodegeneration and provides an essential link between autophagy and the UPS. Nature *447*, 859-863.

Pangman, V.C., Sloan, J., and Guse, L. (2000). An examination of psychometric properties of the mini-mental state examination and the standardized mini-mental state examination: implications for clinical practice. Applied nursing research : ANR *13*, 209-213.

Parsons, R.G., Gafford, G.M., and Helmstetter, F.J. (2006). Translational control via the mammalian target of rapamycin pathway is critical for the formation and stability of long-term fear memory in amygdala neurons. The Journal of neuroscience : the official journal of the Society for Neuroscience *26*, 12977-12983.

Patrick, G.N., Zukerberg, L., Nikolic, M., de la Monte, S., Dikkes, P., and Tsai, L.H. (1999). Conversion of p35 to p25 deregulates Cdk5 activity and promotes neurodegeneration. Nature *402*, 615-622.

Pavitt, G.D. (2013). Less translational control, more memory. eLife *2*, e00895.

Pearson, R.B., Dennis, P.B., Han, J.W., Williamson, N.A., Kozma, S.C., Wettenhall, R.E., and Thomas, G. (1995). The principal target of rapamycin-induced p70s6k inactivation is a novel phosphorylation site within a conserved hydrophobic domain. The EMBO journal *14*, 5279-5287.

Peel, A.L., and Bredesen, D.E. (2003). Activation of the cell stress kinase PKR in Alzheimer's disease and human amyloid precursor protein transgenic mice. Neurobiology of disease *14*, 52-62.

Pei, J.J., An, W.L., Zhou, X.W., Nishimura, T., Norberg, J., Benedikz, E., Gotz, J., and Winblad, B. (2006). P70 S6 kinase mediates tau phosphorylation and synthesis. FEBS letters *580*, 107-114.

Pei, J.J., Bjorkdahl, C., Zhang, H., Zhou, X., and Winblad, B. (2008). p70 S6 kinase and tau in Alzheimer's disease. J Alzheimers Dis *14*, 385-392.

Pei, J.J., and Hugon, J. (2008). mTOR-dependent signalling in Alzheimer's disease. Journal of cellular and molecular medicine *12*, 2525-2532.

Perluigi, M., Di Domenico, F., and Butterfield, D.A. (2015). mTOR signaling in aging and neurodegeneration: At the crossroad between metabolism dysfunction and impairment of autophagy. Neurobiology of disease.

Phinney, A.L., Horne, P., Yang, J., Janus, C., Bergeron, C., and Westaway, D. (2003). Mouse models of Alzheimer's disease: the long and filamentous road. Neurol Res *25*, 590-600.

Pickford, F., Masliah, E., Britschgi, M., Lucin, K., Narasimhan, R., Jaeger, P.A., Small, S., Spencer, B., Rockenstein, E., Levine, B.*, et al.* (2008). The autophagy-related protein beclin 1 shows reduced expression in early Alzheimer disease and regulates amyloid beta accumulation in mice. J Clin Invest *118*, 2190-2199.

Pike, C.J., Cummings, B.J., and Cotman, C.W. (1992). beta-Amyloid induces neuritic dystrophy in vitro: similarities with Alzheimer pathology. Neuroreport *3*, 769-772.

Puighermanal, E., Marsicano, G., Busquets-Garcia, A., Lutz, B., Maldonado, R., and Ozaita, A. (2009). Cannabinoid modulation of hippocampal long-term memory is mediated by mTOR signaling. Nature neuroscience *12*, 1152-1158.

Querfurth, H.W., and LaFerla, F.M. (2010). Alzheimer's disease. N Engl J Med *362*, 329-344.

Quon, D., Wang, Y., Catalano, R., Scardina, J.M., Murakami, K., and Cordell, B. (1991). Formation of beta-amyloid protein deposits in brains of transgenic mice. Nature *352*, 239-241.

Rajapakse, A.G., Yepuri, G., Carvas, J.M., Stein, S., Matter, C.M., Scerri, I., Ruffieux, J., Montani, J.P., Ming, X.F., and Yang, Z. (2011). Hyperactive S6K1 mediates oxidative stress and endothelial dysfunction in aging: inhibition by resveratrol. PloS one *6*, e19237.

Rapoport, M., Dawson, H.N., Binder, L.I., Vitek, M.P., and Ferreira, A. (2002). Tau is essential to beta -amyloid-induced neurotoxicity. Proc Natl Acad Sci U S A *99*, 6364-6369.

Ravikumar, B., Vacher, C., Berger, Z., Davies, J.E., Luo, S., Oroz, L.G., Scaravilli, F., Easton, D.F., Duden, R., O'Kane, C.J., *et al.* (2004). Inhibition of mTOR induces autophagy and reduces toxicity of polyglutamine expansions in fly and mouse models of Huntington disease. Nature genetics *36*, 585-595.

Reddy, P.H., McWeeney, S., Park, B.S., Manczak, M., Gutala, R.V., Partovi, D., Jung, Y., Yau, V., Searles, R., Mori, M., *et al.* (2004). Gene expression profiles of transcripts in amyloid precursor protein transgenic mice: up-regulation of mitochondrial metabolism and apoptotic genes is an early cellular change in Alzheimer's disease. Hum Mol Genet *13*, 1225-1240.

Reinhard, C., Thomas, G., and Kozma, S.C. (1992). A single gene encodes two isoforms of the p70 S6 kinase: activation upon mitogenic stimulation. Proceedings of the National Academy of Sciences of the United States of America *89*, 4052-4056.

Reitz, C., and Mayeux, R. (2014). Alzheimer disease: epidemiology, diagnostic criteria, risk factors and biomarkers. Biochemical pharmacology *88*, 640-651.

Ricciardi, S., Boggio, E.M., Grosso, S., Lonetti, G., Forlani, G., Stefanelli, G., Calcagno, E., Morello, N., Landsberger, N., Biffo, S., *et al.* (2011). Reduced AKT/mTOR signaling and protein synthesis dysregulation in a Rett syndrome animal model. Hum Mol Genet *20*, 1182-1196.

Richardson, A., Galvan, V., Lin, A.L., and Oddo, S. (2014). How longevity research can lead to therapies for Alzheimer's disease: The rapamycin story. Exp Gerontol.

Richardson, A., Galvan, V., Lin, A.L., and Oddo, S. (2015). How longevity research can lead to therapies for Alzheimer's disease: The rapamycin story. Exp Gerontol *68*, 51-58.

Rissman, R.A., Poon, W.W., Blurton-Jones, M., Oddo, S., Torp, R., Vitek, M.P., LaFerla, F.M., Rohn, T.T., and Cotman, C.W. (2004). Caspase-cleavage of tau is an early event in Alzheimer disease tangle pathology. J Clin Invest *114*, 121-130.

Roberson, E.D., Scearce-Levie, K., Palop, J.J., Yan, F., Cheng, I.H., Wu, T., Gerstein, H., Yu, G.Q., and Mucke, L. (2007). Reducing endogenous tau ameliorates amyloid beta-induced deficits in an Alzheimer's disease mouse model. Science *316*, 750-754.

Rogaev, E.I., Sherrington, R., Rogaeva, E.A., Levesque, G., Ikeda, M., Liang, Y., Chi, H., Lin, C., Holman, K., Tsuda, T.*, et al.* (1995). Familial Alzheimer's disease in kindreds with missense mutations in a gene on chromosome 1 related to the Alzheimer's disease type 3 gene. Nature *376*, 775-778.

Rohn, T.T., Head, E., Nesse, W.H., Cotman, C.W., and Cribbs, D.H. (2001). Activation of caspase-8 in the Alzheimer's disease brain. Neurobiol Dis *8*, 1006-1016.

Rubinsztein, D.C. (2006). The roles of intracellular protein-degradation pathways in neurodegeneration. Nature *443*, 780-786.

Rubinsztein, D.C., Marino, G., and Kroemer, G. (2011). Autophagy and aging. Cell *146*, 682-695.

Ruvinsky, I., and Meyuhas, O. (2006). Ribosomal protein S6 phosphorylation: from protein synthesis to cell size. Trends Biochem Sci *31*, 342-348.

Sajdel-Sulkowska, E.M., and Marotta, C.A. (1984). Alzheimer's disease brain: alterations in RNA levels and in a ribonuclease-inhibitor complex. Science *225*, 947-949.

Sandhu, F.A., Salim, M., and Zain, S.B. (1991). Expression of the human beta-amyloid protein of Alzheimer's disease specifically in the brains of transgenic mice. J Biol Chem *266*, 21331-21334.

Santini, E., Huynh, T.N., and Klann, E. (2014). Mechanisms of translation control underlying long-lasting synaptic plasticity and the consolidation of long-term memory. Progress in molecular biology and translational science *122*, 131-167.

Schauwecker, P.E., and Steward, O. (1997). Genetic determinants of susceptibility to excitotoxic cell death: implications for gene targeting approaches. Proc Natl Acad Sci U S A *94*, 4103-4108.

Scheuner, D., Eckman, C., Jensen, M., Song, X., Citron, M., Suzuki, N., Bird, T.D., Hardy, J., Hutton, M., Kukull, W.*, et al.* (1996). Secreted amyloid beta-protein similar to that in the senile plaques of Alzheimer's disease is increased in vivo by the presenilin 1 and 2 and APP mutations linked to familial Alzheimer's disease. Nat Med *2*, 864-870.

Selkoe, D.J. (1991). The molecular pathology of Alzheimer's disease. Neuron *6*, 487-498.

Selkoe, D.J. (2001). Alzheimer's disease: genes, proteins, and therapy. Physiological reviews *81*, 741-766.

Selman, C., Tullet, J.M., Wieser, D., Irvine, E., Lingard, S.J., Choudhury, A.I., Claret, M., Al-Qassab, H., Carmignac, D., Ramadani, F.*, et al.* (2009). Ribosomal protein S6 kinase 1 signaling regulates mammalian life span. Science *326*, 140-144.

Shao, J., and Diamond, M.I. (2007). Polyglutamine diseases: emerging concepts in pathogenesis and therapy. Hum Mol Genet *16 Spec No. 2*, R115-123.

Sheng, M., Sabatini, B.L., and Sudhof, T.C. (2012). Synapses and Alzheimer's disease. Cold Spring Harb Perspect Biol *4*.

Sherrington, R., Rogaev, E.I., Liang, Y., Rogaeva, E.A., Levesque, G., Ikeda, M., Chi, H., Lin, C., Li, G., Holman, K.*, et al.* (1995). Cloning of a gene bearing missense mutations in early-onset familial Alzheimer's disease. Nature *375*, 754-760.

Shima, H., Pende, M., Chen, Y., Fumagalli, S., Thomas, G., and Kozma, S.C. (1998). Disruption of the p70(s6k)/p85(s6k) gene reveals a small mouse phenotype and a new functional S6 kinase. The EMBO journal *17*, 6649-6659.

Song, C., Murray, T.A., Kimura, R., Wakui, M., Ellsworth, K., Javedan, S.P., Marxer-Miller, S., Lukas, R.J., and Wu, J. (2005). Role of alpha7-nicotinic acetylcholine receptors in tetanic stimulation-induced gamma oscillations in rat hippocampal slices. Neuropharmacology *48*, 869-880.

Speakman, J.R., and Mitchell, S.E. (2011). Caloric restriction. Molecular aspects of medicine *32*, 159-221.

Spilman, P., Podlutskaya, N., Hart, M.J., Debnath, J., Gorostiza, O., Bredesen, D., Richardson, A., Strong, R., and Galvan, V. (2010). Inhibition of mTOR by rapamycin abolishes cognitive deficits and reduces amyloid-beta levels in a mouse model of Alzheimer's disease. PloS one *5*, e9979.

St George-Hyslop, P.H., Tanzi, R.E., Polinsky, R.J., Haines, J.L., Nee, L., Watkins, P.C., Myers, R.H., Feldman, R.G., Pollen, D., Drachman, D.*, et al.* (1987). The genetic defect causing familial Alzheimer's disease maps on chromosome 21. Science *235*, 885-890.

Steinhilb, M.L., Dias-Santagata, D., Fulga, T.A., Felch, D.L., and Feany, M.B. (2007). Tau phosphorylation sites work in concert to promote neurotoxicity in vivo. Molecular biology of the cell *18*, 5060-5068.

Steward, O., Schauwecker, P.E., Guth, L., Zhang, Z., Fujiki, M., Inman, D., Wrathall, J., Kempermann, G., Gage, F.H., Saatman, K.E.*, et al.* (1999). Genetic approaches to neurotrauma research: opportunities and potential pitfalls of murine models. Exp Neurol *157*, 19-42.

Sturchler-Pierrat, C., Abramowski, D., Duke, M., Wiederhold, K.H., Mistl, C., Rothacher, S., Ledermann, B., Burki, K., Frey, P., Paganetti, P.A.*, et al.* (1997). Two amyloid precursor protein transgenic mouse models with Alzheimer disease-like pathology. Proc Natl Acad Sci U S A *94*, 13287-13292.

Su, J.H., Cummings, B.J., and Cotman, C.W. (1994). Early phosphorylation of tau in Alzheimer's disease occurs at Ser-202 and is preferentially located within neurites. Neuroreport *5*, 2358-2362.

Suzuki, N., Cheung, T.T., Cai, X.D., Odaka, A., Otvos, L., Jr., Eckman, C., Golde, T.E., and Younkin, S.G. (1994). An increased percentage of long amyloid beta protein secreted by familial amyloid beta protein precursor (beta APP717) mutants. Science *264*, 1336-1340.

Takashima, A., Noguchi, K., Sato, K., Hoshino, T., and Imahori, K. (1993). Tau protein kinase I is essential for amyloid beta-protein-induced neurotoxicity. Proc Natl Acad Sci U S A *90*, 7789-7793.

Tan, L., Wang, X., Ni, Z.F., Zhu, X., Wu, W., Zhu, L.Q., and Liu, D. (2013). A systematic analysis of genomic changes in Tg2576 mice. Molecular neurobiology *47*, 883-891.

Tang, S.J., Reis, G., Kang, H., Gingras, A.C., Sonenberg, N., and Schuman, E.M. (2002). A rapamycin-sensitive signaling pathway contributes to long-term synaptic plasticity in the hippocampus. Proceedings of the National Academy of Sciences of the United States of America *99*, 467-472.

Tang, Z., Bereczki, E., Zhang, H., Wang, S., Li, C., Ji, X., Branca, R.M., Lehtio, J., Guan, Z., Filipcik, P.*, et al.* (2013). Mammalian target of rapamycin (mTor) mediates tau protein dyshomeostasis: implication for Alzheimer disease. The Journal of biological chemistry *288*, 15556-15570.

Tang, Z., Ioja, E., Bereczki, E., Hultenby, K., Li, C., Guan, Z., Winblad, B., and Pei, J.J. (2015). mTor mediates tau localization and secretion: Implication for Alzheimer's disease. Biochimica et biophysica acta *1853*, 1646-1657.

Tanida, I. (2011). Autophagy basics. Microbiol Immunol *55*, 1-11.

Tanida, I., Minematsu-Ikeguchi, N., Ueno, T., and Kominami, E. (2005). Lysosomal turnover, but not a cellular level, of endogenous LC3 is a marker for autophagy. Autophagy *1*, 84-91.

Thies, W., Bleiler, L., and Alzheimer's, A. (2013). 2013 Alzheimer's disease facts and figures. Alzheimer's & dementia : the journal of the Alzheimer's Association *9*, 208-245.

Tian, Y., Bustos, V., Flajolet, M., and Greengard, P. (2011). A small-molecule enhancer of autophagy decreases levels of A{beta} and APP-CTF via Atg5-dependent autophagy pathway. Faseb J.

Tramutola, A., Triplett, J.C., Di Domenico, F., Niedowicz, D.M., Murphy, M.P., Coccia, R., Perluigi, M., and Butterfield, D.A. (2015). Alteration of mTOR signaling occurs early in the progression

of Alzheimer disease (AD): analysis of brain from subjects with pre-clinical AD, amnestic mild cognitive impairment and late-stage AD. J Neurochem *133*, 739-749.

Trinczek, B., Biernat, J., Baumann, K., Mandelkow, E.M., and Mandelkow, E. (1995). Domains of tau protein, differential phosphorylation, and dynamic instability of microtubules. Mol Biol Cell *6*, 1887-1902.

Troca-Marin, J.A., Alves-Sampaio, A., and Montesinos, M.L. (2012). Deregulated mTOR-mediated translation in intellectual disability. Progress in neurobiology *96*, 268-282.

Troy, C.M., Rabacchi, S.A., Friedman, W.J., Frappier, T.F., Brown, K., and Shelanski, M.L. (2000). Caspase-2 mediates neuronal cell death induced by beta-amyloid. J Neurosci *20*, 1386-1392.

Tuval-Kochen, L., Paglin, S., Keshet, G., Lerenthal, Y., Nakar, C., Golani, T., Toren, A., Yahalom, J., Pfeffer, R., and Lawrence, Y. (2013). Eukaryotic initiation factor 2alpha--a downstream effector of mammalian target of rapamycin--modulates DNA repair and cancer response to treatment. PloS one *8*, e77260.

Um, S.H., Frigerio, F., Watanabe, M., Picard, F., Joaquin, M., Sticker, M., Fumagalli, S., Allegrini, P.R., Kozma, S.C., Auwerx, J.*, et al.* (2004). Absence of S6K1 protects against age- and diet-induced obesity while enhancing insulin sensitivity. Nature *431*, 200-205.

Vassar, R., Bennett, B.D., Babu-Khan, S., Kahn, S., Mendiaz, E.A., Denis, P., Teplow, D.B., Ross, S., Amarante, P., Loeloff, R.*, et al.* (1999). Beta-secretase cleavage of Alzheimer's amyloid precursor protein by the transmembrane aspartic protease BACE. Science *286*, 735-741.

Vellai, T., Takacs-Vellai, K., Zhang, Y., Kovacs, A.L., Orosz, L., and Muller, F. (2003). Genetics: influence of TOR kinase on lifespan in C. elegans. Nature *426*, 620.

Wang, X., and Proud, C.G. (2006). The mTOR pathway in the control of protein synthesis. Physiology (Bethesda) *21*, 362-369.

Wang, Y., and Mandelkow, E. (2012). Degradation of tau protein by autophagy and proteasomal pathways. Biochemical Society transactions *40*, 644-652.

Welsh, K.A., Butters, N., Hughes, J.P., Mohs, R.C., and Heyman, A. (1992). Detection and staging of dementia in Alzheimer's disease. Use of the neuropsychological measures developed for the Consortium to Establish a Registry for Alzheimer's Disease. Arch Neurol *49*, 448-452.

Westerman, M.A., Cooper-Blacketer, D., Mariash, A., Kotilinek, L., Kawarabayashi, T., Younkin, L.H., Carlson, G.A., Younkin, S.G., and Ashe, K.H. (2002). The relationship between Abeta and memory in the Tg2576 mouse model of Alzheimer's disease. The Journal of neuroscience : the official journal of the Society for Neuroscience *22*, 1858-1867.

Wolfe, M.S., Xia, W., Ostaszewski, B.L., Diehl, T.S., Kimberly, W.T., and Selkoe, D.J. (1999). Two transmembrane aspartates in presenilin-1 required for presenilin endoproteolysis and gamma-secretase activity. Nature *398*, 513-517.

Wu, J.J., Liu, J., Chen, E.B., Wang, J.J., Cao, L., Narayan, N., Fergusson, M.M., Rovira, II, Allen, M., Springer, D.A.*, et al.* (2013). Increased mammalian lifespan and a segmental and tissue-specific slowing of aging after genetic reduction of mTOR expression. Cell Rep *4*, 913-920.

Wullschleger, S., Loewith, R., and Hall, M.N. (2006). TOR signaling in growth and metabolism. Cell *124*, 471-484.

Yang, D.S., Stavrides, P., Mohan, P.S., Kaushik, S., Kumar, A., Ohno, M., Schmidt, S.D., Wesson, D., Bandyopadhyay, U., Jiang, Y.*, et al.* (2011). Reversal of autophagy dysfunction in the TgCRND8 mouse model of Alzheimer's disease ameliorates amyloid pathologies and memory deficits. Brain *134*, 258-277.

Yankner, B.A., Dawes, L.R., Fisher, S., Villa-Komaroff, L., Oster-Granite, M.L., and Neve, R.L. (1989). Neurotoxicity of a fragment of the amyloid precursor associated with Alzheimer's disease. Science *245*, 417-420.

Yu, W.H., Cuervo, A.M., Kumar, A., Peterhoff, C.M., Schmidt, S.D., Lee, J.H., Mohan, P.S., Mercken, M., Farmery, M.R., Tjernberg, L.O.*, et al.* (2005). Macroautophagy--a novel Beta-amyloid peptide-generating pathway activated in Alzheimer's disease. J Cell Biol *171*, 87-98.

Yu, W.H., Dorado, B., Figueroa, H.Y., Wang, L., Planel, E., Cookson, M.R., Clark, L.N., and Duff, K.E. (2009). Metabolic activity determines efficacy of macroautophagic clearance of pathological oligomeric alpha-synuclein. The American journal of pathology *175*, 736-747.

Zeng, L.H., Rensing, N.R., and Wong, M. (2009). The mammalian target of rapamycin signaling pathway mediates epileptogenesis in a model of temporal lobe epilepsy. The Journal of neuroscience : the official journal of the Society for Neuroscience *29*, 6964-6972.

Zhao, M., Su, J., Head, E., and Cotman, C.W. (2003). Accumulation of caspase cleaved amyloid precursor protein represents an early neurodegenerative event in aging and in Alzheimer's disease. Neurobiol Dis *14*, 391-403.

Zhou, X.W., Tanila, H., and Pei, J.J. (2008). Parallel increase in p70 kinase activation and tau phosphorylation (S262) with Abeta overproduction. FEBS letters *582*, 159-164.